ISR Science Highlights

Ian McCrea
STFC Rutherford Appleton Laboratory

ISR Science: Science at all scales!

- Large-scale structures
  - Morphology of the ionosphere
  - Large-scale convection (effect of solar wind coupling)
  - Flow channels (heating and composition effects)
  - Blobs and patches (formation and development)
  - Holes and troughs (high-latitude and middle latitude)

- Meso-scale structures
  - Gradients and scintillations (comms/space weather applications)
  - Auroral arcs and electrodynamics (what happens near an arc?)
  - Thin layer phenomena
  - Gravity waves and TIDs

ISR Science: Science at all scales!

- Micro-scale structures
  - Natural plasma heating
  - Non-thermal distribution functions (non-Maxwellians, E and F regions)
  - HF plasma heating
  - Natural plasma instabilities (e.g. NEIALs,)
  - Small-scale plasma waves (coherent structures)

- Temporal structures
  - Day-to-day variability
  - Statistical studies (ion heating, ion upflows)
  - Long-term trends (e.g. upper atmosphere cooling)

Large-scale structure
I: Morphology of the ionosphere

- Large-scale structure of the ionosphere varies significantly as a function of :
  - Geographic/Geomagnetic location
  - Season
  - Solar activity
  - Magnetospheric coupling
  - Atmospheric dynamics

- Because of large range/altitude coverage, pointing flexibility and multi-parameter fitting, ISRs are superb tools for revealing the main structures in the plasma.

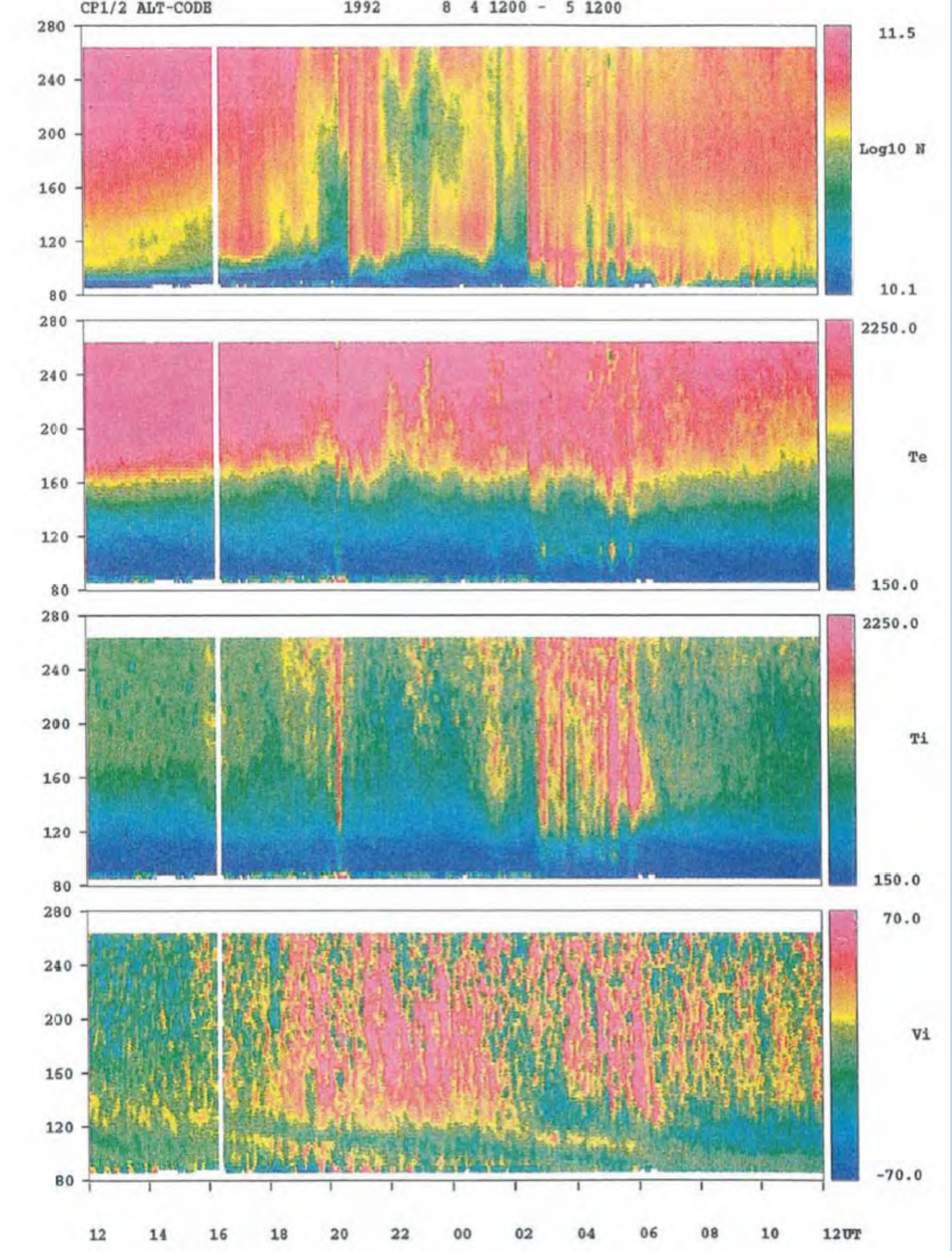

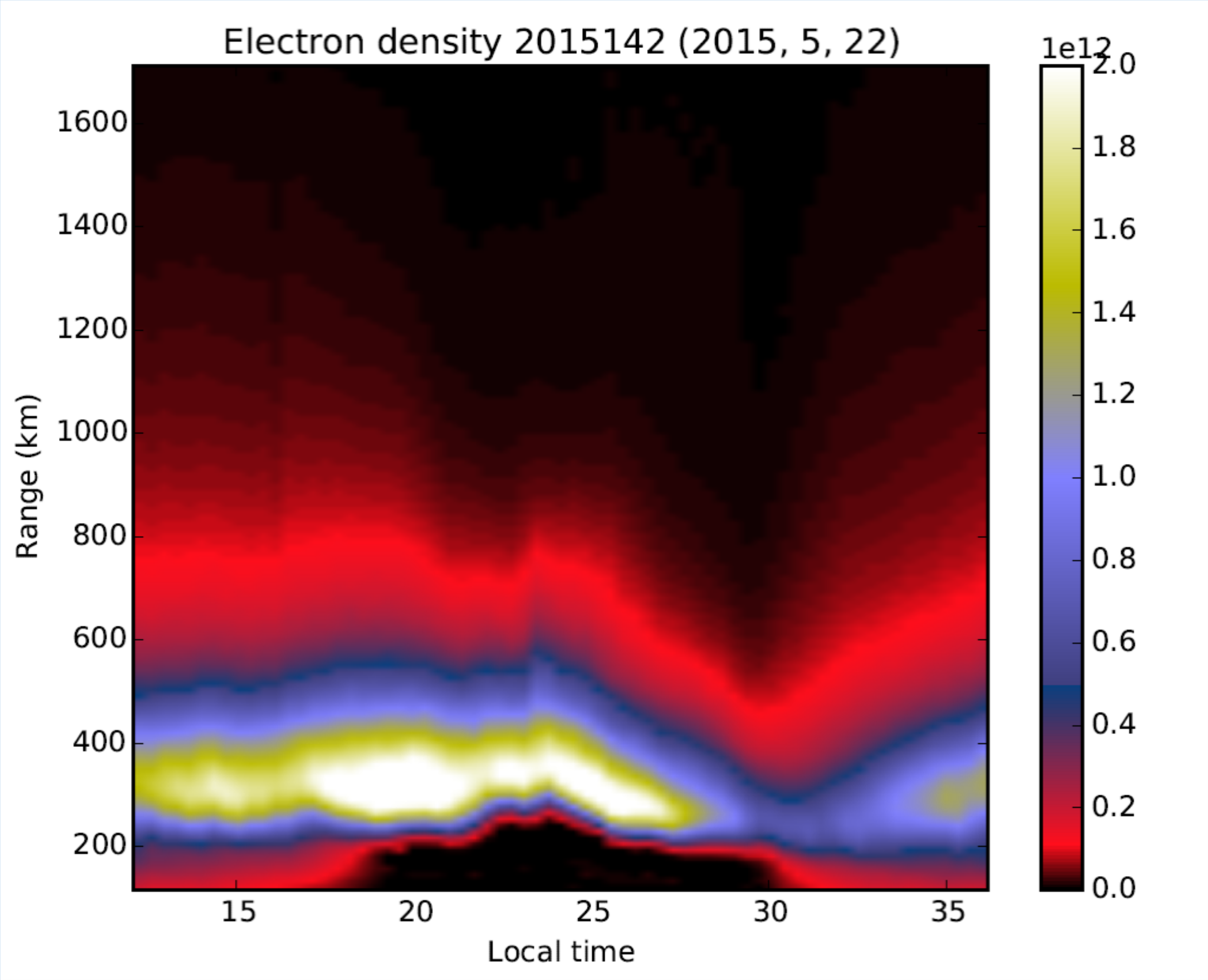

Electron density 2015142 (2015, 5, 22)
Range (km)
1600
1400
1200
1000
800
600
400
200
15
20
25
30
35
Local time
1e12
2.0
1.8
1.6
1.4
1.2
1.0
0.8
0.6
0.4
0.2
0.0

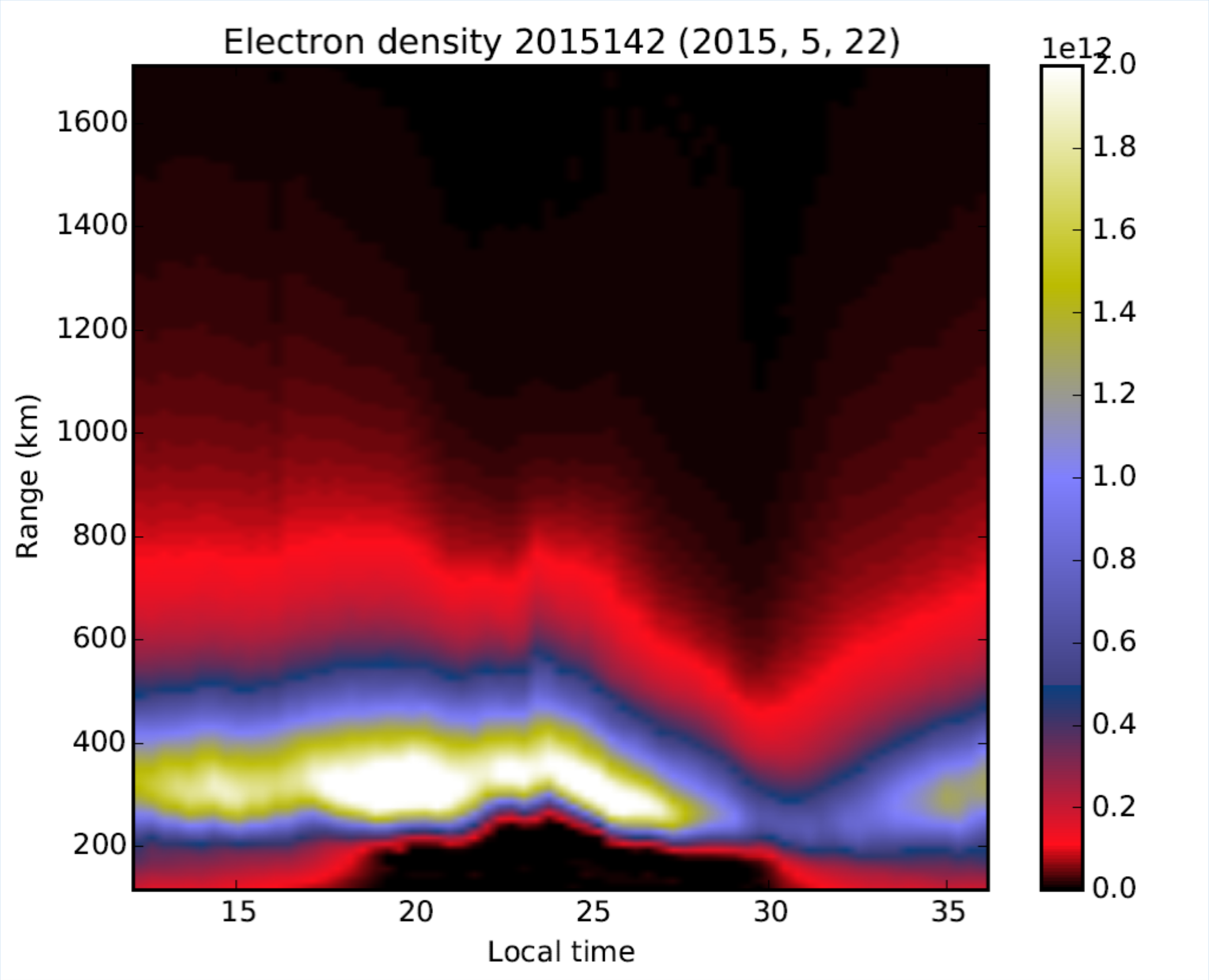

Low-latitude data: Arecibo

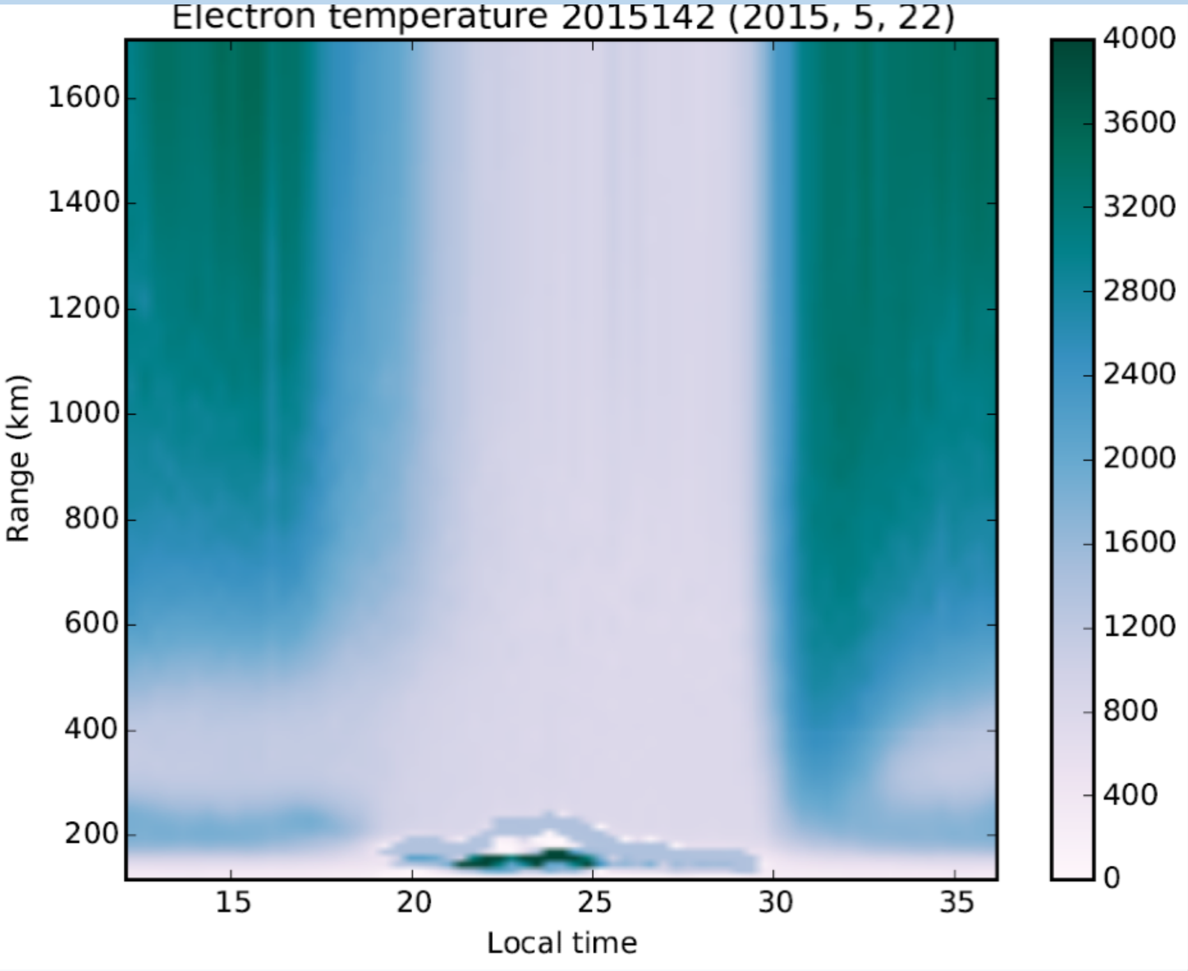
Electron temperature 2015142 (2015, 5, 22)
Range (km)
1600
1400
1200
1000
800
600
400
200
15
20
25
30
35
Local time
4000
3600
3200
2800
2400
2000
1600
1200
800
400
0

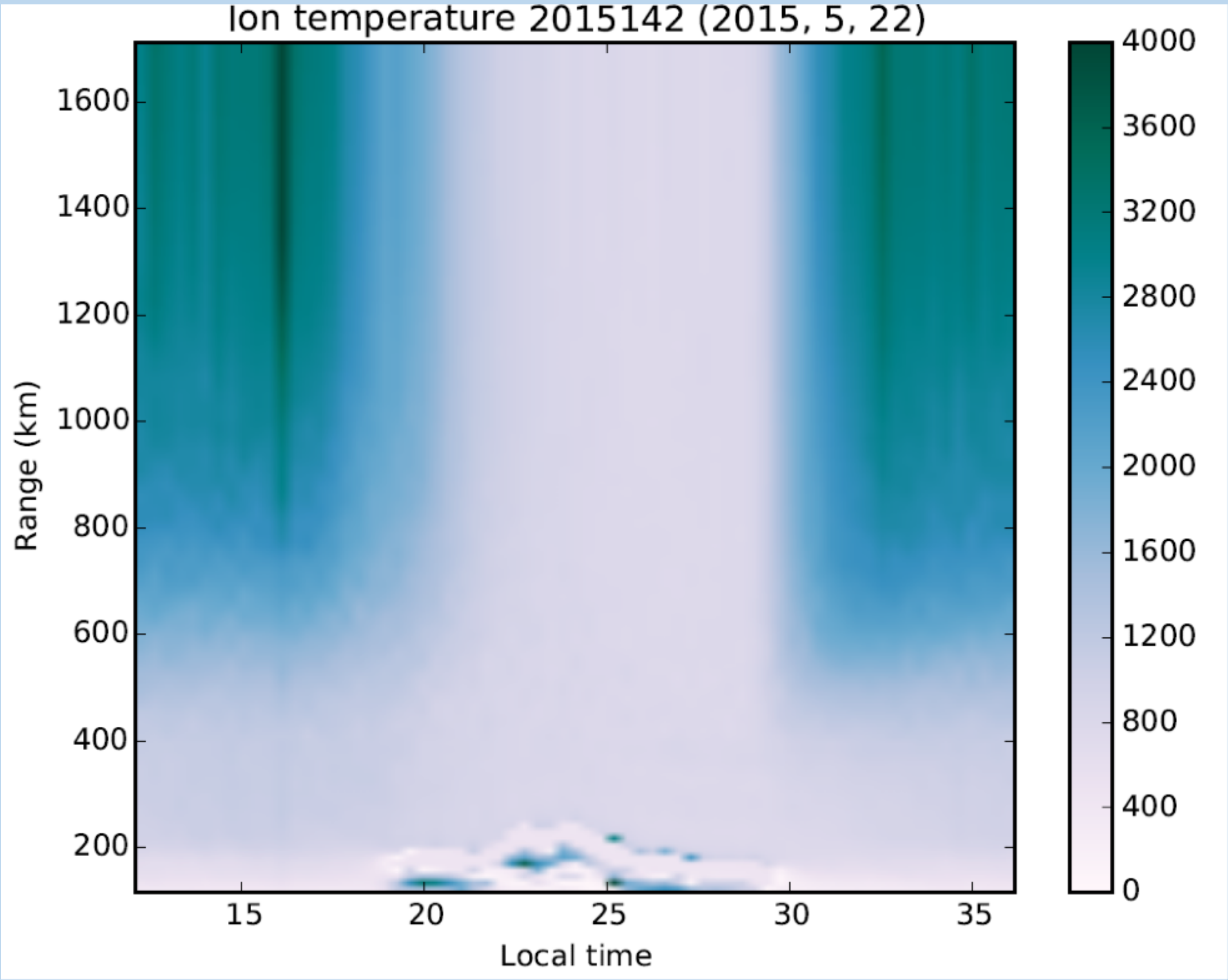
Ion temperature 2015142 (2015, 5, 22)
Range (km)
1600
1400
1200
1000
800
600
400
200
15
20
25
30
35
Local time
4000
3600
3200
2800
2400
2000
1600
1200
800
400
0

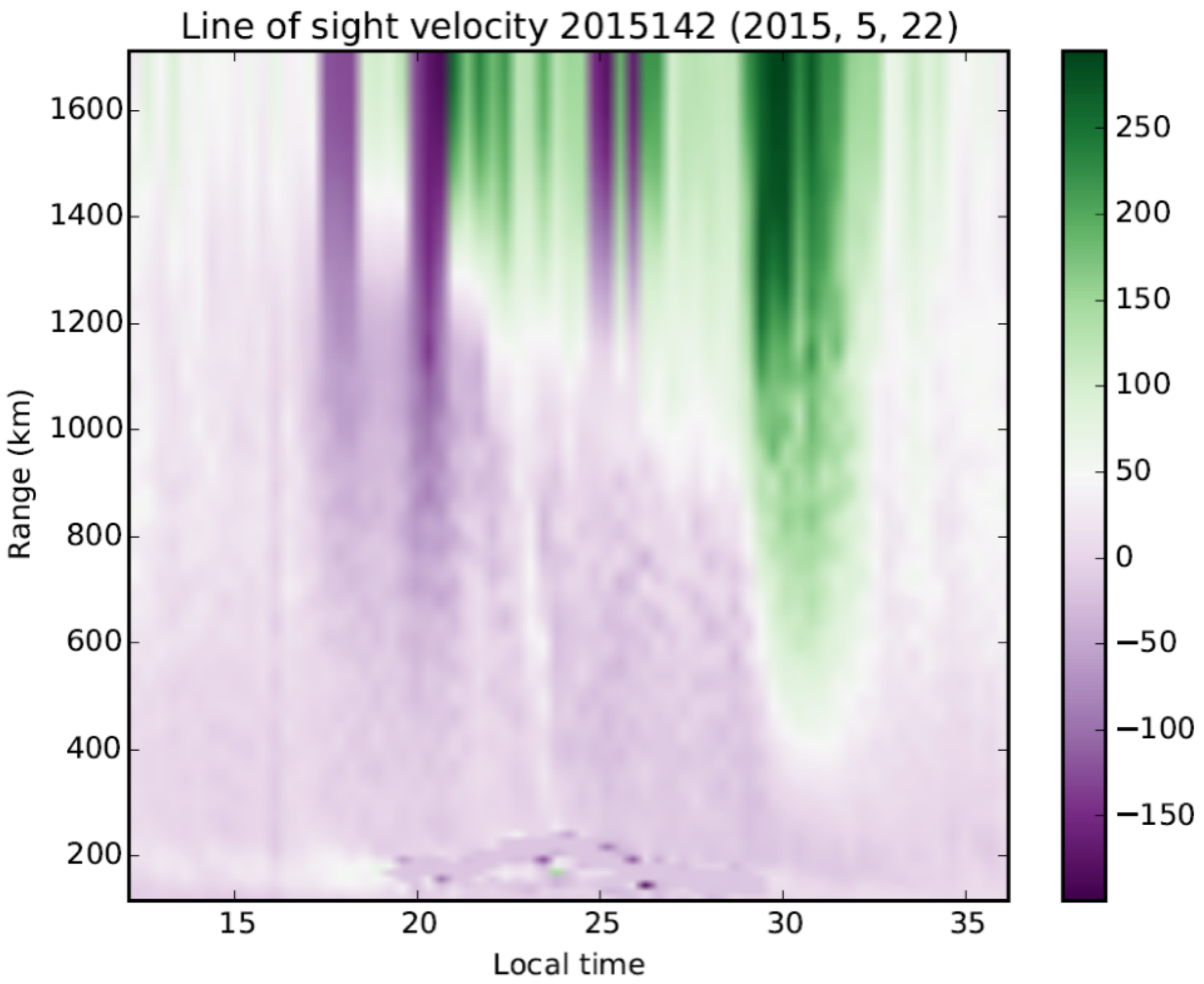

Line of sight velocity 2015142 (2015, 5, 22)
Range (km)
Local time
1600
1400
1200
1000
800
600
400
200
15
20
25
30
35
250
200
150
100
50
0
−50
−100
−150

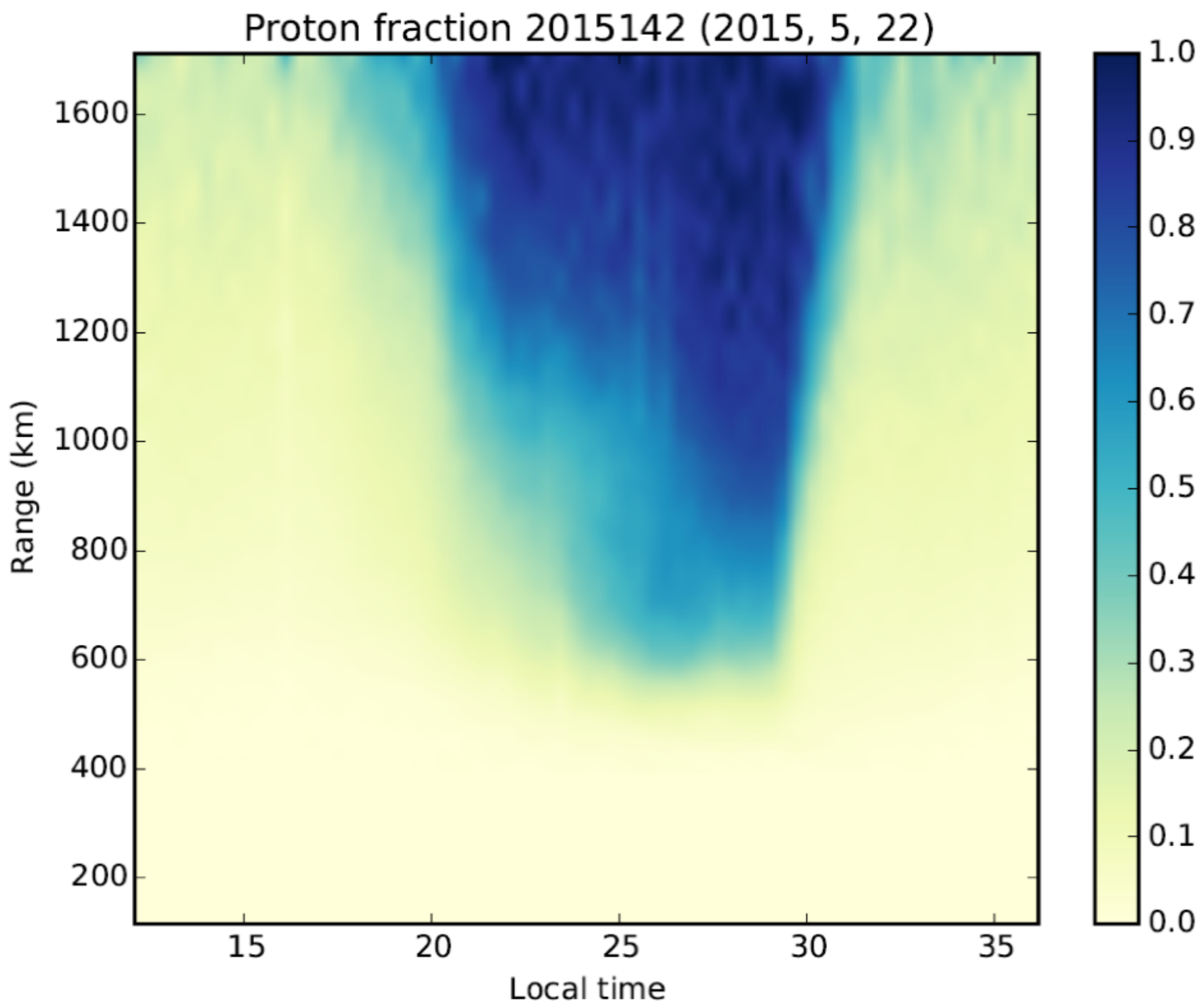

Proton fraction 2015142 (2015, 5, 22)
Range (km)
Local time
1600
1400
1200
1000
800
600
400
200
15
20
25
30
35
1.0
0.9
0.8
0.7
0.6
0.5
0.4
0.3
0.2
0.1
0.0

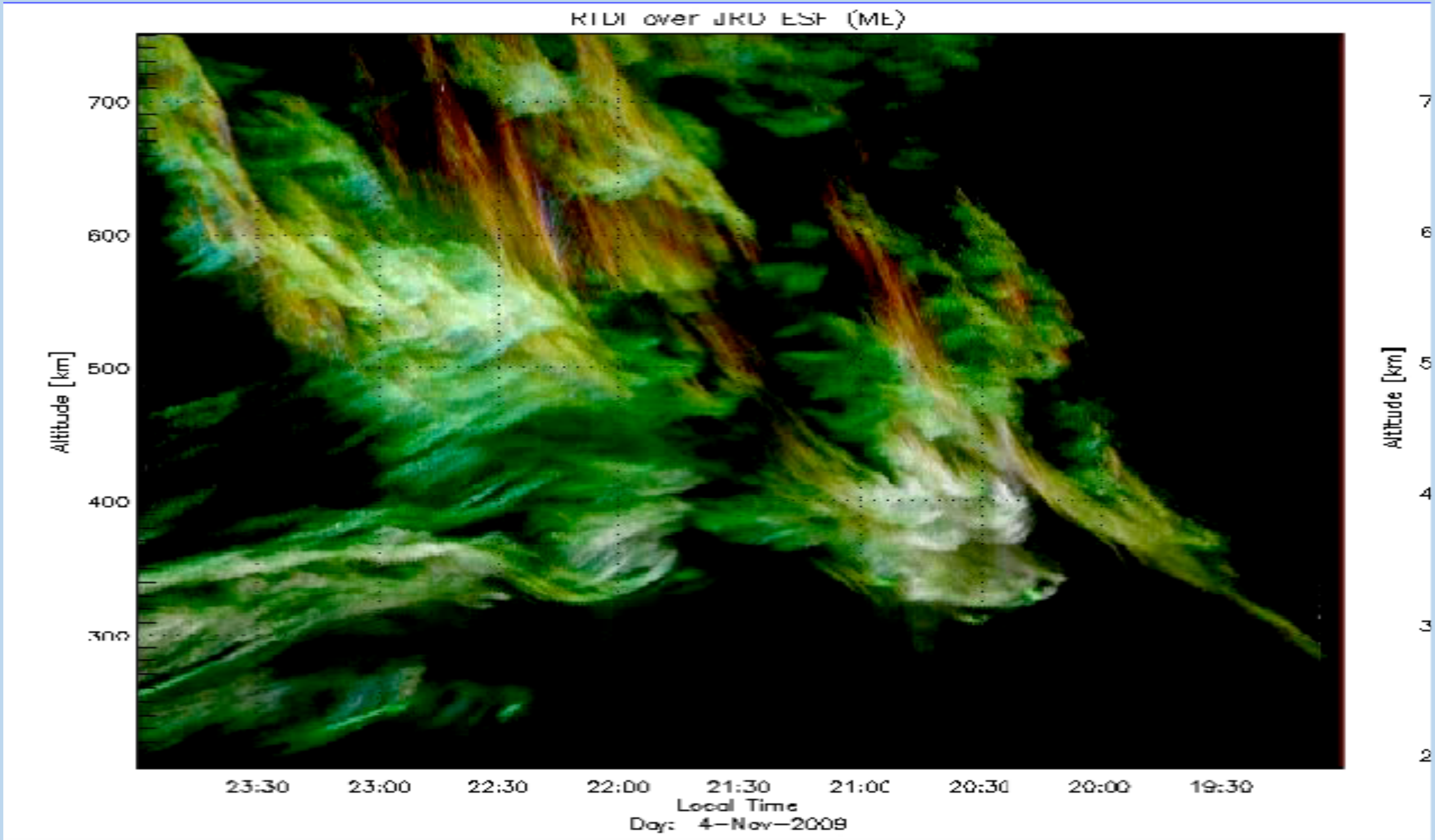
RTDI over JRO ESF (ME)
Altitude [km]
700
600
500
400
300
23:30
23:00
22:30
22:00
21:30
21:00
20:30
20:00
19:30
Local Time
Day: 4-Nov-2009
Altitude [km]

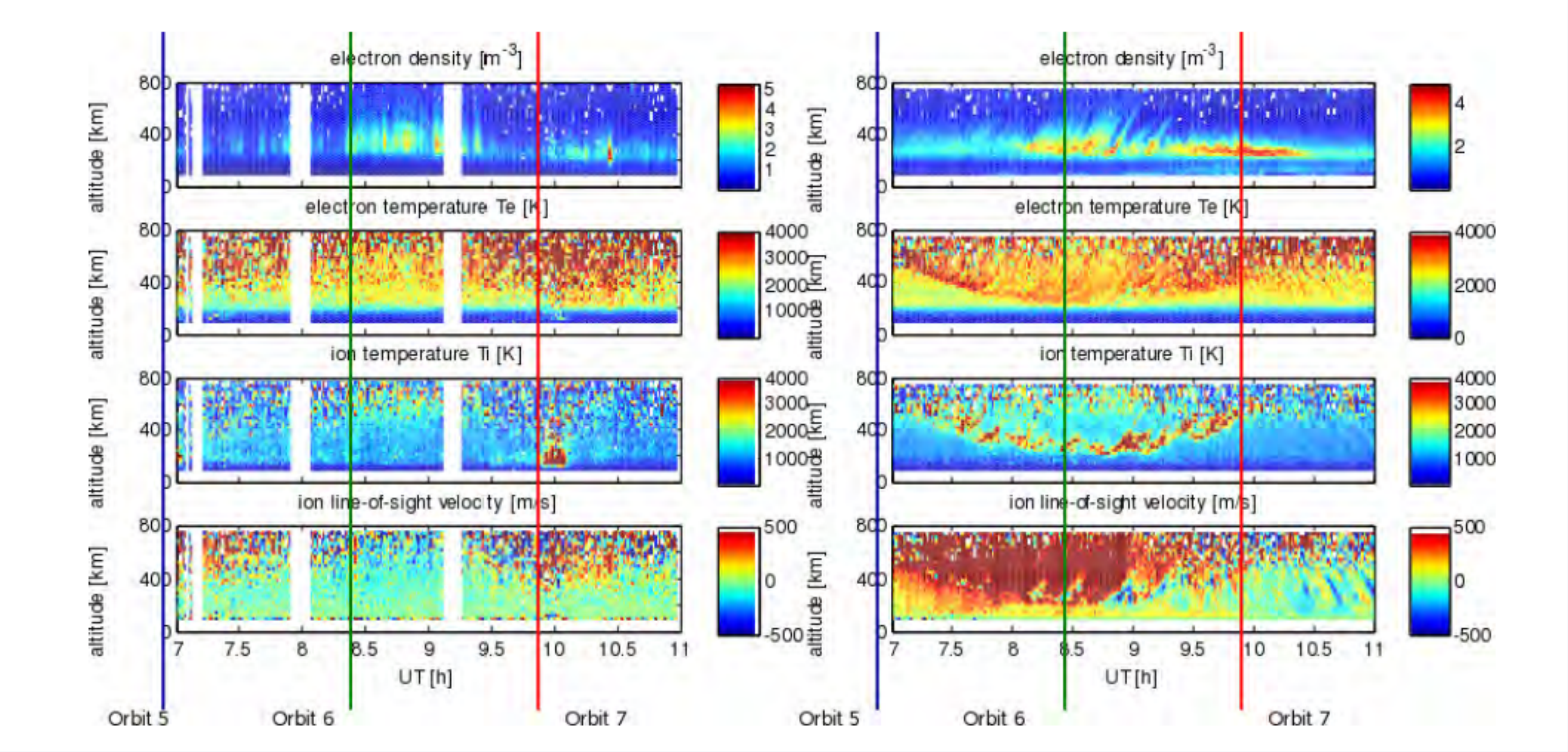

ESR 42m Dish

Tromso VHF radar (low elevation north)

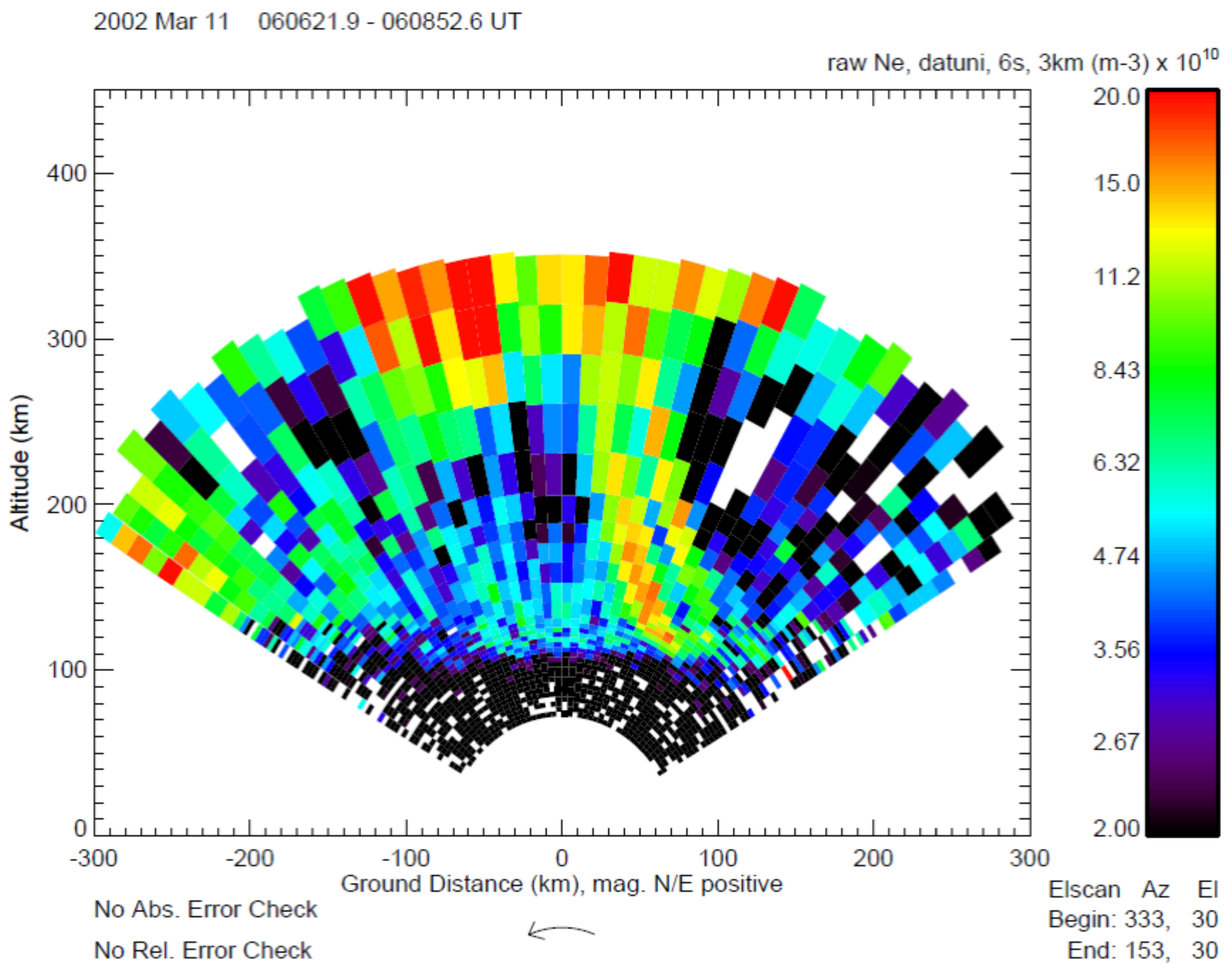
2002 Mar 11 060621.9 - 060852.6 UT
raw Ne, datuni, 6s, 3km (m-3) x 10^10
20.0
15.0
11.2
8.43
6.32
4.74
3.56
2.67
2.00
Altitude (km)
400
300
200
100
0
-300
-200
-100
0
100
200
300
Ground Distance (km), mag. N/E positive
No Abs. Error Check
No Rel. Error Check
Elscan Az El
Begin: 333, 30
End: 153, 30

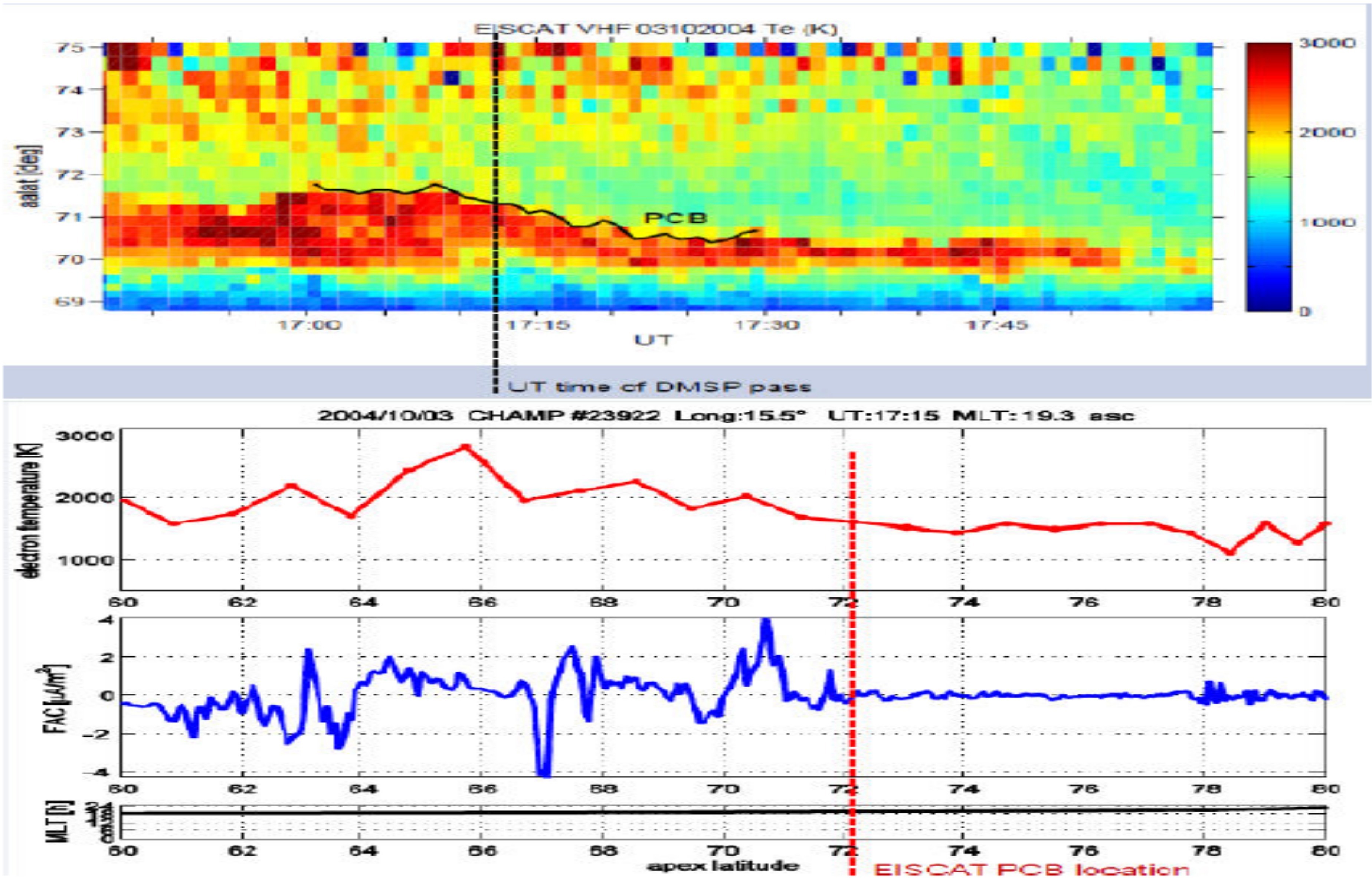
EISCAT VHF 03102004 Te (K)
aalat [deg]
PCB
UT
17:00
17:15
17:30
17:45
UT time of DMSP pass
2004/10/03 CHAMP #23922 Long:15.5° UT:17:15 MLT:19.3 asc
electron temperature [K]
FAC [μA/m²]
MLT [h]
apex latitude
EISCAT PCB location

Large-scale structure
II: Large-scale convection

Scanning modes (e.g. EISCAT and Sondrestrom) enable large-scale monitoring of the plasma convection pattern, especially using tristatic velocity e.g. from EISCAT remote sites.

Tristatic and beam-swinging approaches are both possible

Key issues include response to large and small scale responses to IMF variation, implications for electrodynamics and coupling, relationships to other parameters.

ISRs have been key systems in demonstrating the dynamical coupling of the ionosphere to the magnetosphere and solar wind, especially in FTEs, and determining location and time constants of responses.

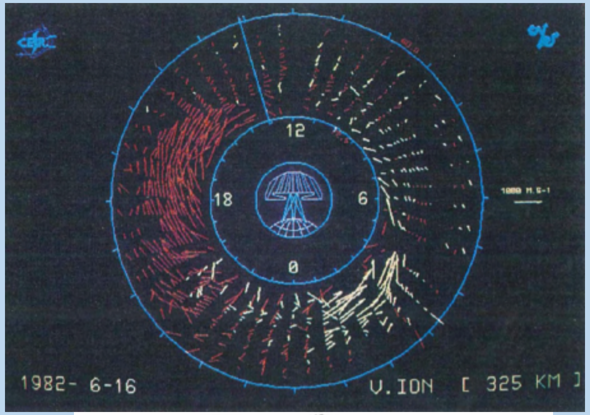

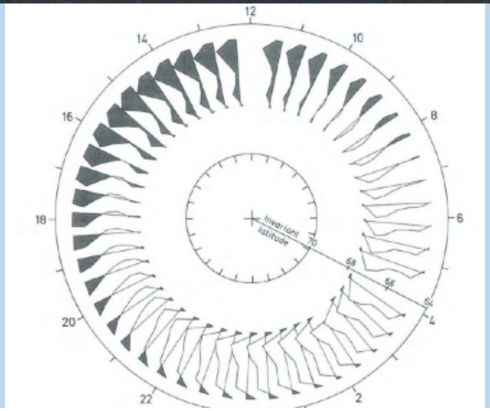

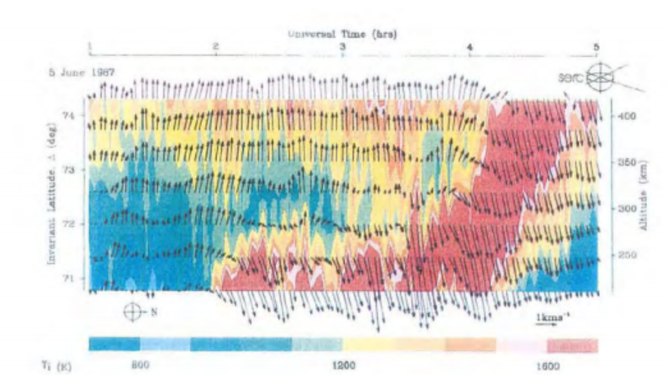

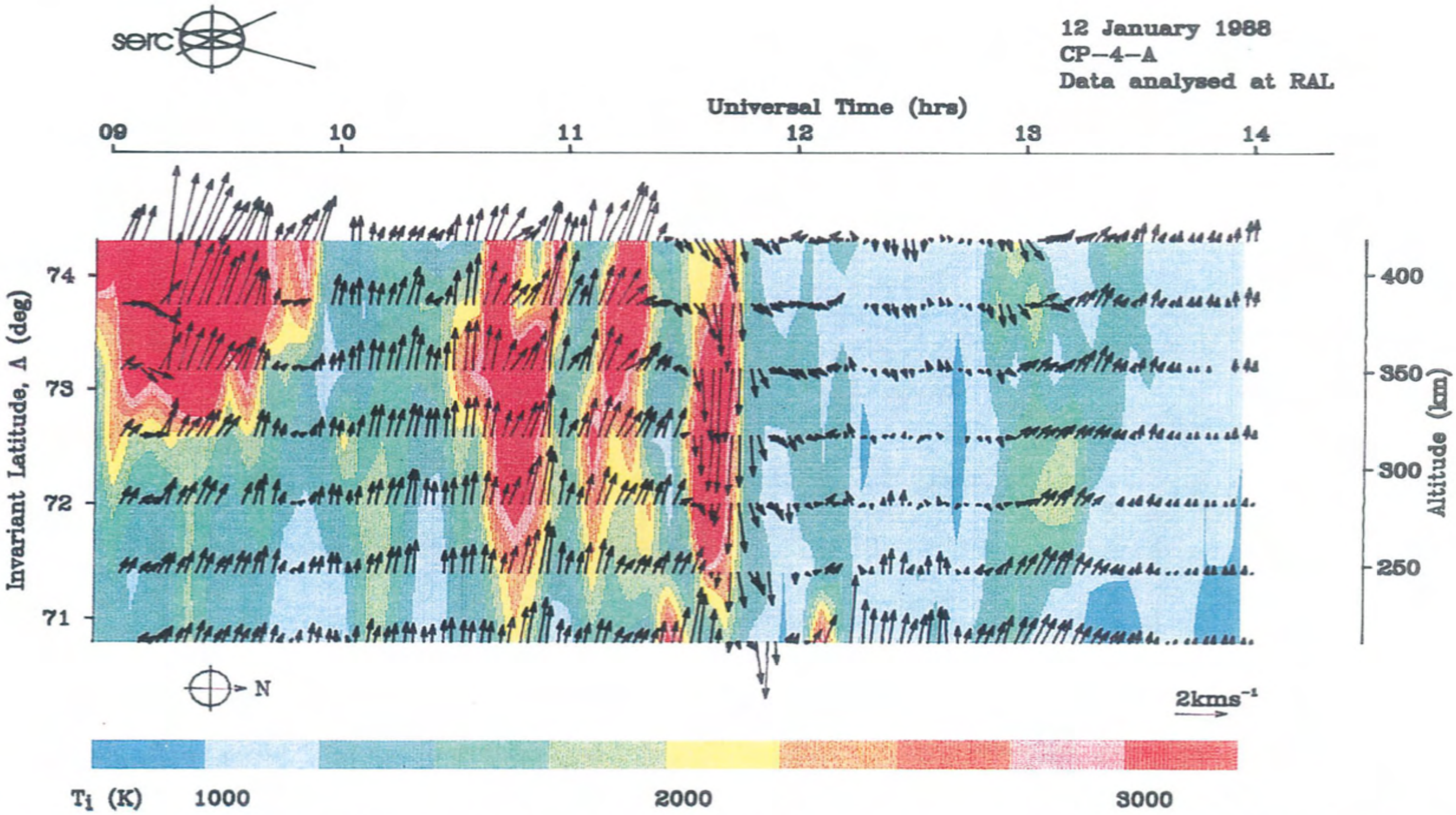

serc
12 January 1988
CP-4-A
Data analysed at RAL
Universal Time (hrs)
09
10
11
12
13
14
Invariant Latitude, Λ (deg)
74
73
72
71
Altitude (km)
400
350
300
250
N
2kms⁻¹
Tᵢ (K)
1000
2000
3000

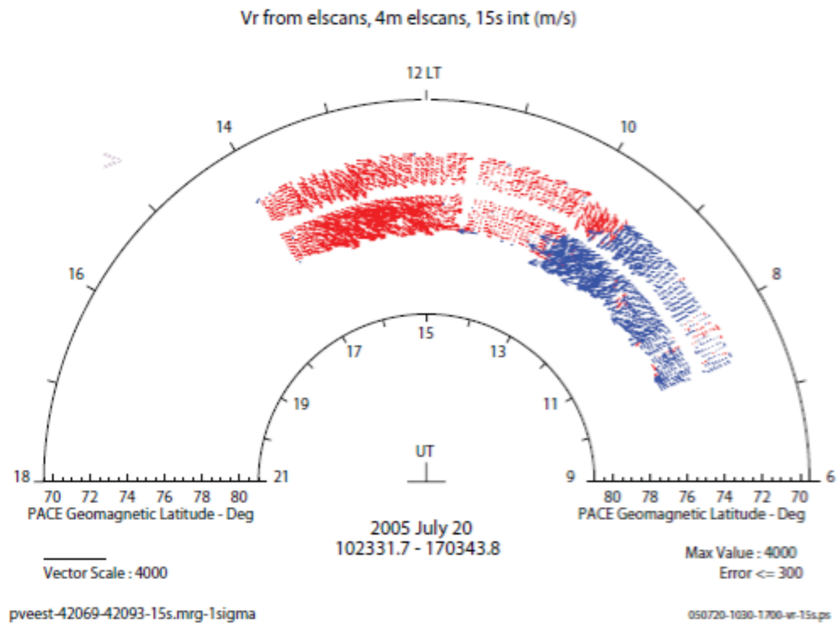
Vr from elscans, 4m elscans, 15s int (m/s)
12 LT
14
10
16
8
15
17
13
19
11
18
21
UT
9
6
70 72 74 76 78 80
PACE Geomagnetic Latitude - Deg
80 78 76 74 72 70
PACE Geomagnetic Latitude - Deg
2005 July 20
102331.7 - 170343.8
Vector Scale : 4000
Max Value : 4000
Error <= 300
pveest-42069-42093-15s.mrg-1sigma
050720-1030-1700-vr-15s.ps

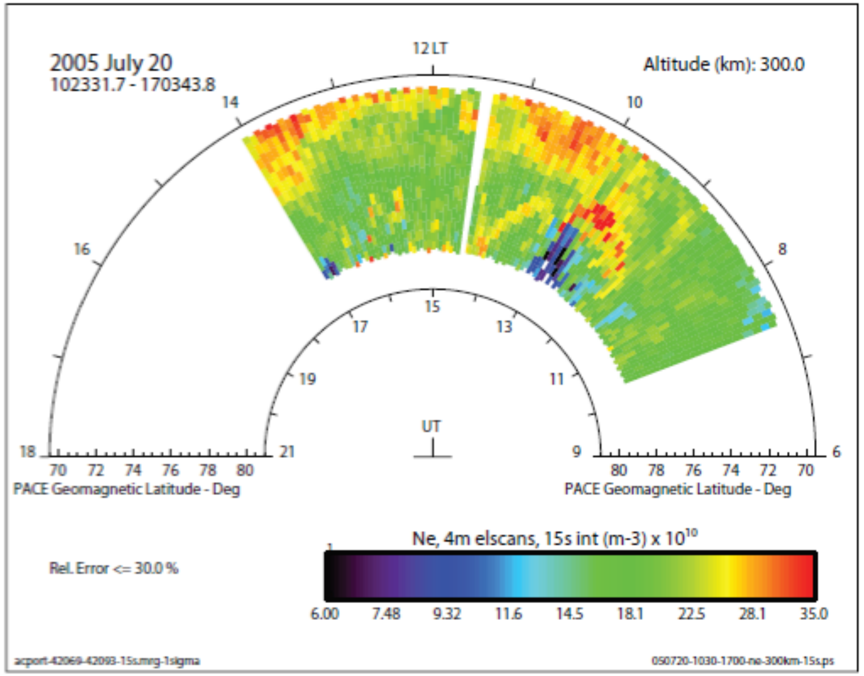
2005 July 20
102331.7 - 170343.8
Altitude (km): 300.0
12 LT
14
10
16
8
15
17
13
19
11
18
21
UT
9
6
70 72 74 76 78 80
PACE Geomagnetic Latitude - Deg
80 78 76 74 72 70
PACE Geomagnetic Latitude - Deg
Ne, 4m elscans, 15s int (m-3) x 10^10
Rel. Error <= 30.0 %
6.00 7.48 9.32 11.6 14.5 18.1 22.5 28.1 35.0
acport-42069-42093-15s.mrg-1sigma
050720-1030-1700-ne-300km-15s.ps

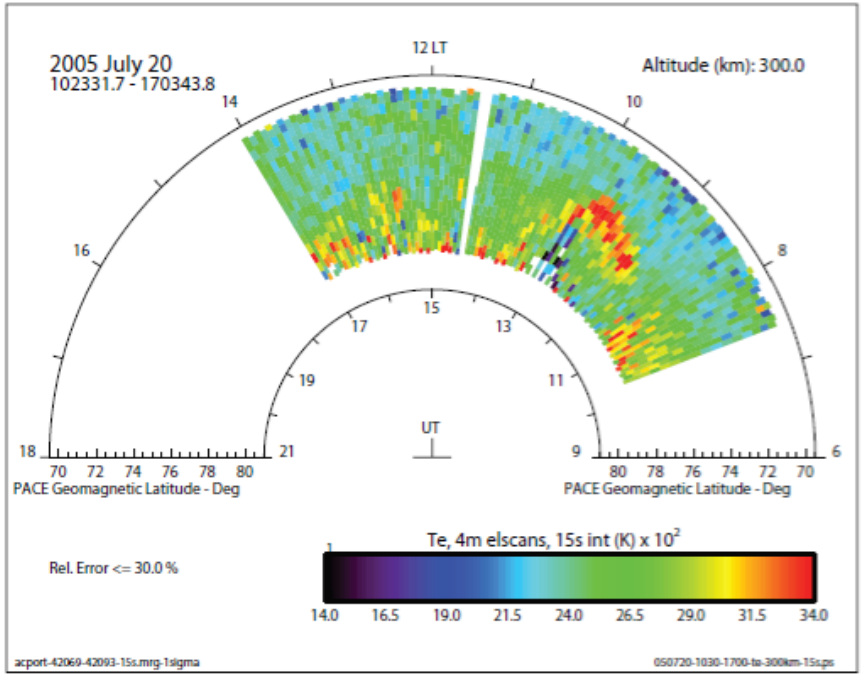
2005 July 20
102331.7 - 170343.8
Altitude (km): 300.0
12 LT
14
10
16
8
15
17
13
19
11
18
21
UT
9
6
70 72 74 76 78 80
PACE Geomagnetic Latitude - Deg
80 78 76 74 72 70
PACE Geomagnetic Latitude - Deg
Te, 4m elscans, 15s int (K) x 10^2
Rel. Error <= 30.0 %
14.0 16.5 19.0 21.5 24.0 26.5 29.0 31.5 34.0
acport-42069-42093-15s.mrg-1sigma
050720-1030-1700-te-300km-15s.ps

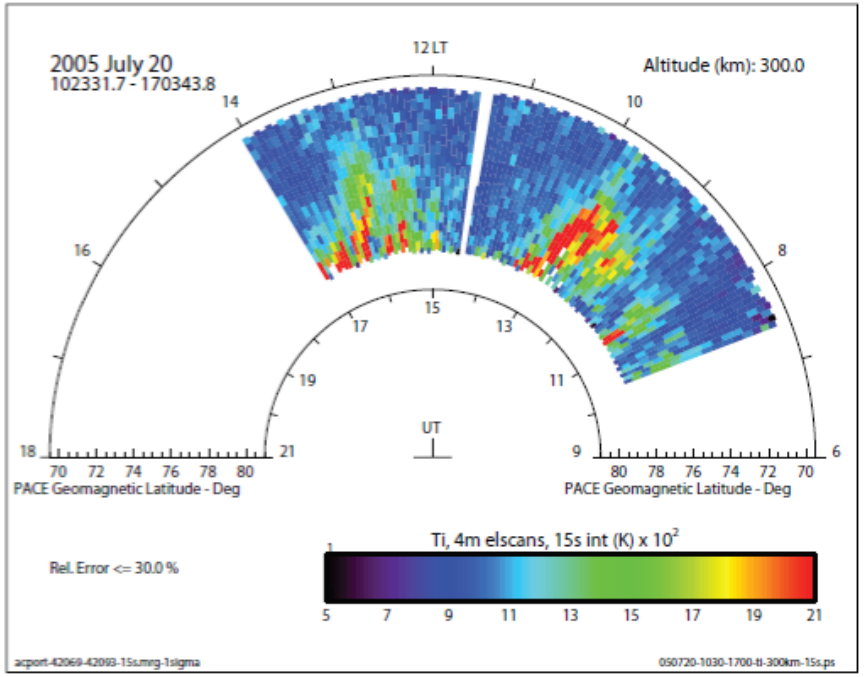
2005 July 20
102331.7 - 170343.8
Altitude (km): 300.0
12 LT
14
10
16
8
15
17
13
19
11
18
21
UT
9
6
70 72 74 76 78 80
PACE Geomagnetic Latitude - Deg
80 78 76 74 72 70
PACE Geomagnetic Latitude - Deg
Ti, 4m elscans, 15s int (K) x 10^2
Rel. Error <= 30.0 %
5 7 9 11 13 15 17 19 21
acport-42069-42093-15s.mrg-1sigma
050720-1030-1700-ti-300km-15s.ps

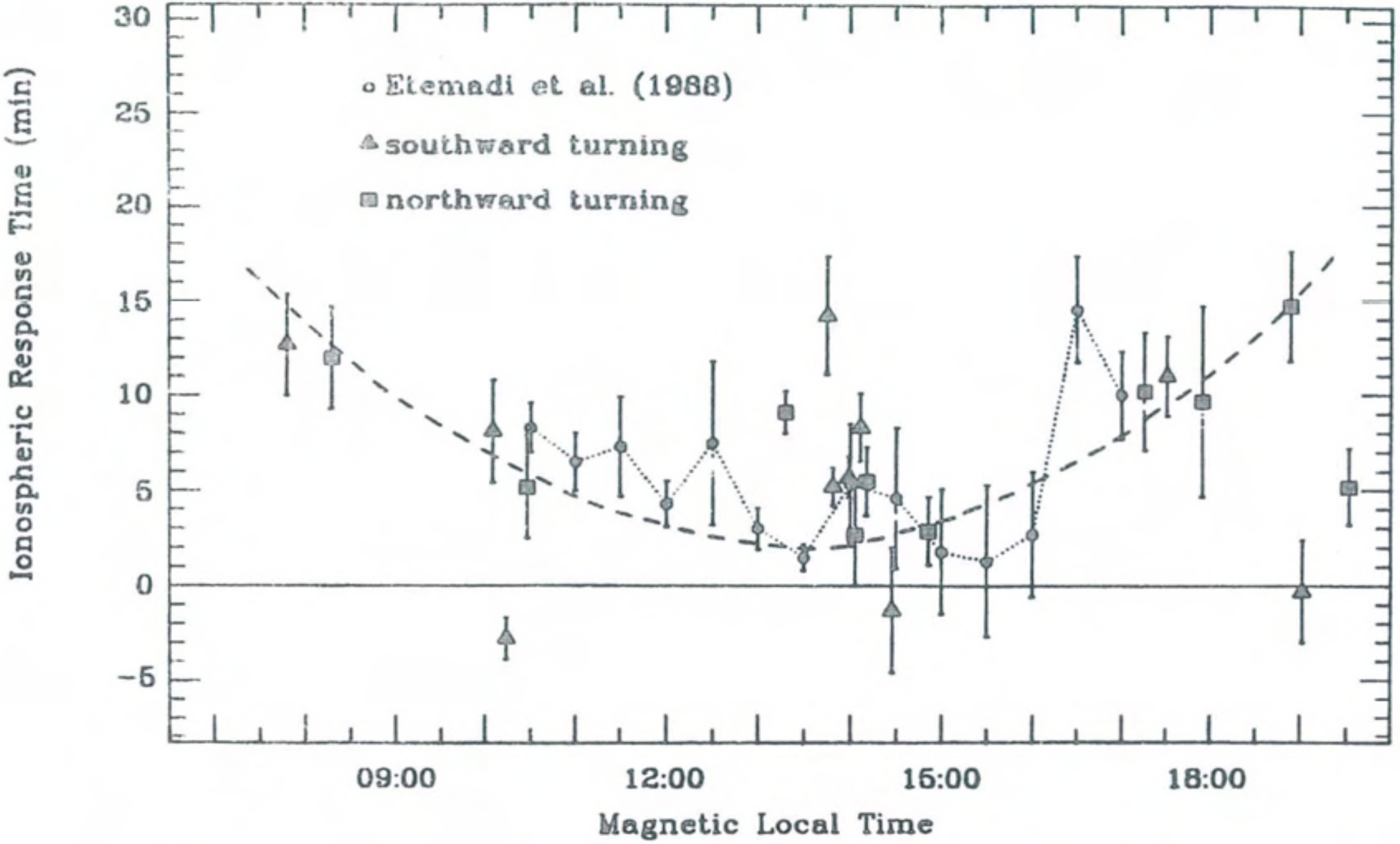

30
25
20
15
10
5
0
−5
Ionospheric Response Time (min)
Etemadi et al. (1988)
southward turning
northward turning
09:00
12:00
15:00
18:00
Magnetic Local Time

Large-scale structure III: Flow channels

These are examples of smaller-scale responses to specific events, such as FTEs, most often seen on the dayside

Transient flow channels seem to be a regular feature of the dayside cusp

Illustrates response of flux tubes to solar wind-magnetosphere coupling processes, occur over a range of By and Bz conditions

Convecting flux tubes can display dispersed precipitation into ionosphere

High-speed flow drives ion frictional heating, changes chemistry, density structure

Shows how IMF and MI coupling can

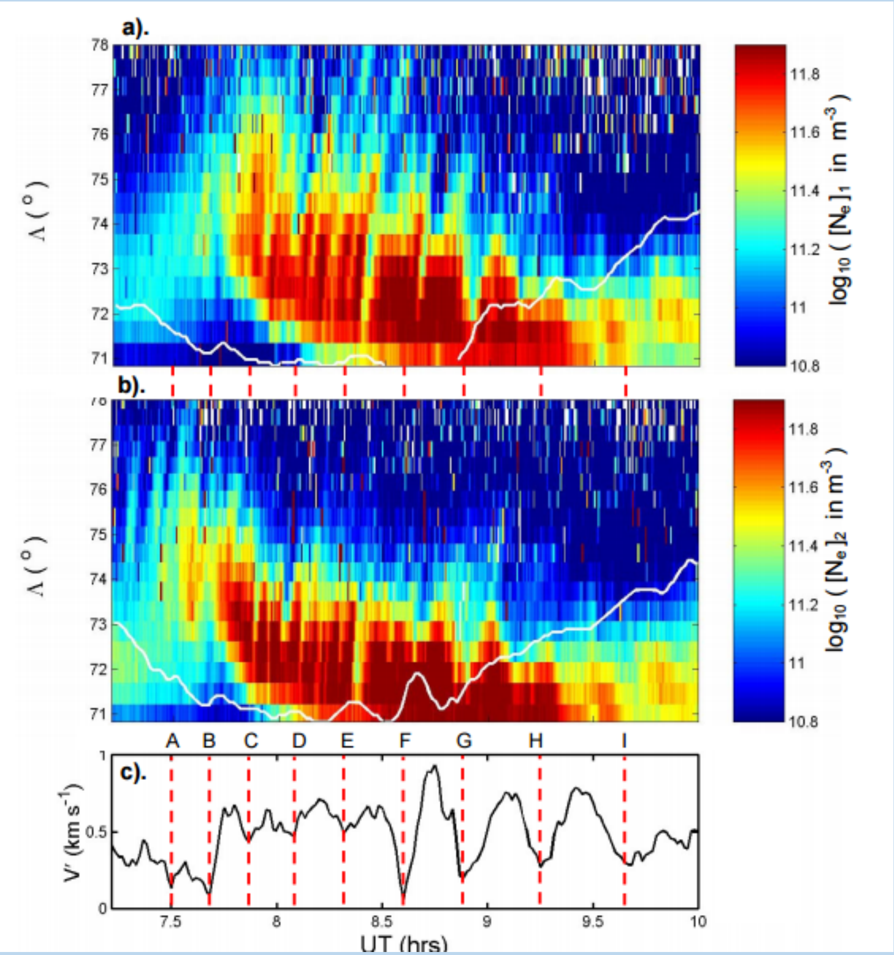

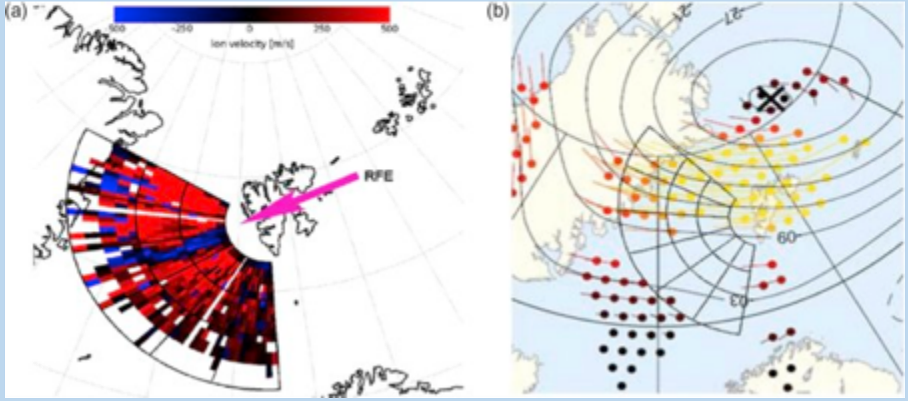

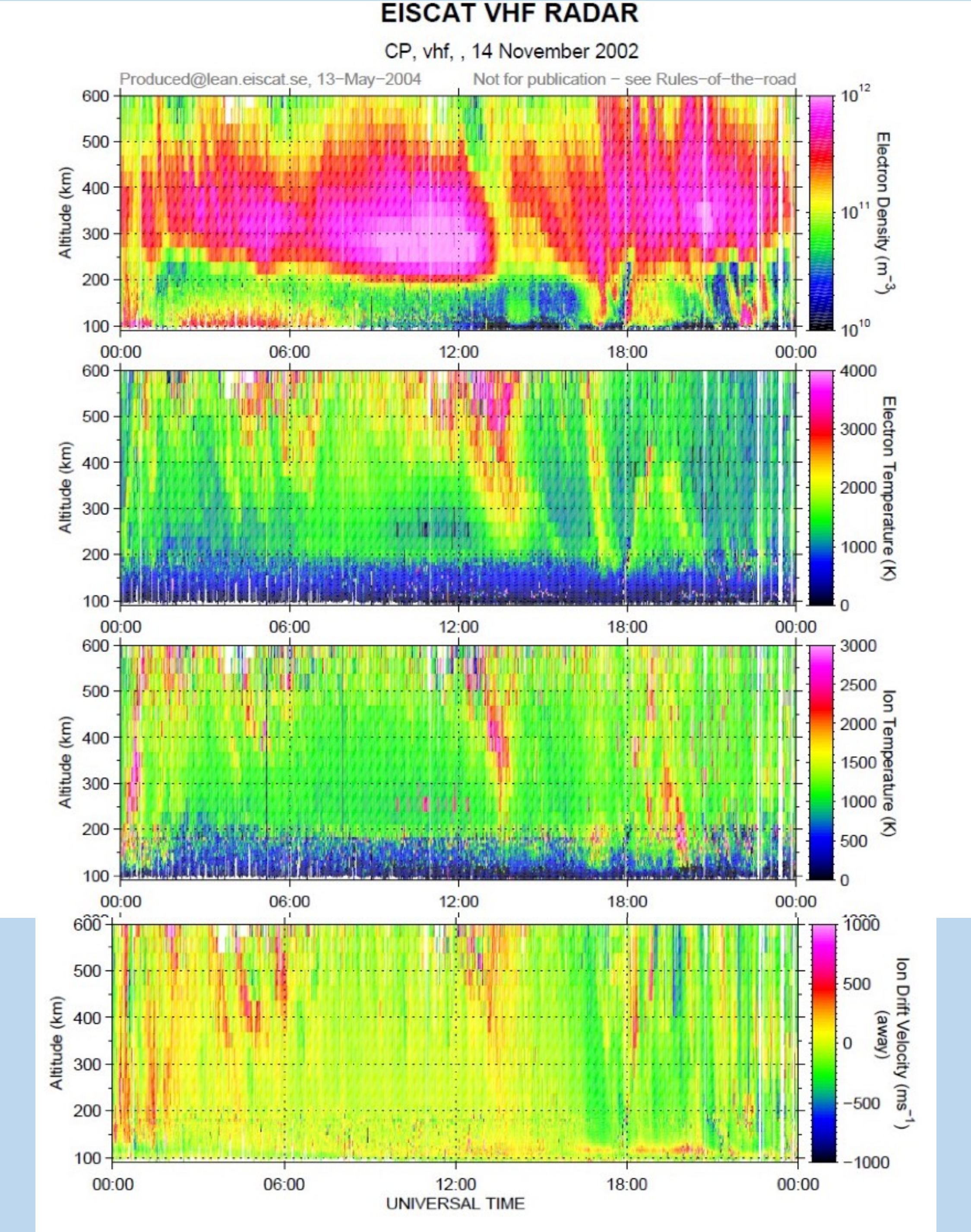
EISCAT VHF RADAR
CP, vhf, , 14 November 2002
Produced@lean.eiscat.se, 13-May-2004
Not for publication – see Rules-of-the-road
Altitude (km)
Electron Density (m^-3)
Electron Temperature (K)
Ion Temperature (K)
Ion Drift Velocity (ms^-1) (away)
00:00
06:00
12:00
18:00
00:00
UNIVERSAL TIME

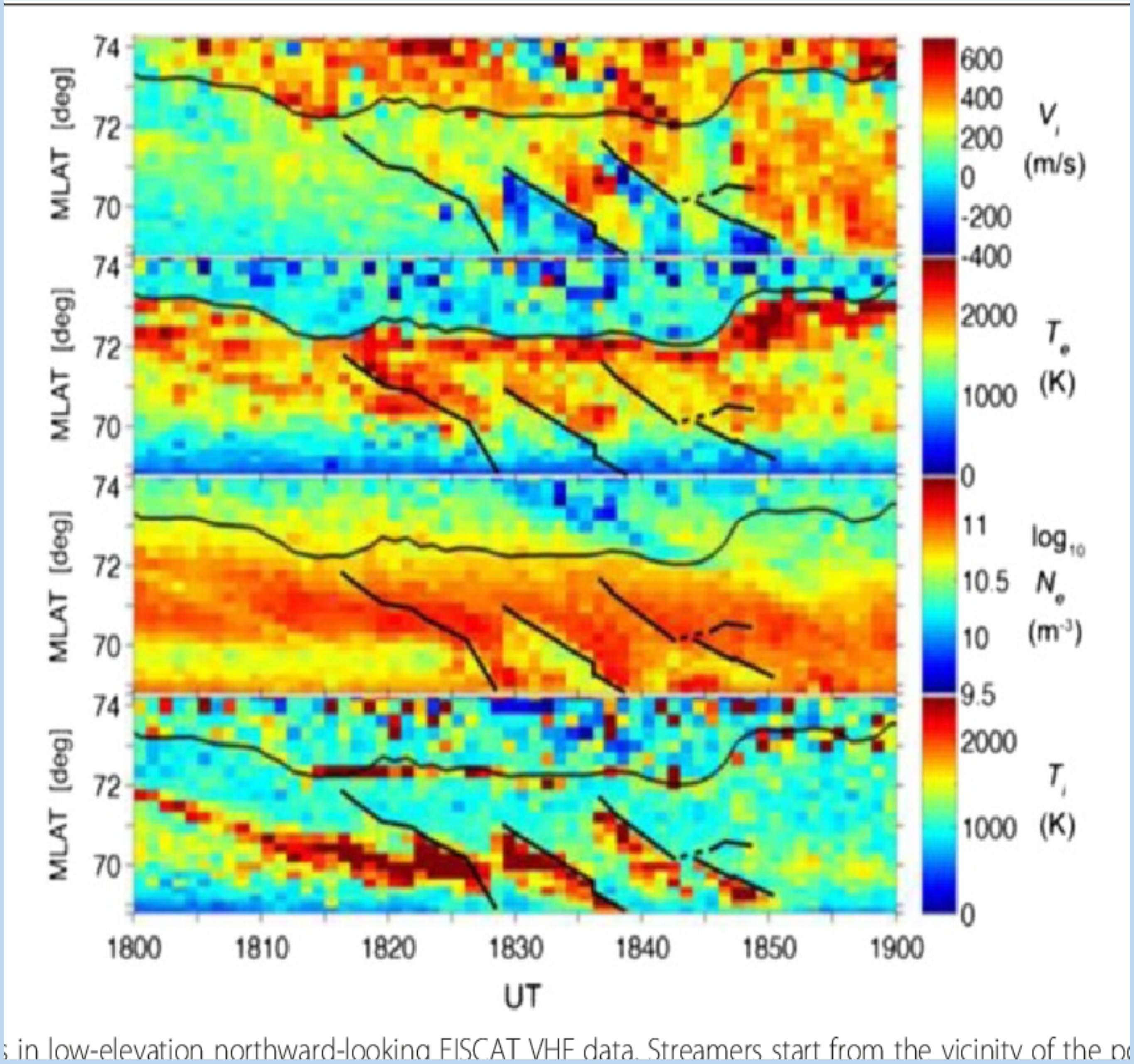
MLAT [deg]
V_i (m/s)
T_e (K)
log10 N_e (m^-3)
T_i (K)
1800
1810
1820
1830
1840
1850
1900
UT
; in low-elevation northward-looking EISCAT VHF data. Streamers start from the vicinity of the po

Large-scale structure IV: Blobs and patches

The product of the processes we just discussed: small-scale structuring and large-scale convection.

Local production but global-scale propagation

Lots of small-scale structure embedded in large-scale structure, implications for radio communications, positioning, timing etc.

Patches (polar cap) and blobs (lower latitudes) can have a variety of formation mechanisms (direct deposition, segmentation, convection effects), scale sizes, positions and time histories as conditions change.

Full time history not observable from a single ISR, need other data to put ISR data in context.

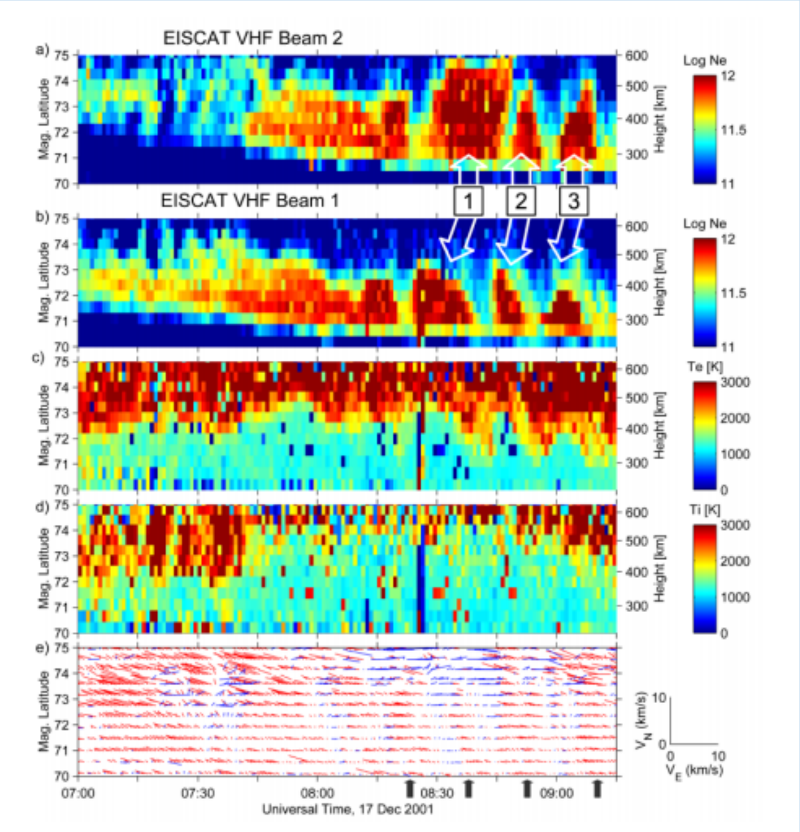

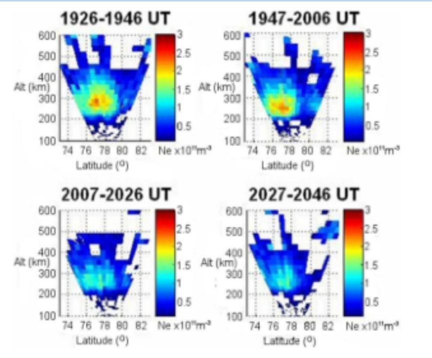

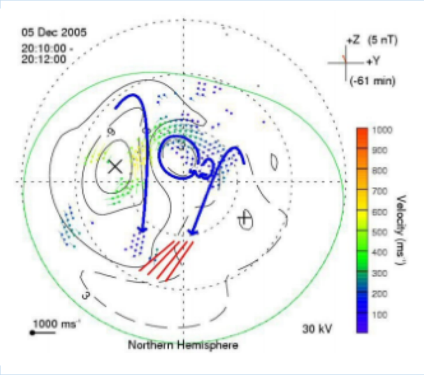

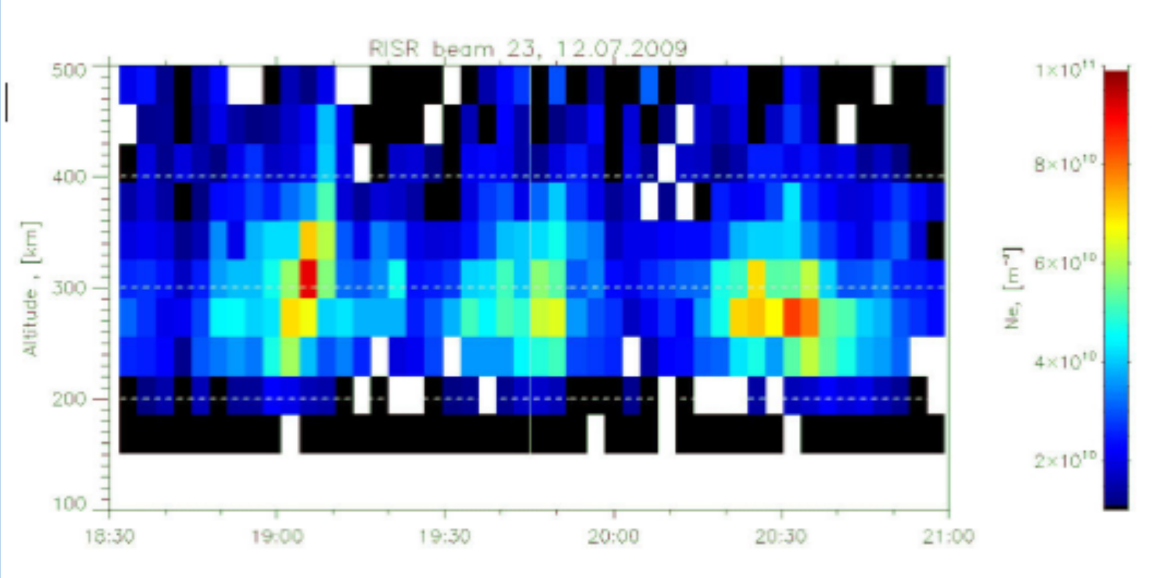
RISR beam 23, 12.07.2009
Altitude , [km]
500
400
300
200
100
18:30
19:00
19:30
20:00
20:30
21:00
Ne, [m⁻³]
1×10¹¹
8×10¹⁰
6×10¹⁰
4×10¹⁰
2×10¹⁰

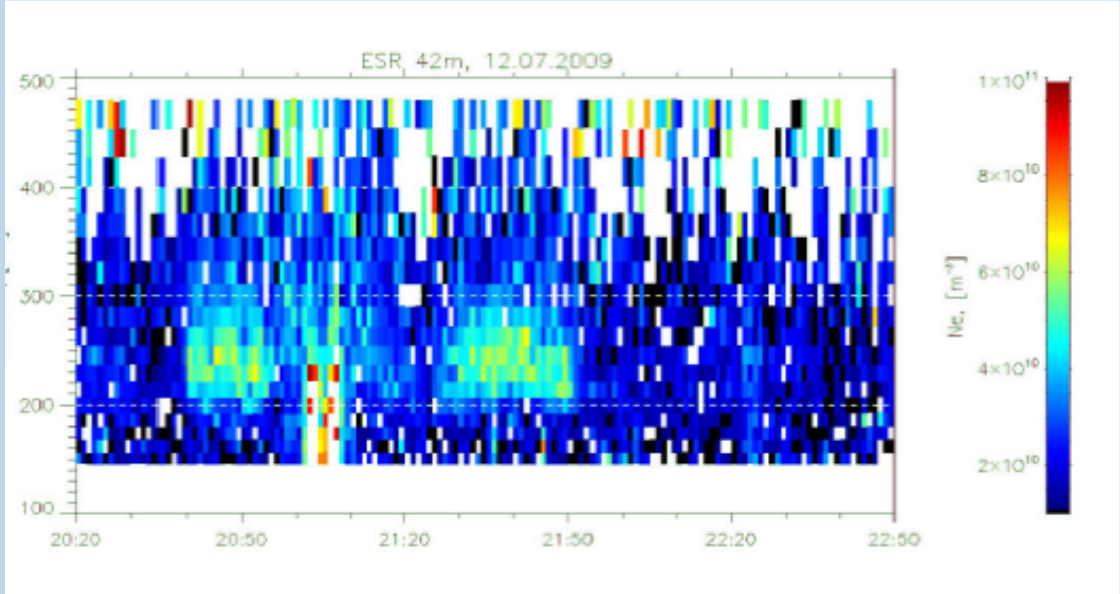
ESR 42m, 12.07.2009
500
400
300
200
100
20:20
20:50
21:20
21:50
22:20
22:50
Ne, [m⁻³]
1×10¹¹
8×10¹⁰
6×10¹⁰
4×10¹⁰
2×10¹⁰

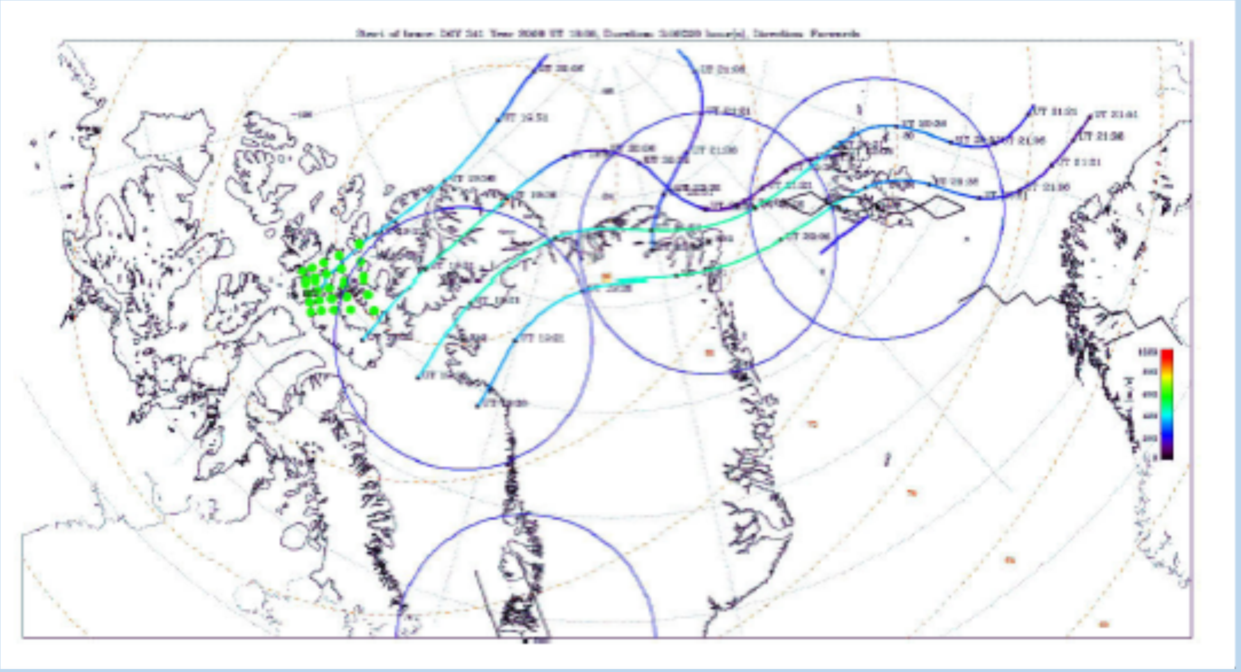

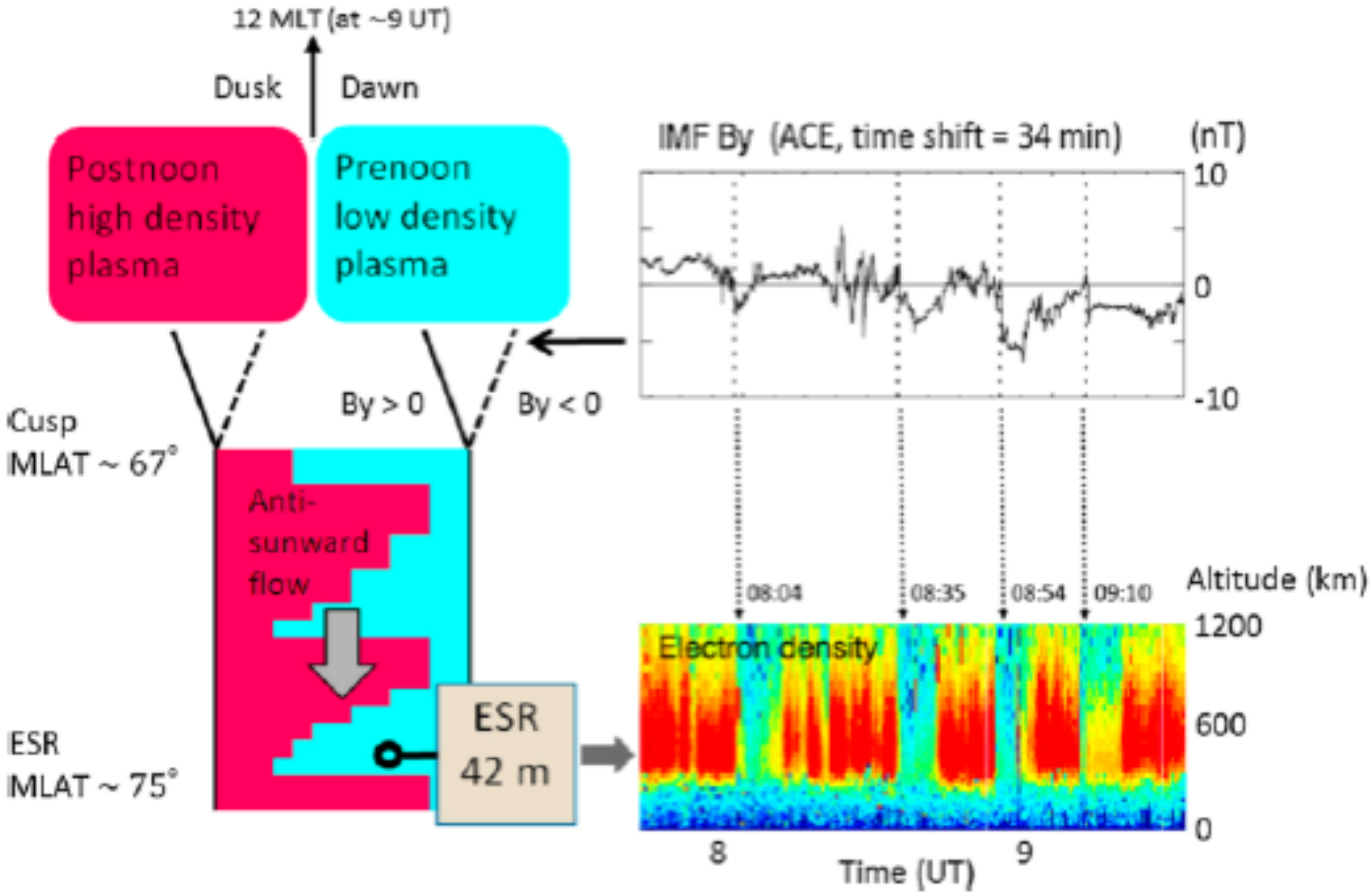

12 MLT (at ~9 UT)
Dusk
Dawn
Postnoon high density plasma
Prenoon low density plasma
IMF By (ACE, time shift = 34 min)
(nT)
10
0
-10
By > 0
By < 0
Cusp MLAT ~ 67°
Anti-sunward flow
ESR MLAT ~ 75°
ESR 42 m
08:04
08:35
08:54
09:10
Altitude (km)
1200
600
0
Electron density
8
9
Time (UT)

Large-scale structure V: Troughs and holes

The flip side of high density structures

Some regions of the ionosphere, e.g . equatorward of auroral zone, connect to regions of magnetosphere which are not a good plasma source.

These regions can be subjected to mechanisms that deplete the plasma e.g. enhanced plasma velocity, ion temperature, reaction rate.

Troughs and holes can form anywhere that depletion happens faster than production.

For that to happen, production can decrease, or recombination/transport can increase.

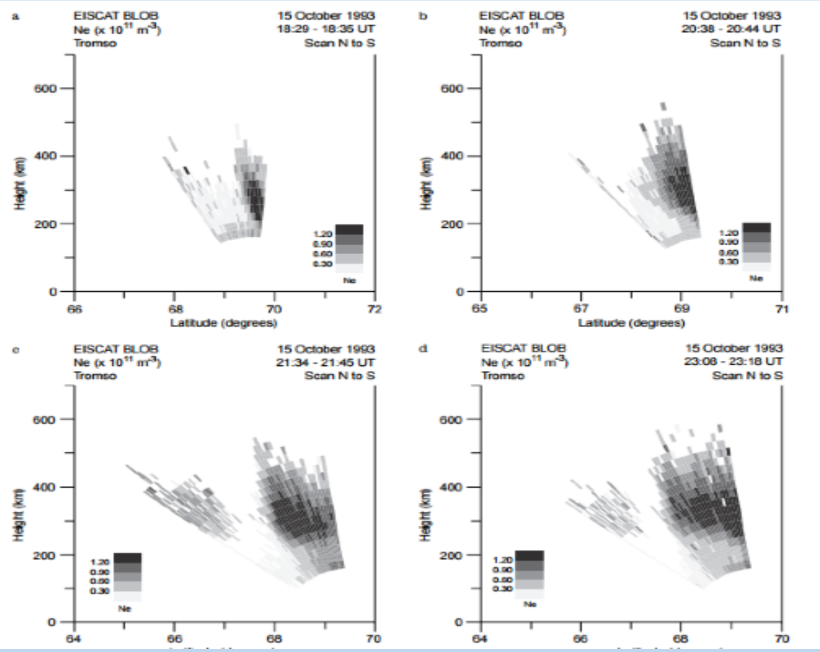

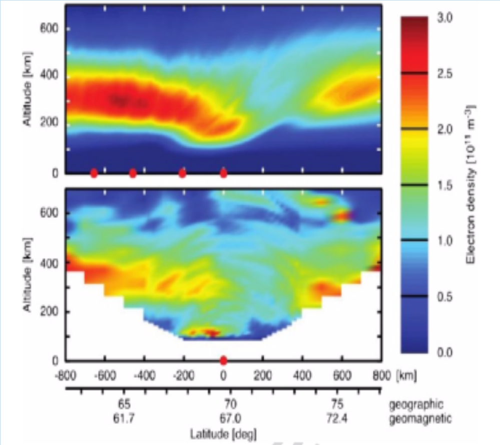

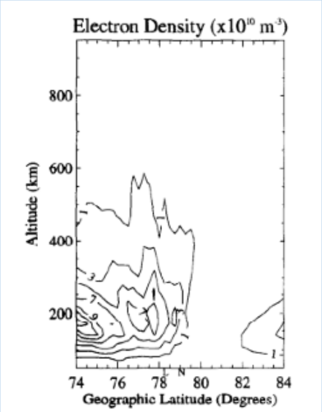

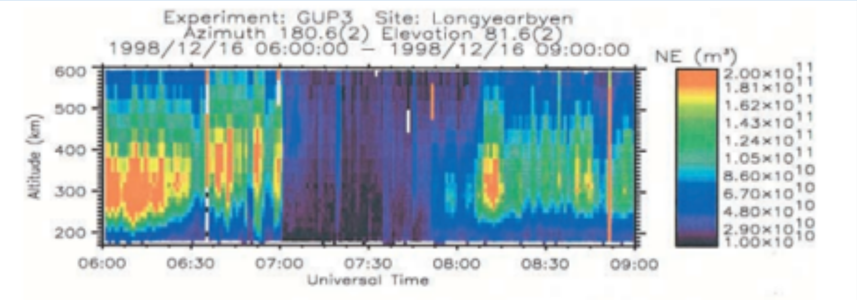

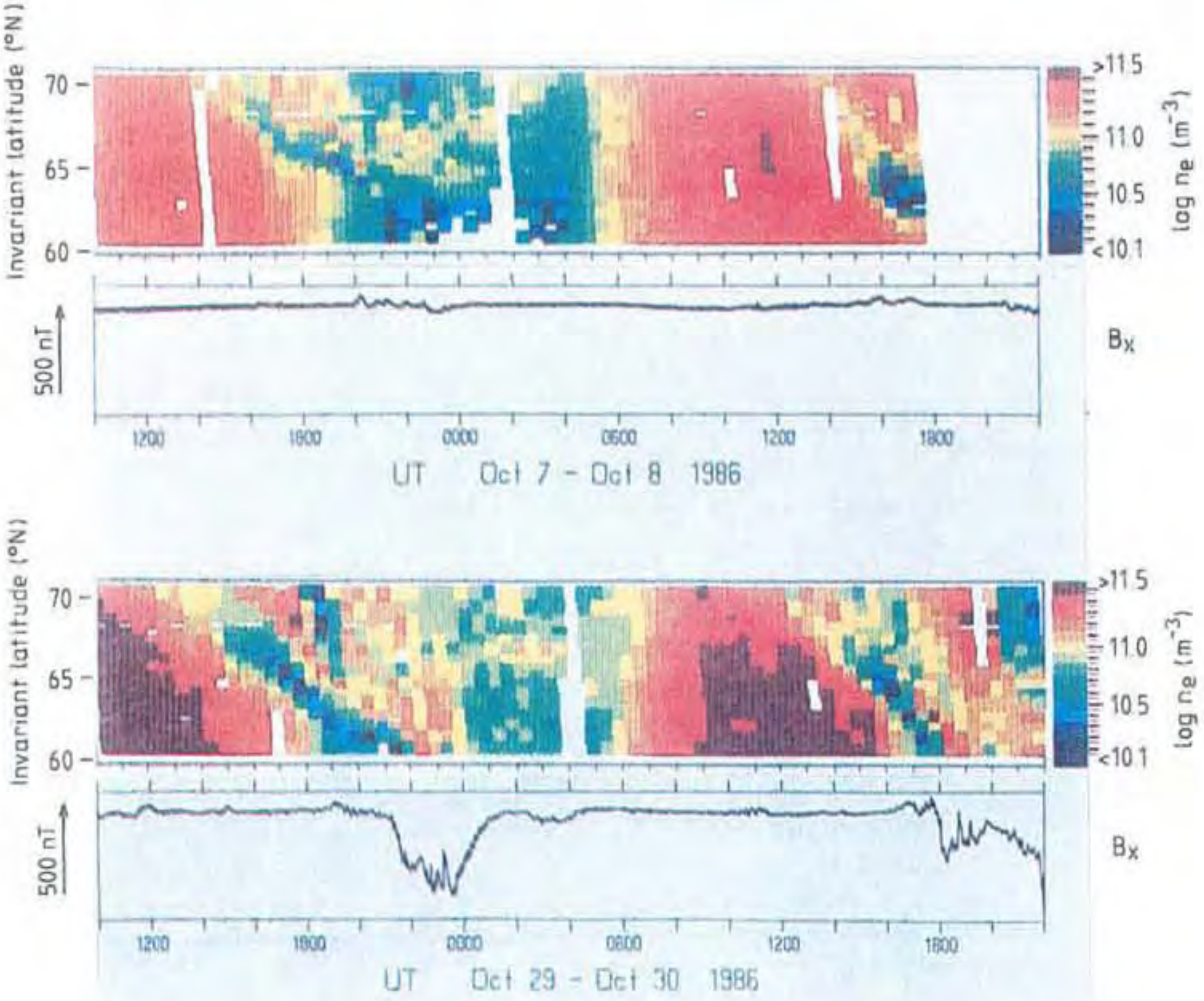
Invariant latitude (°N)
70
65
60
>11.5
11.0
10.5
<10.1
log ne (m-3)
Bx
500 nT
1200
1800
0000
0600
1200
1800
UT Oct 7 - Oct 8 1986
Invariant latitude (°N)
70
65
60
>11.5
11.0
10.5
<10.1
log ne (m-3)
Bx
500 nT
1200
1800
0000
0600
1200
1800
UT Oct 29 - Oct 30 1986

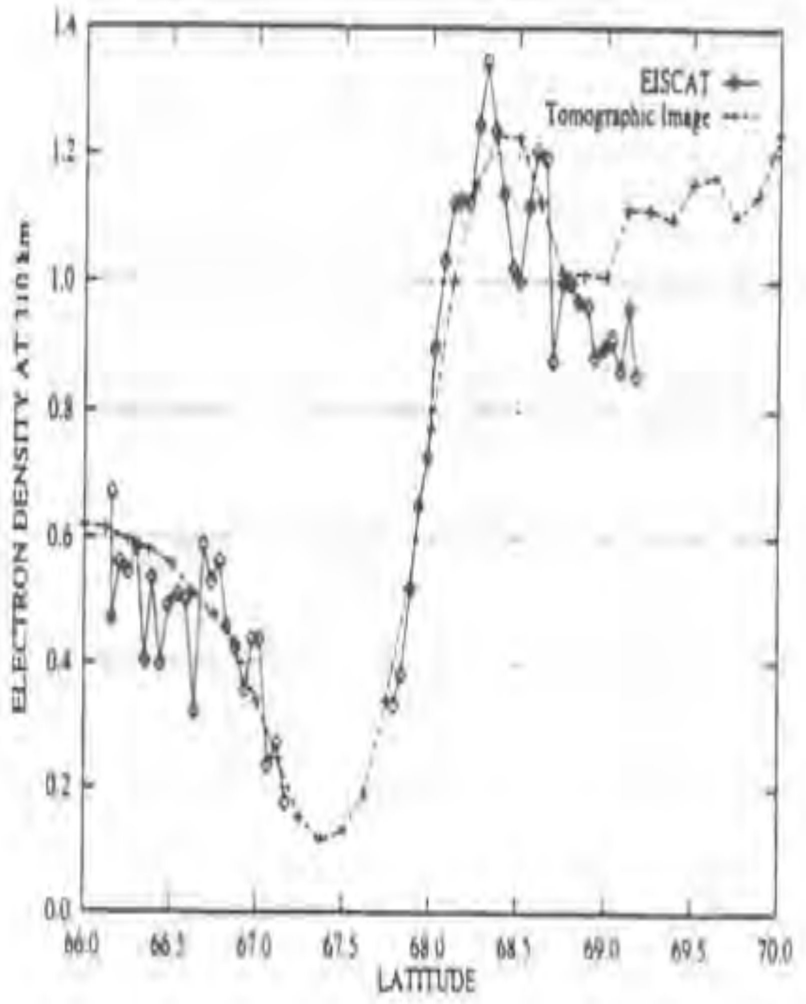
EISCAT
Tomographic Image
ELECTRON DENSITY
1.4
1.2
1.0
0.8
0.6
0.4
0.2
0.0
66.0
67.0
67.5
68.0
68.5
69.0
69.5
70.0
LATITUDE

Meso-scale structure
I: Gradients, TEC and scintillation

ISRs frequently see highly structured density and strong gradients

Structure is interesting in itself, but also has practical implications because these irregularities cause phase and amplitude fluctuations (scintillation) in radio signals

Phase and amplitude scintillation do not necessarily occur together (different irreg scales)

Example by Chartier et al (2016) shows (predominantly) phase scintillation during density enhancements at Tromso

These enhancements are predominantly in the E-region density

Magnitude of phase scintillation is not proportional to the background density

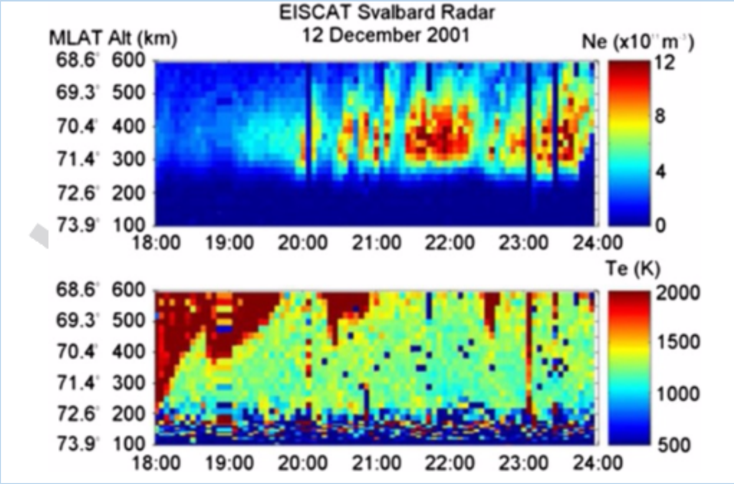

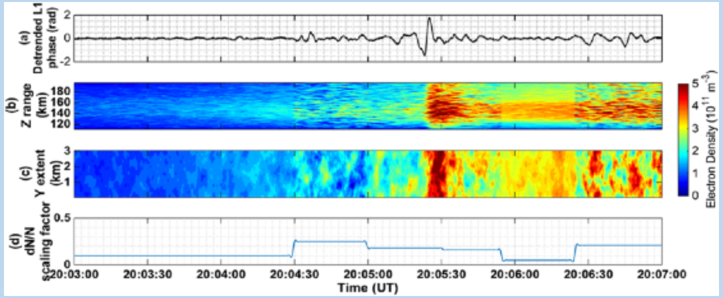

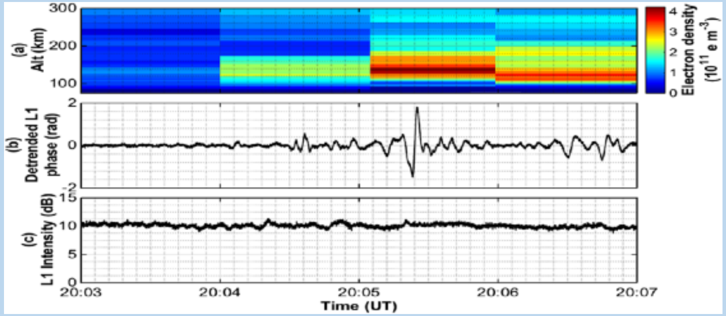

Meso-scale structure
II: Auroral arcs and electrodynamics

ISRs can make unique observations of aurora, in a way not possible for rockets and satellites

In particular, high time resolution velocities helped us understand small-scale arc electrodynamics

ISRs needs complementary data e.g. from auroral imagers to do this kind of science

What seems to be continuous density structure in radar data is revealed to be made of made of multiple arc elements

Optical measurements make clear that the largest fields are adjacent to the arcs

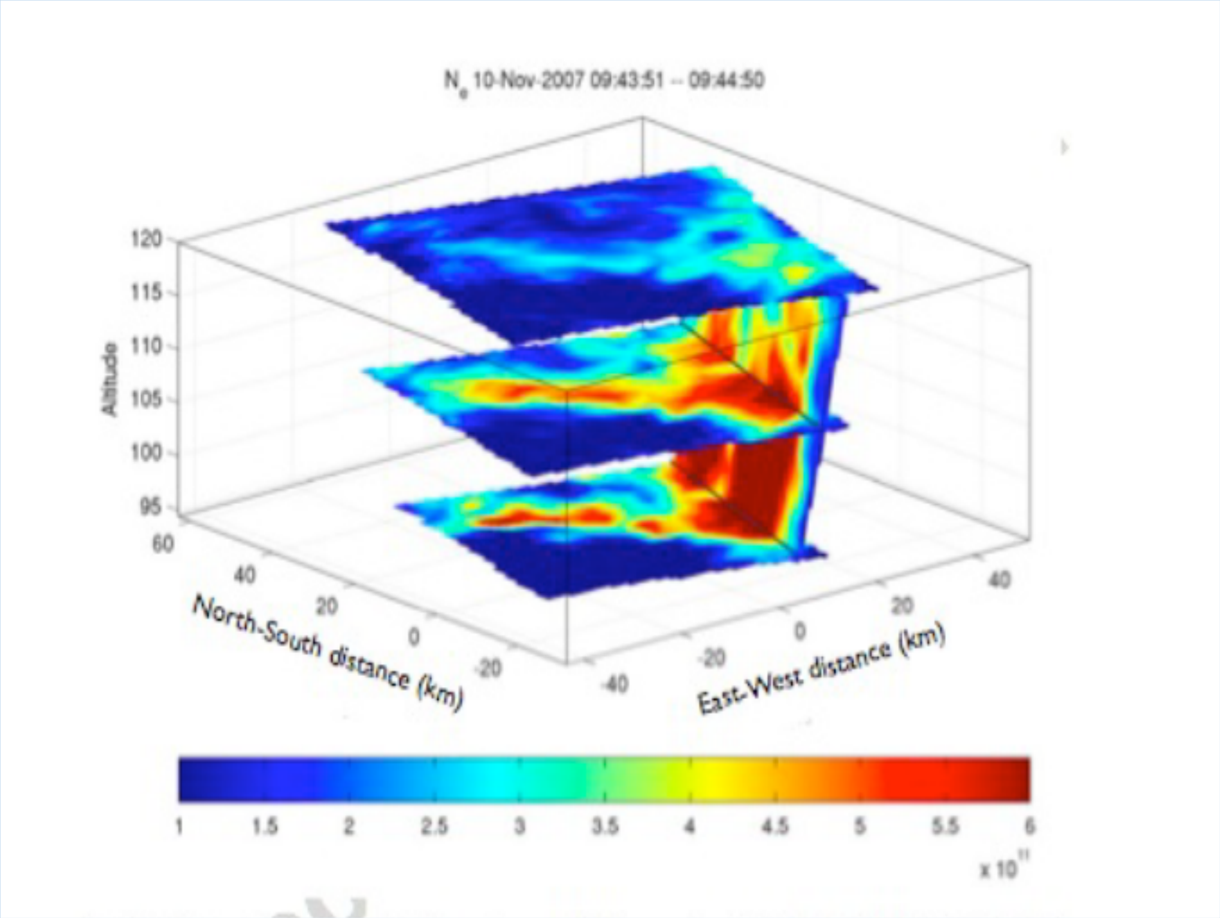

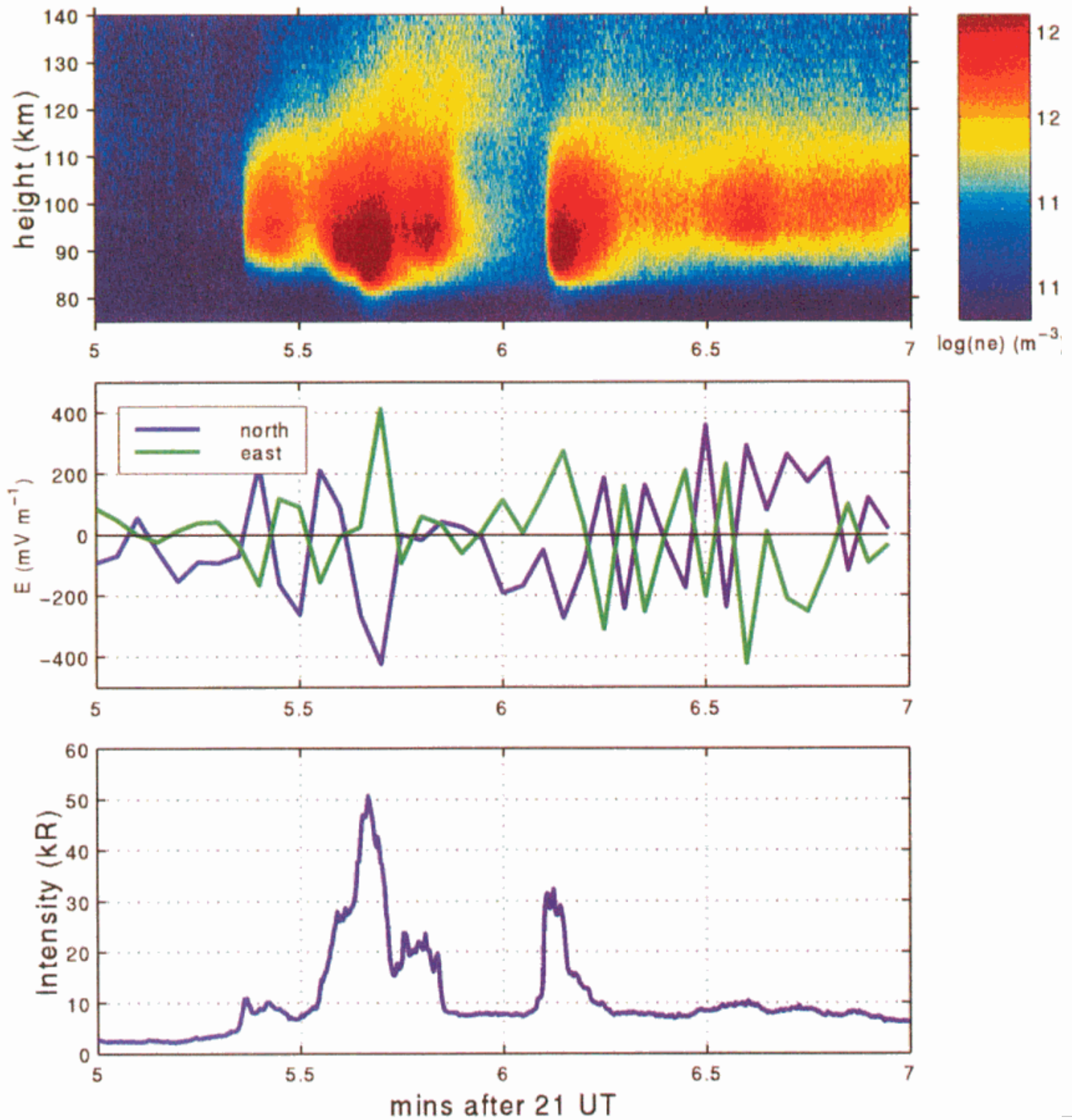
height (km)
log(ne) (m⁻³)
north
east
E (mV m⁻¹)
Intensity (kR)
mins after 21 UT

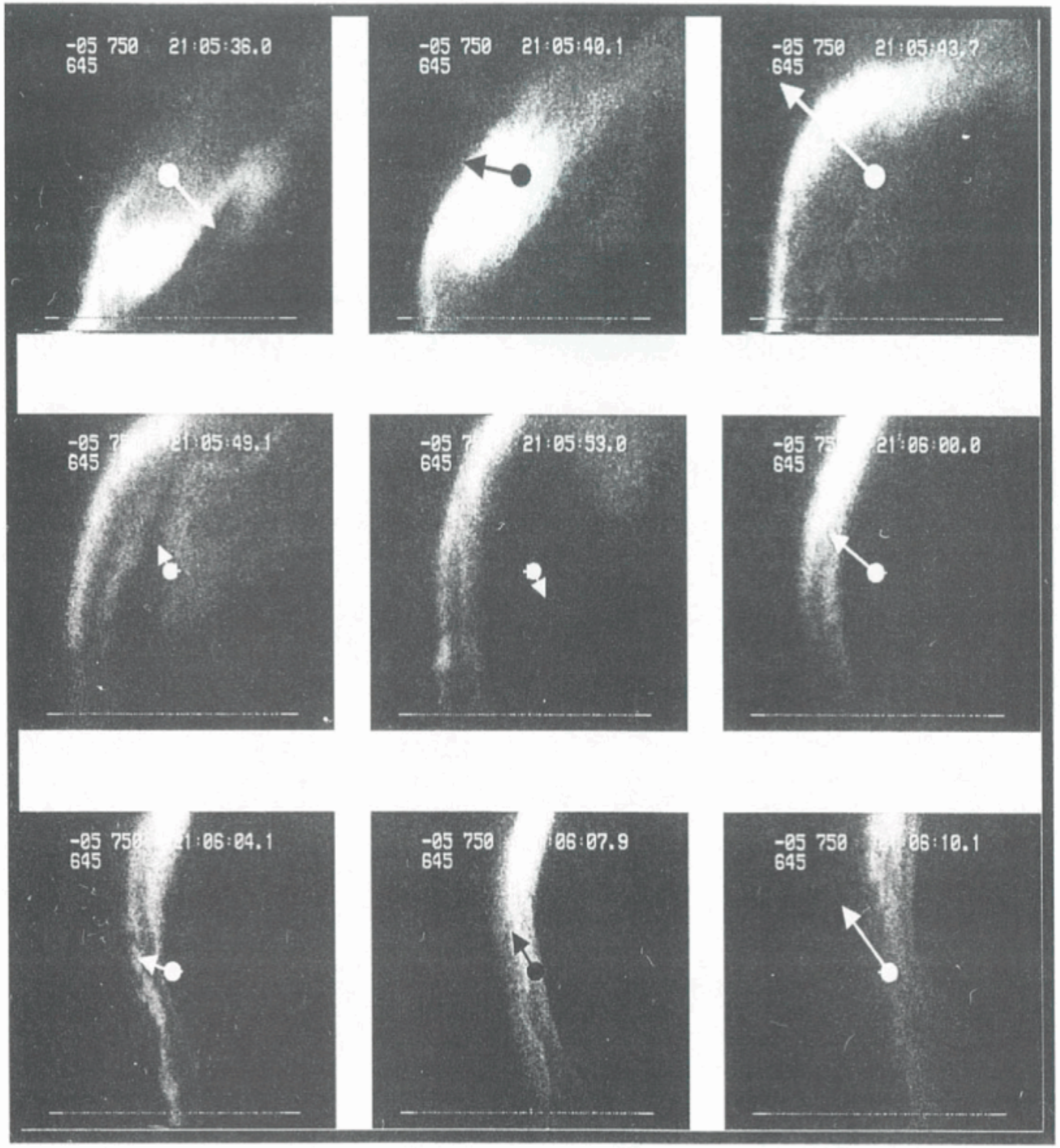
-05 750 21:05:36.0
645
-05 750 21:05:40.1
645
-05 750 21:05:43.7
645
21:05:49.1
645
21:05:53.0
645
21:06:00.0
645
21:06:04.1
645
-05 750 06:07.9
645
-05 750 06:10.1
645

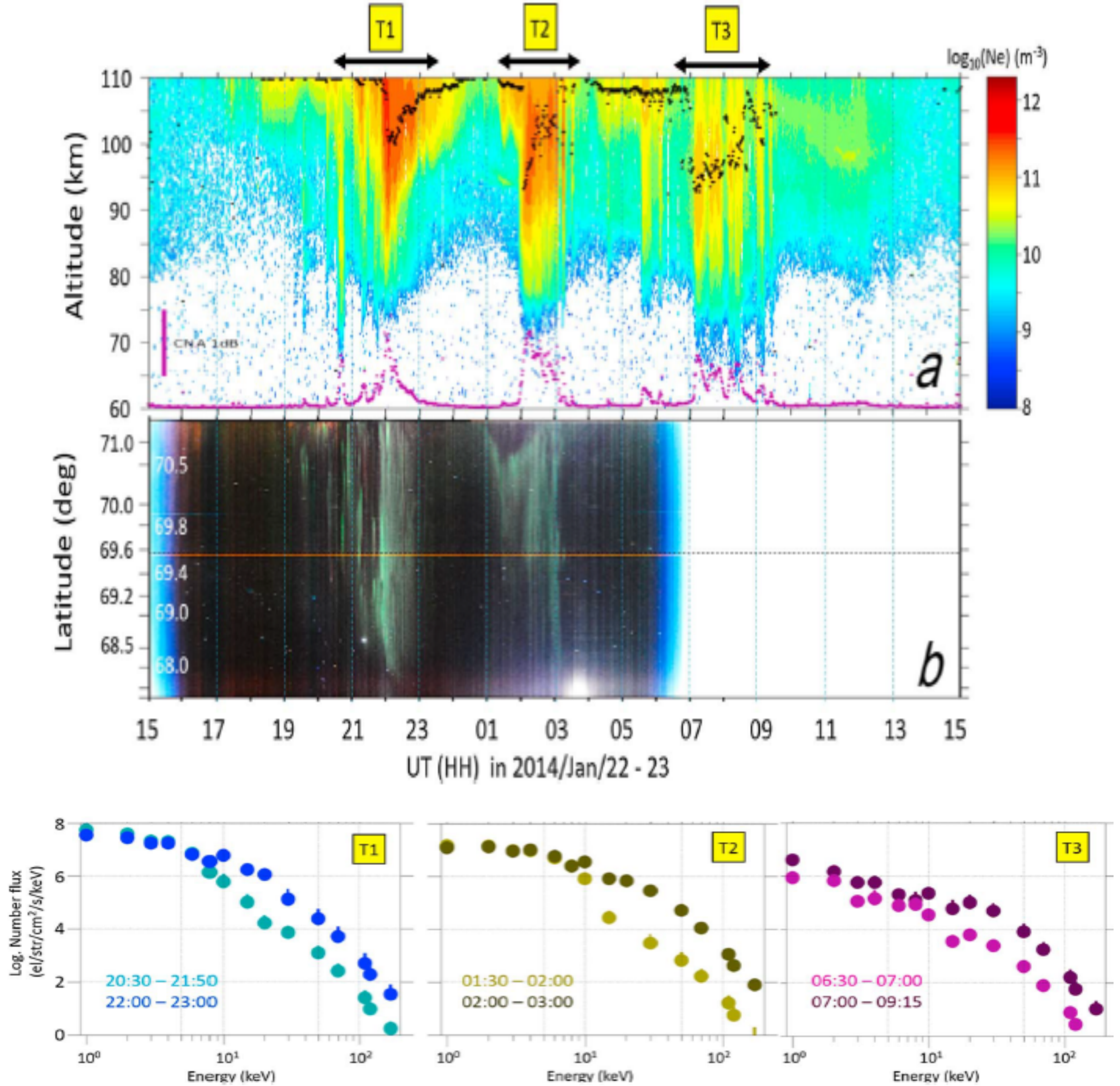
T1
T2
T3
log10(Ne) (m-3)
Altitude (km)
CNA 1dB
a
Latitude (deg)
b
UT (HH) in 2014/Jan/22 - 23
Log. Number flux (el/str/cm2/s/keV)
Energy (keV)
20:30 – 21:50
22:00 – 23:00
01:30 – 02:00
02:00 – 03:00
06:30 – 07:00
07:00 – 09:15

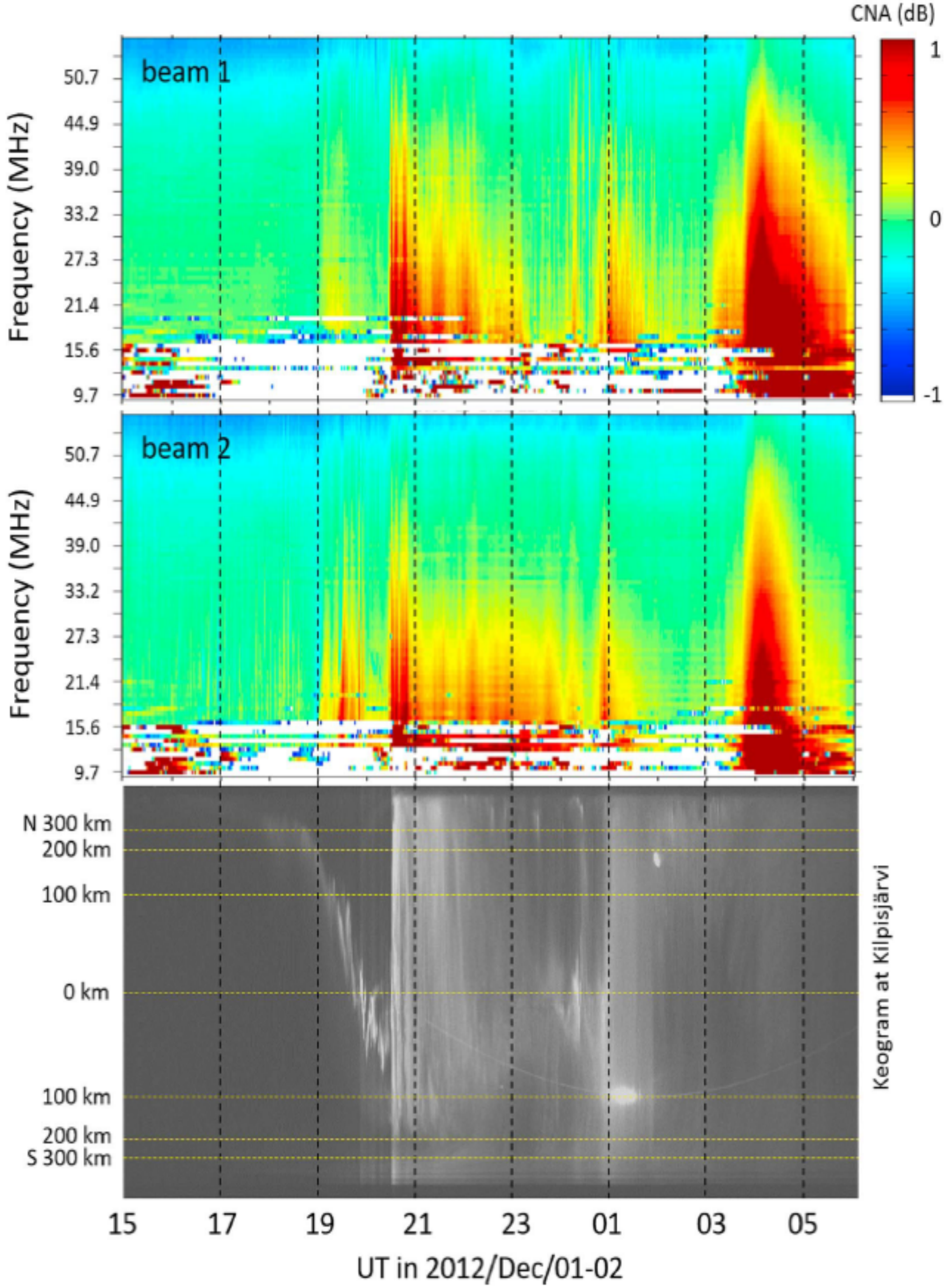
CNA (dB)
beam 1
beam 2
Frequency (MHz)
N 300 km
200 km
100 km
0 km
100 km
200 km
S 300 km
Keogram at Kilpisjärvi
UT in 2012/Dec/01-02

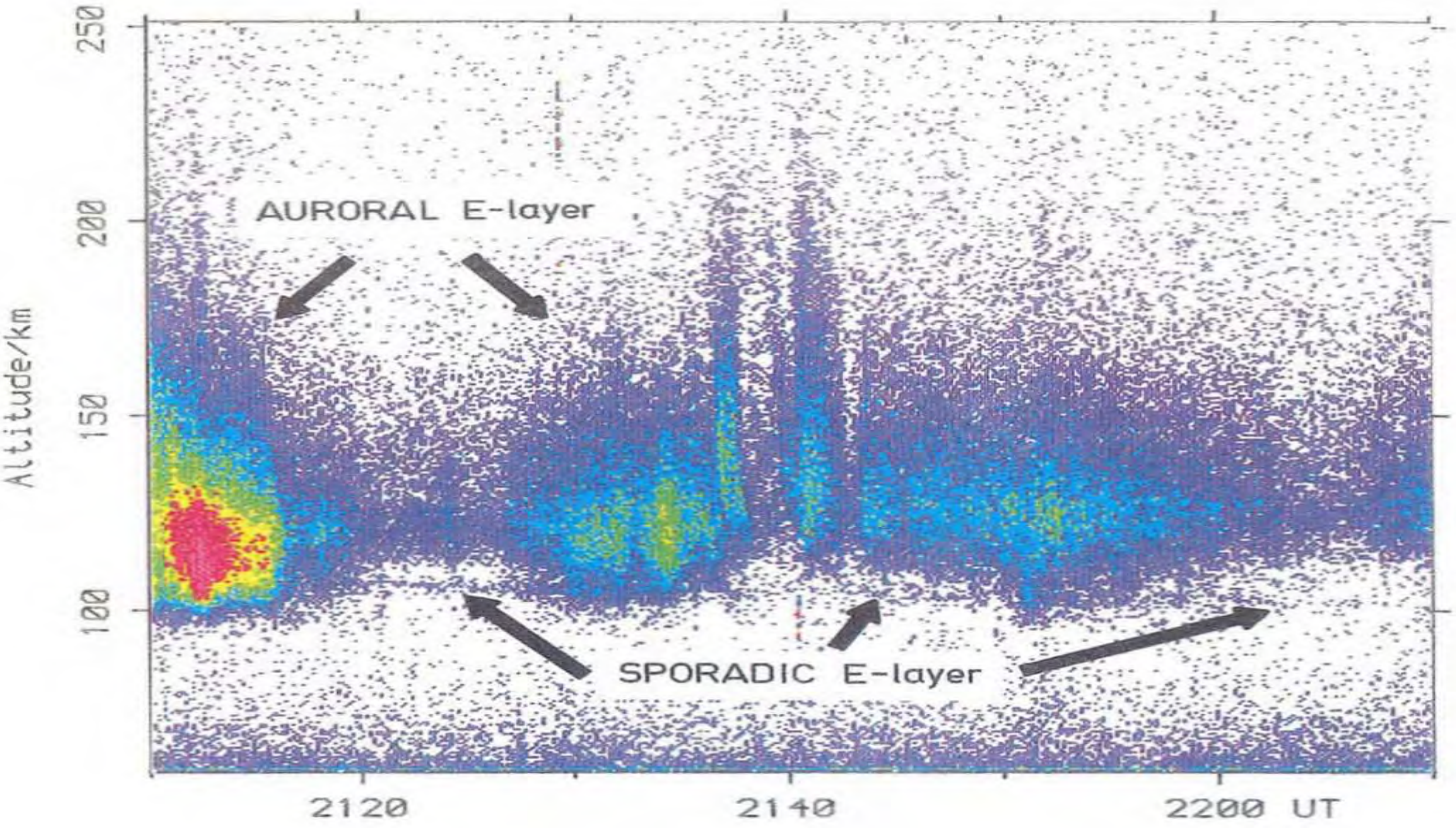

250
200
150
100
Altitude/km
AURORAL E-layer
SPORADIC E-layer
2120
2140
2200 UT

Meso-scale structure III: Thin layer phenomena

- ISRs are very well suited to probing spatial structure and temporal evolution in thin layers (PMSE, Sporadic E)
- Good range resolution makes it possible to probe internal structure
- Artificial heating has shed light on particle size and charging
- Phased arrays can measure horizontal extent and distribution as well as layer thickness

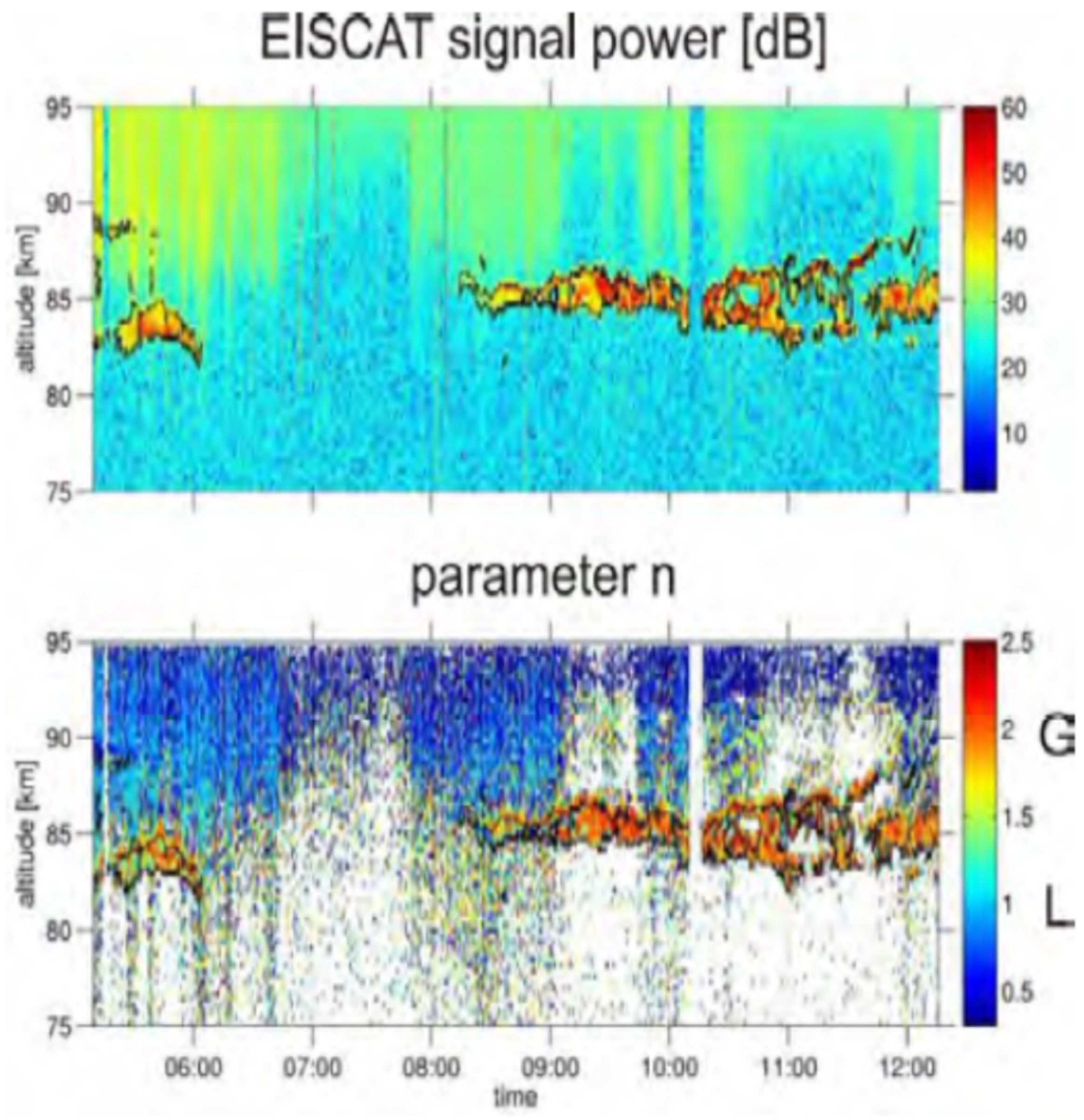

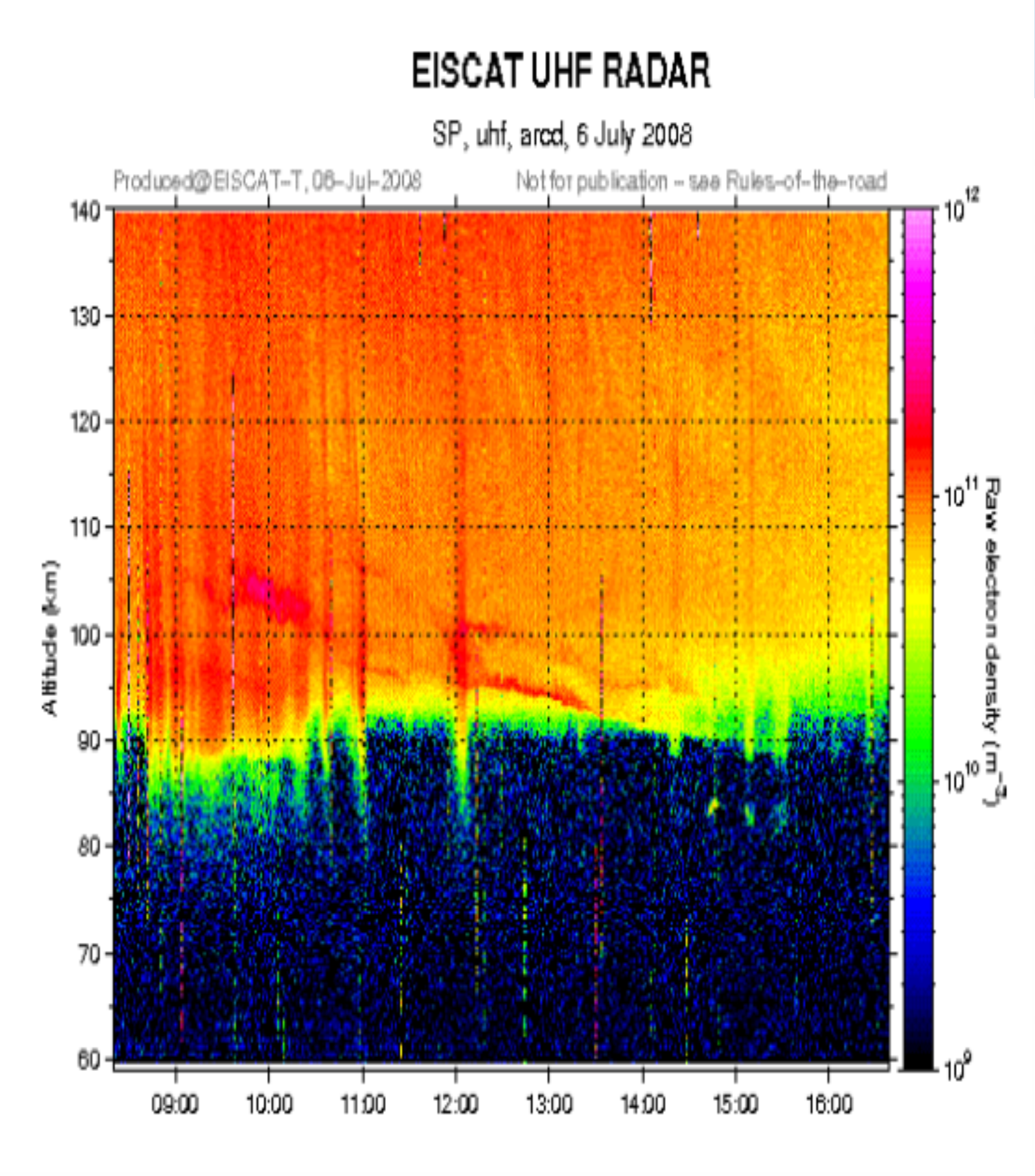

EISCAT UHF RADAR
SP, uhf, arcd, 6 July 2008
Produced@EISCAT-T, 08-Jul-2008
Not for publication – see Rules-of-the-road
Altitude (km)
Raw electron density (m⁻³)
09:00
10:00
11:00
12:00
13:00
14:00
15:00
16:00

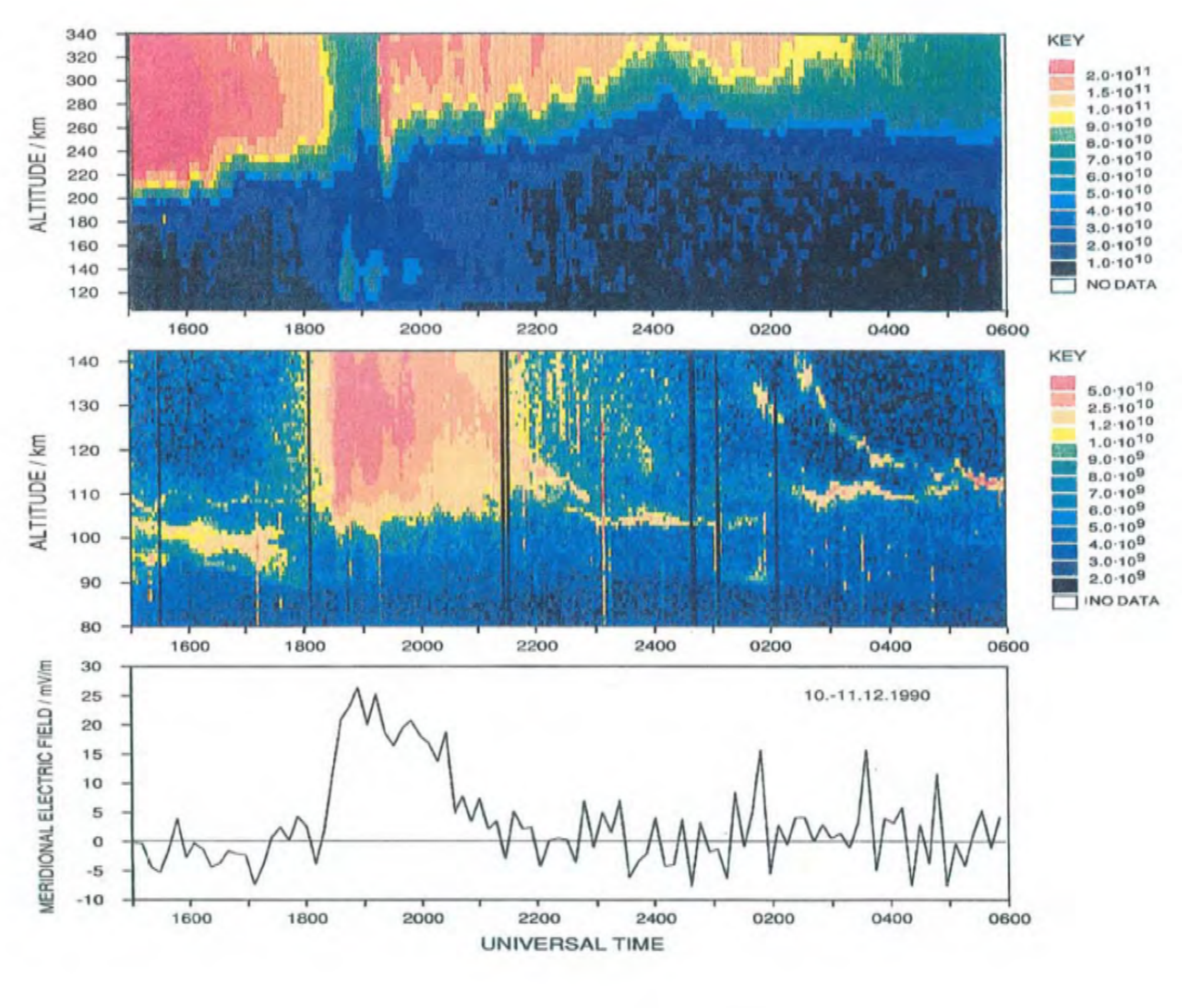

ALTITUDE / km
KEY
NO DATA
MERIDIONAL ELECTRIC FIELD / mV/m
10.-11.12.1990
UNIVERSAL TIME
1600
1800
2000
2200
2400
0200
0400
0600

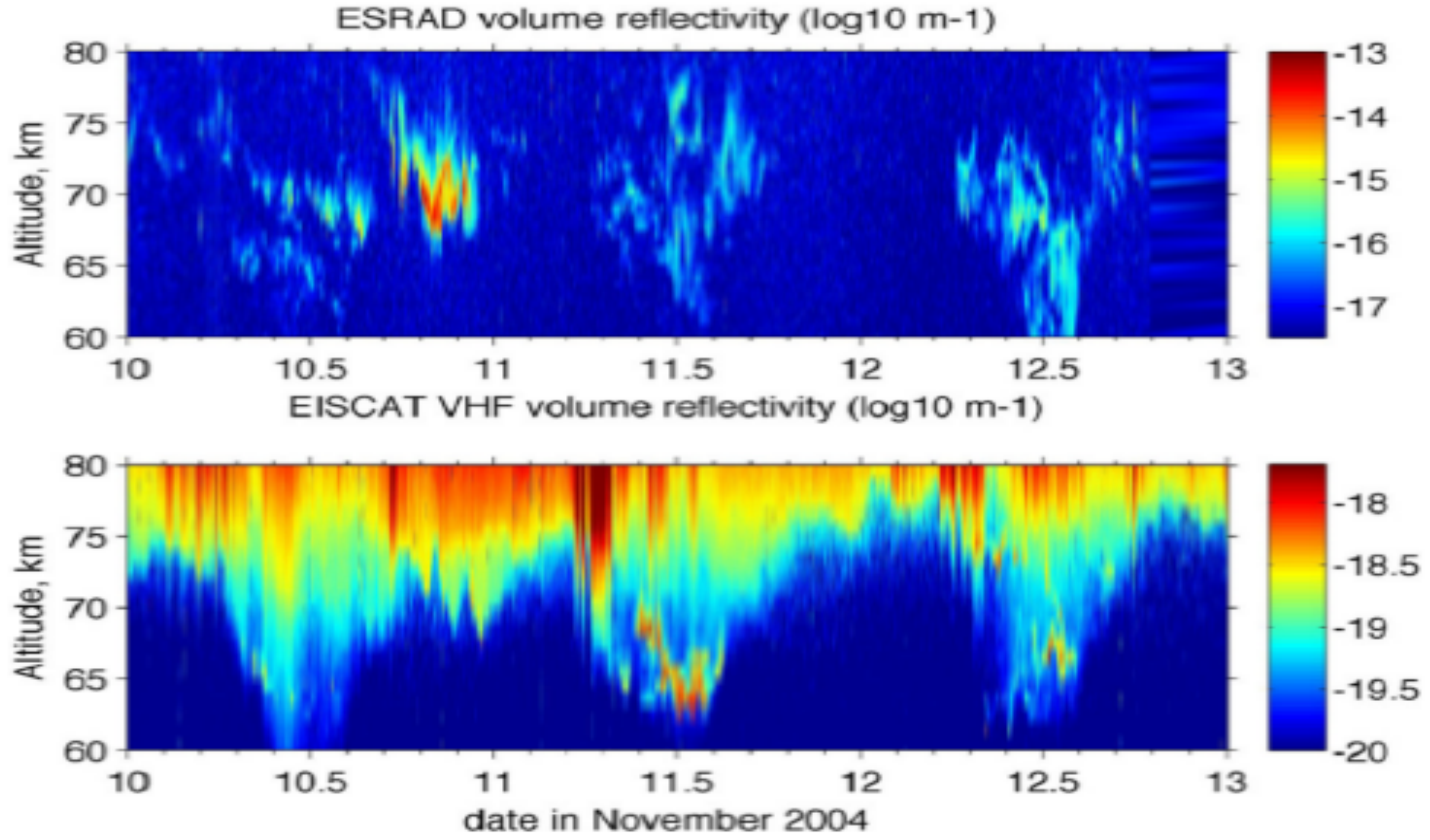

ESRAD volume reflectivity (log10 m-1)
Altitude, km
80
75
70
65
60
10
10.5
11
11.5
12
12.5
13
-13
-14
-15
-16
-17
EISCAT VHF volume reflectivity (log10 m-1)
Altitude, km
80
75
70
65
60
10
10.5
11
11.5
12
12.5
13
-18
-18.5
-19
-19.5
-20
date in November 2004

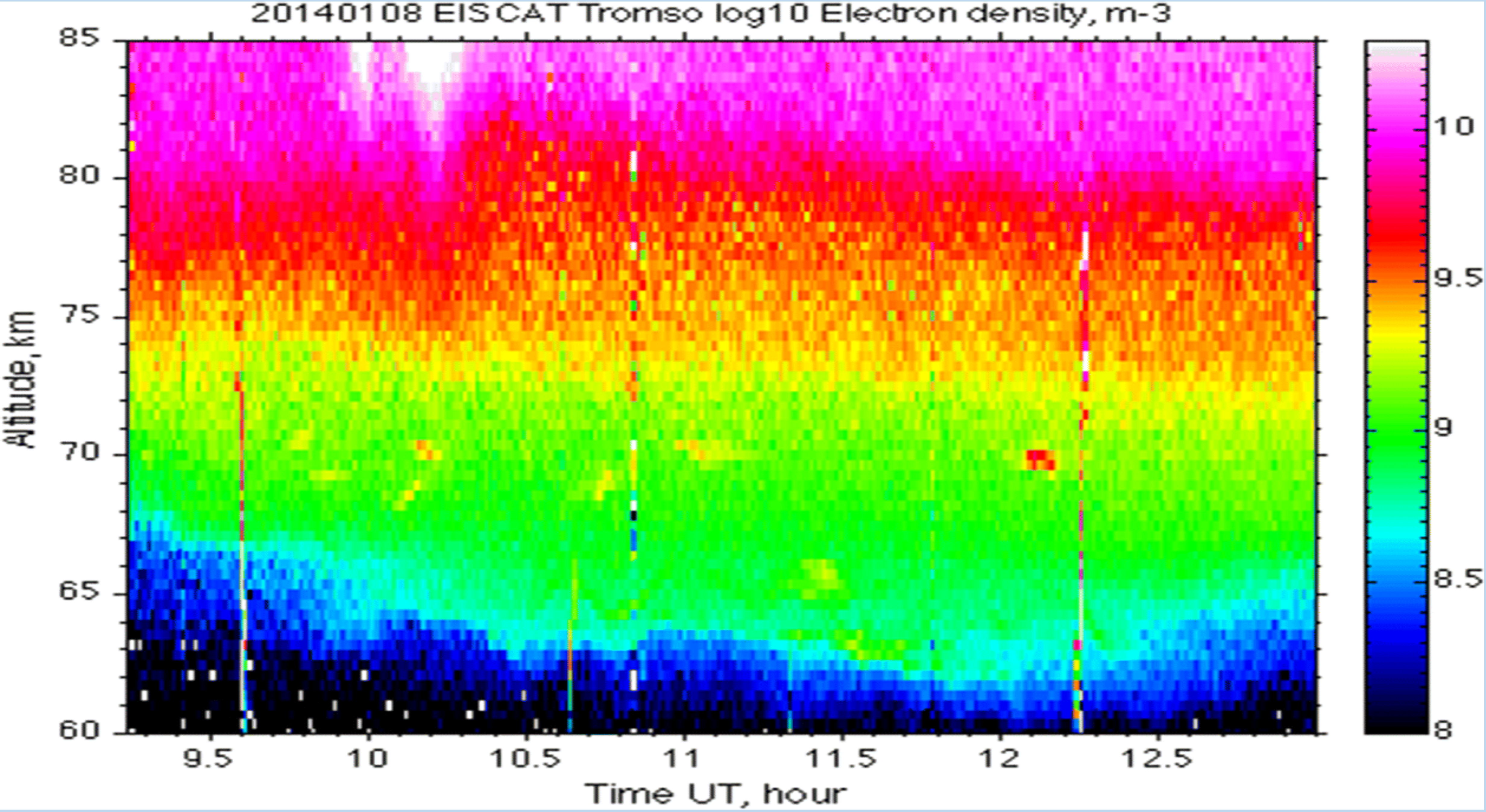

20140108 EISCAT Tromso log10 Electron density, m-3
Altitude, km
85
80
75
70
65
60
9.5
10
10.5
11
11.5
12
12.5
Time UT, hour
10
9.5
9
8.5
8

Meso-scale structure:
IV: Large and medium-scale TIDs

ISRs cannot sense AGWs directly, but do so through their effect on the ionosphere (TIDs)

These signatures are common, often best seen under quiet conditions

Seasonal distribution is biased by Ne variation

TID characteristics can be explored most directly through effects on field-aligned velocity

LS and MSTID: periods > 15 min, Most commonly 0.5-07h, 1.1-1.3h.

Can also use ISRs to investigate some source mechanisms

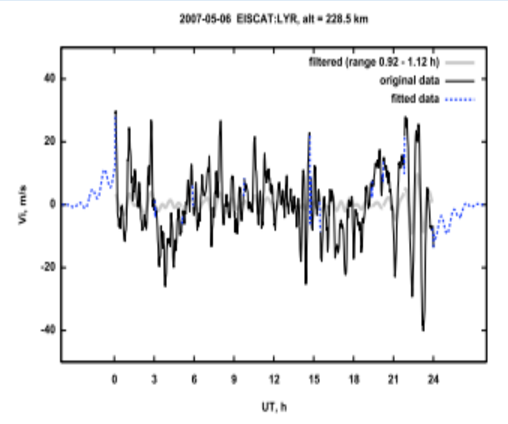

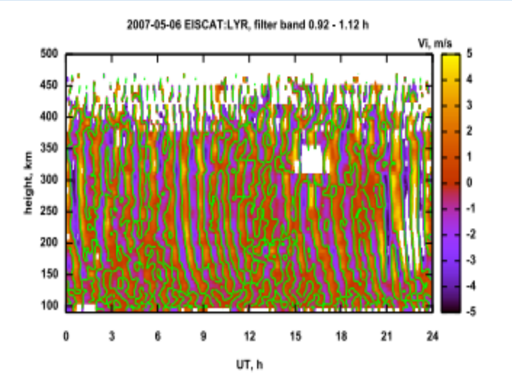

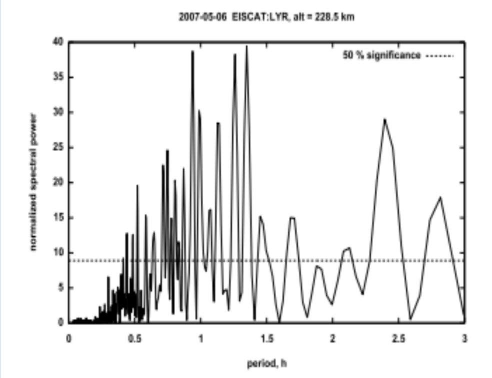

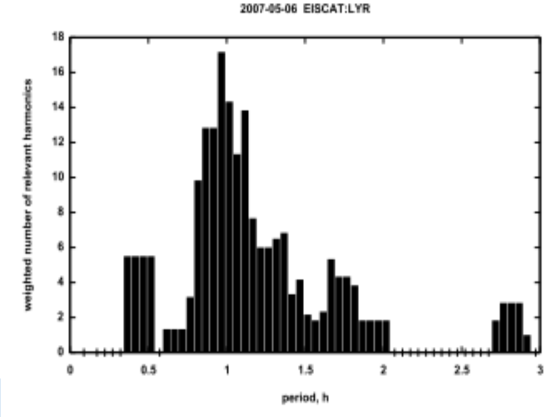

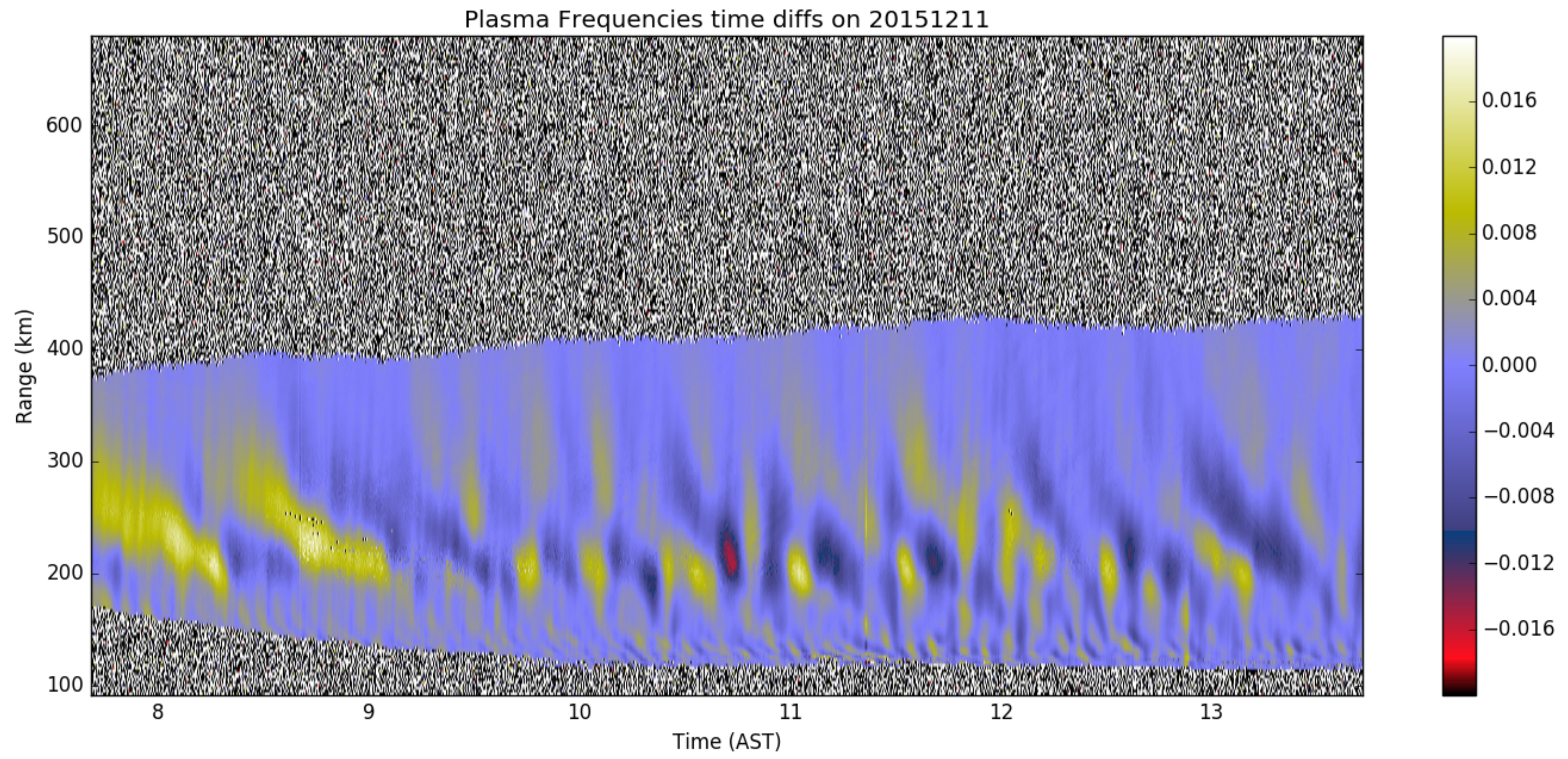
Plasma Frequencies time diffs on 20151211
Range (km)
600
500
400
300
200
100
8
9
10
11
12
13
Time (AST)
0.016
0.012
0.008
0.004
0.000
−0.004
−0.008
−0.012
−0.016

Small-scale structure: I: Natural plasma heating

- As we saw on Tuesday, the ion temperature is governed by an energy balance equation

$$T_i \sim T_n + m_n(\underline{V}_i-\underline{V}_n)^2/3k + (m_i+m_n)(T_e-Ti)\nu_{ie}/(m_i{*}\nu_{in})$$

- E-region electron temperature has a similar relationship due to "anomalous collisions" caused by wave processes
- Relationships like this can be used to infer parameters which cannot be measured
- Remember that much of the F-region chemistry is temperature dependents
- Also important to understand the regimes in which these relationships begin to break down (fitting assumptions unreliable)

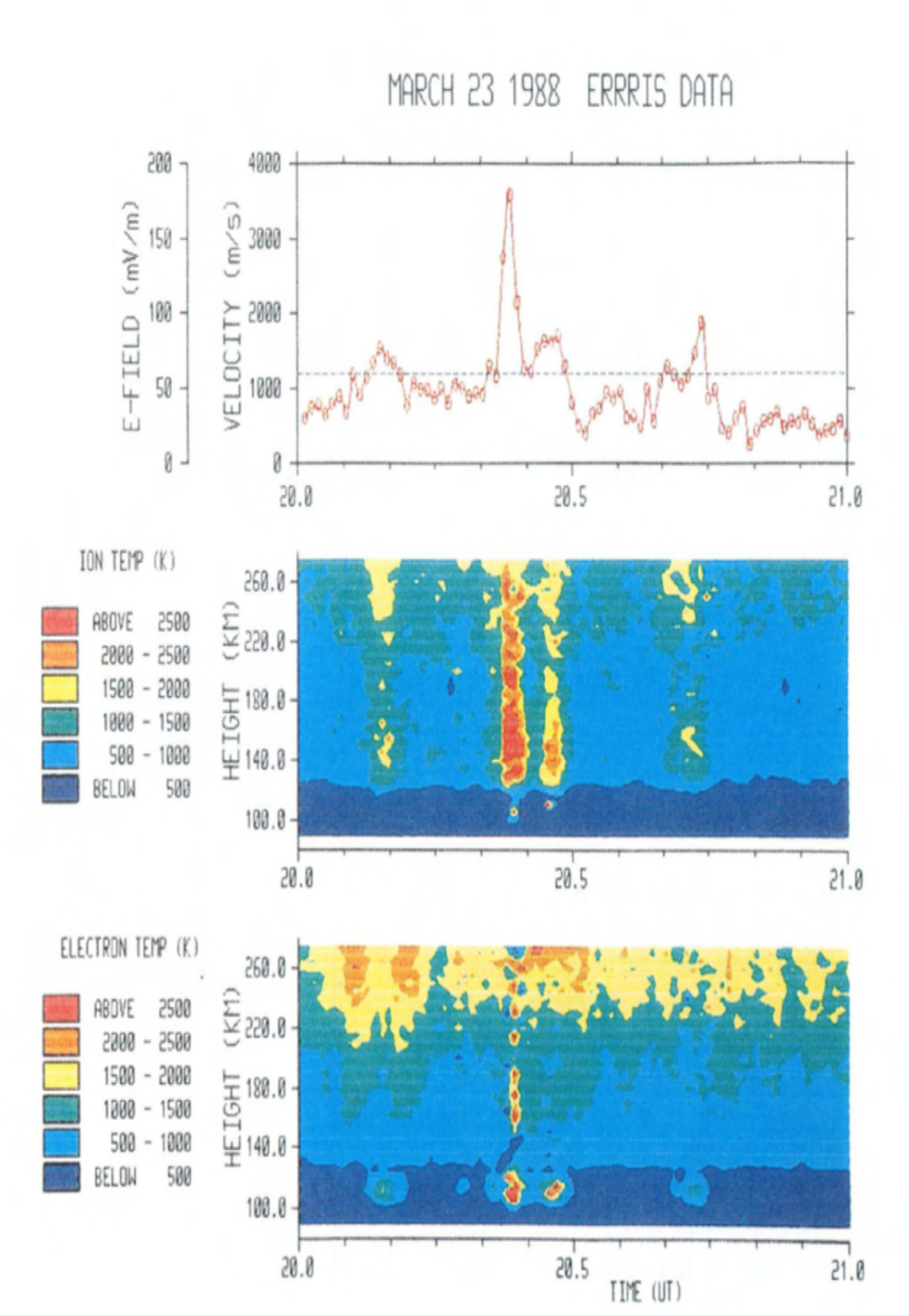

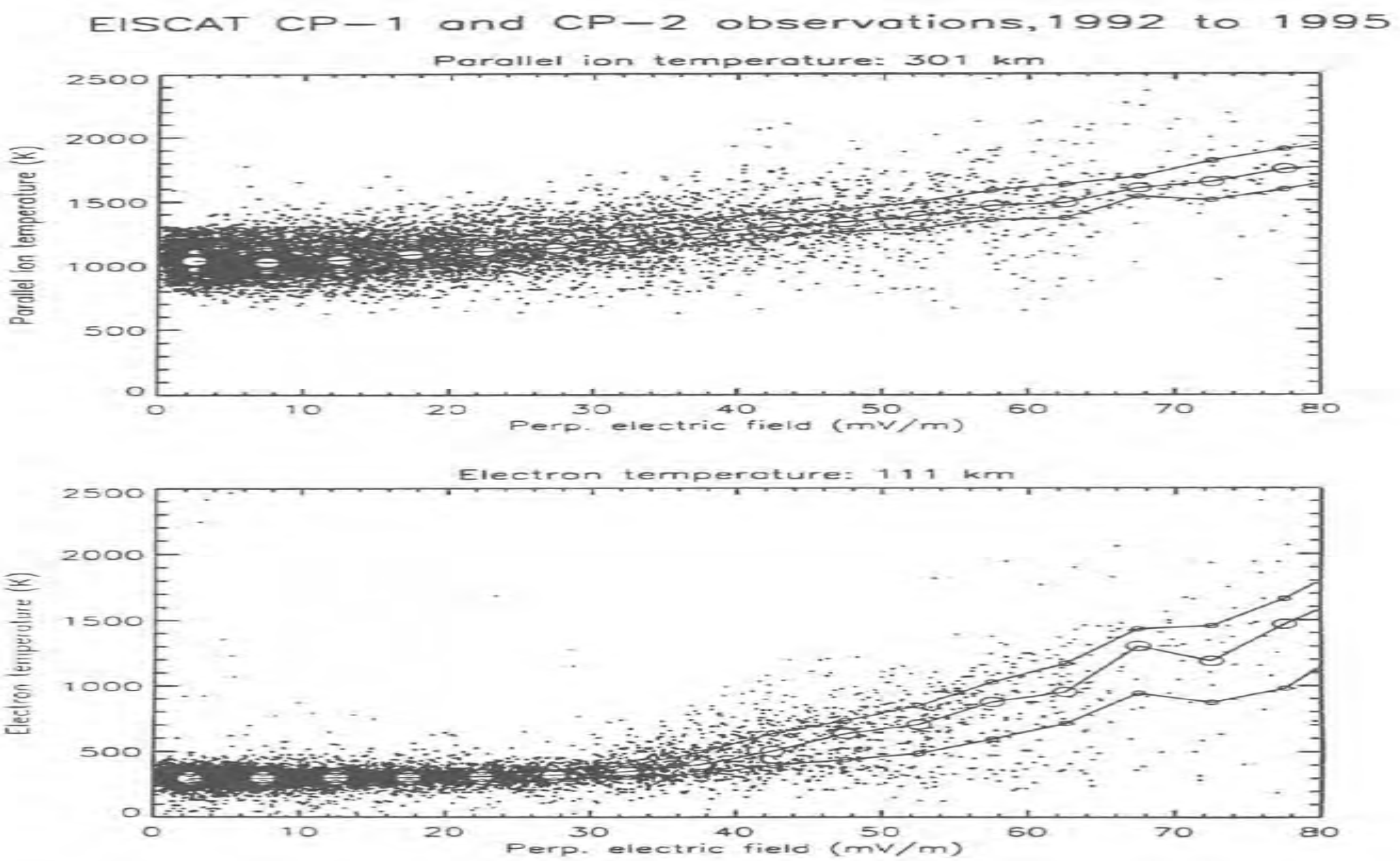
EISCAT CP-1 and CP-2 observations,1992 to 1995
Parallel ion temperature: 301 km
Parallel ion temperature (K)
2500
2000
1500
1000
500
0
0
10
20
30
40
50
60
70
80
Perp. electric field (mV/m)
Electron temperature: 111 km
Electron temperature (K)
2500
2000
1500
1000
500
0
0
10
20
30
40
50
60
70
80
Perp. electric field (mV/m)

Small-scale Structure
II: Non-thermal distribution functions

All our standard parameter fitting is based on assumption of equilibrium plasmas (isotropic Maxwellian distributions)

We know this assumption breaks down when plasma convection is strongly driven by electric fields

This is particularly true in the F-region, because O^+-O collisions are strongly backscattering

Molecular species have more isotropic collisions

Limiting case is a toroidial distribution

Partition coefficient tells how anisotropic the plasma is.

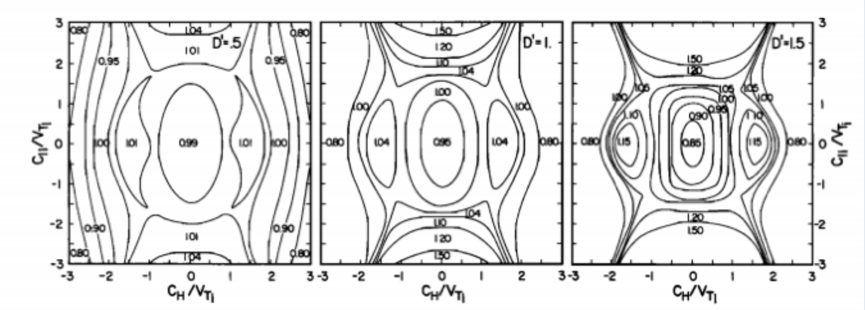

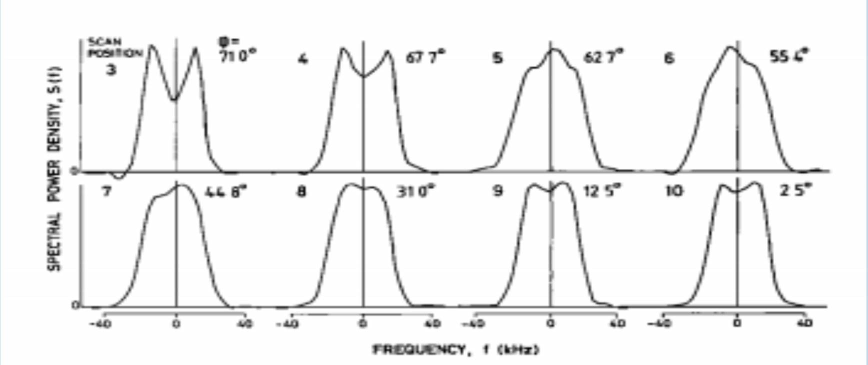

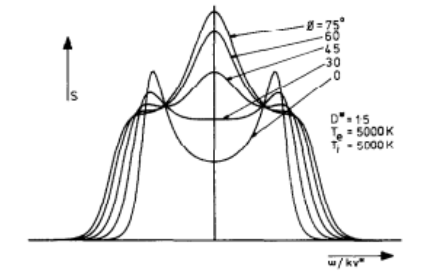

Fig. 7. Incoherent scatter spectra for the generalised relaxation model with $D^* = 1.5$ and equal electron and 3-D ion temperatures of 5000 K, for aspect angles, Φ, of 0°, 30°, 45°, 60° and 75°. The corresponding line-of-sight ion velocity distributions are given in Fig. 1. The phase speeds are normalised to v^*.

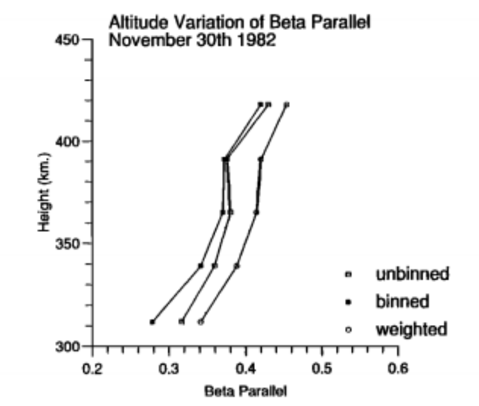

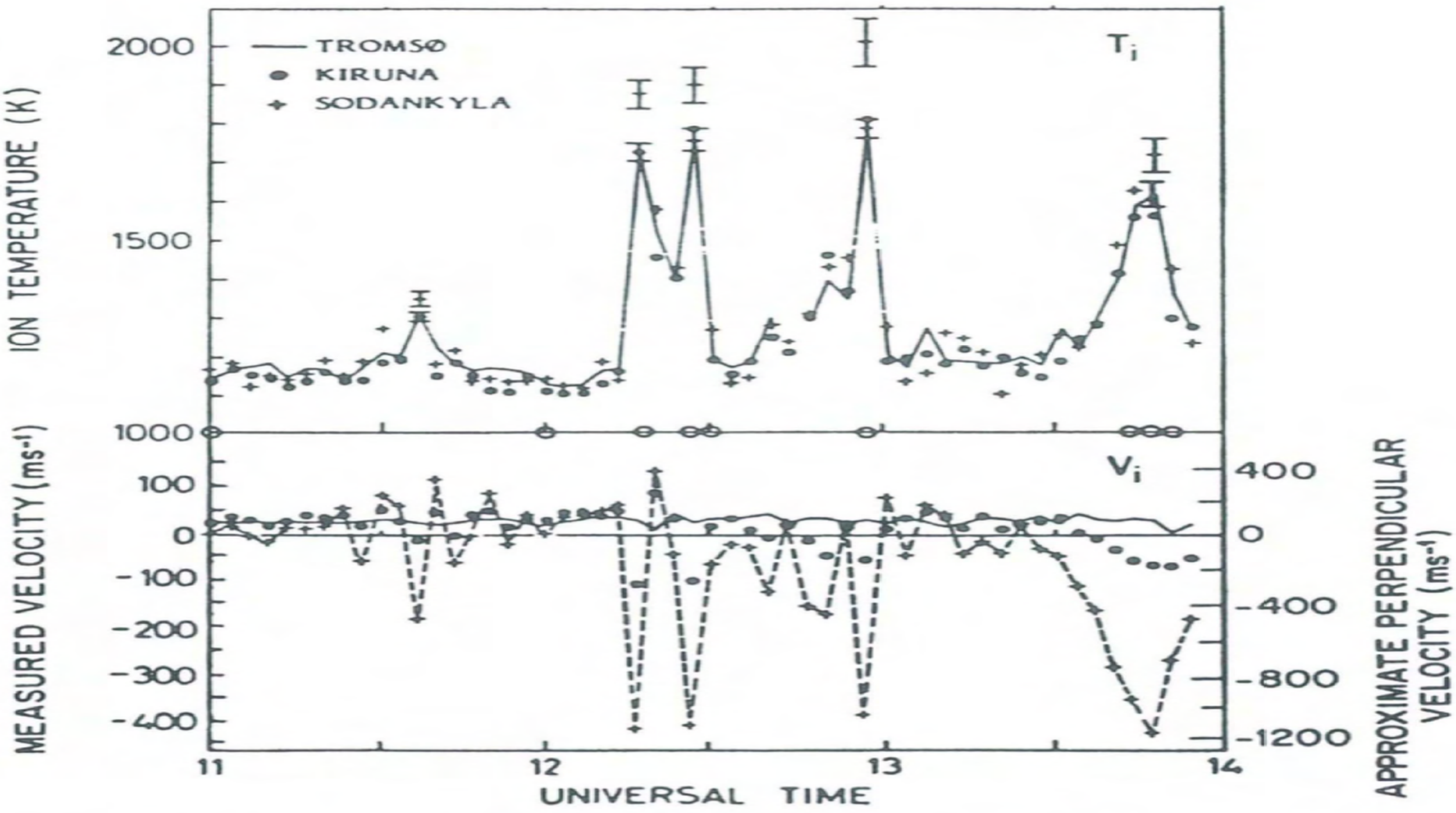

TROMSØ
KIRUNA
SODANKYLA
T_i
V_i
ION TEMPERATURE (K)
2000
1500
1000
MEASURED VELOCITY (ms⁻¹)
100
0
-100
-200
-300
-400
APPROXIMATE PERPENDICULAR VELOCITY (ms⁻¹)
400
0
-400
-800
-1200
11
12
13
14
UNIVERSAL TIME

Small-scale Structure III: HF plasma heating

- HF Heating facilities (at EISCAT and now at Arecibo) have been very important to the ISR science programme
- ISR becomes a critical diagnostic for controlled plasma physics experiments
- Not just variations in the main plasma parameters, but also changes in the IS spectra enable probing of the plasma physics
- ISR radars are used in conjunction with multiple other techniques, e.g. optical imagers, radio receivers, other radars, satellites

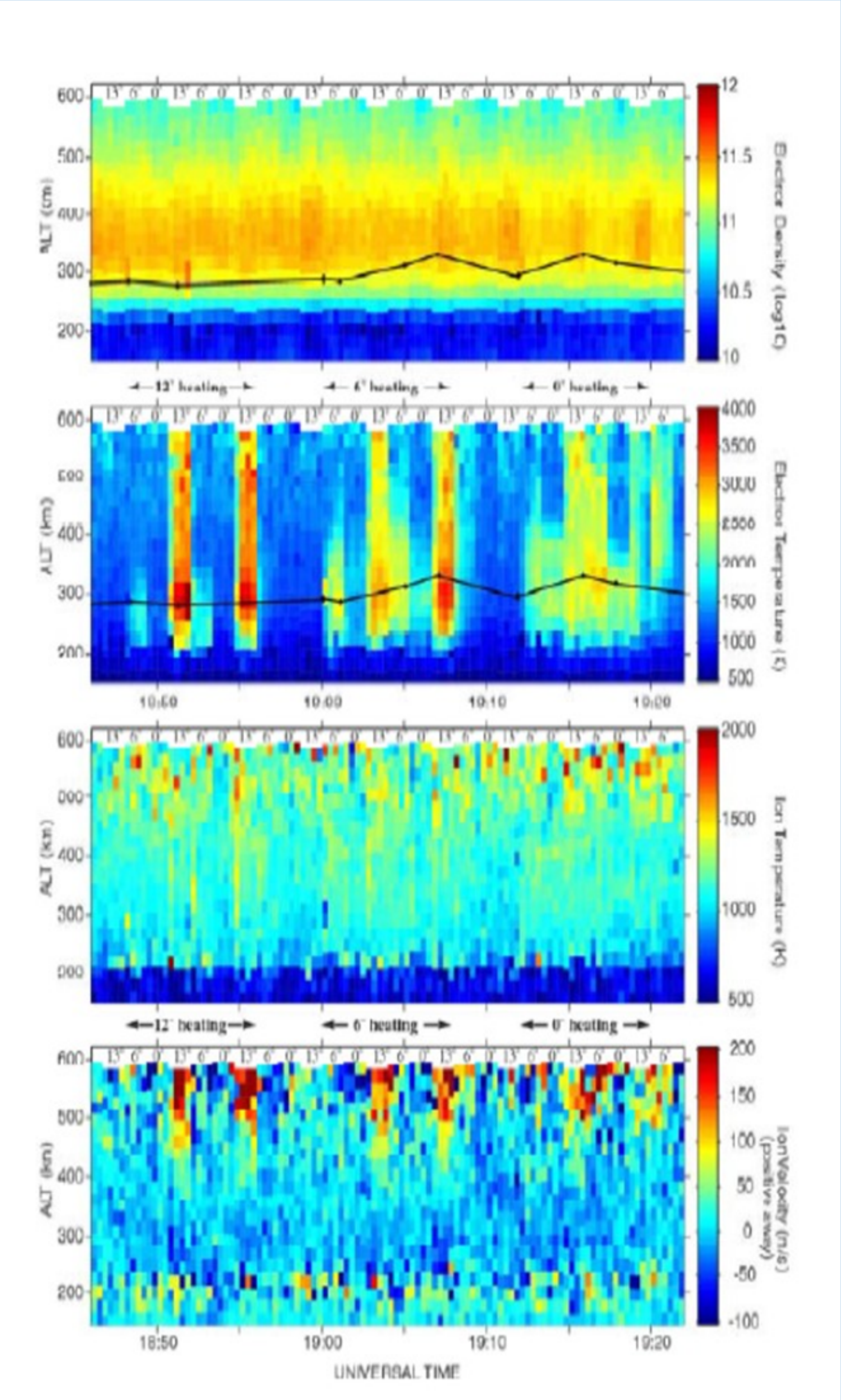

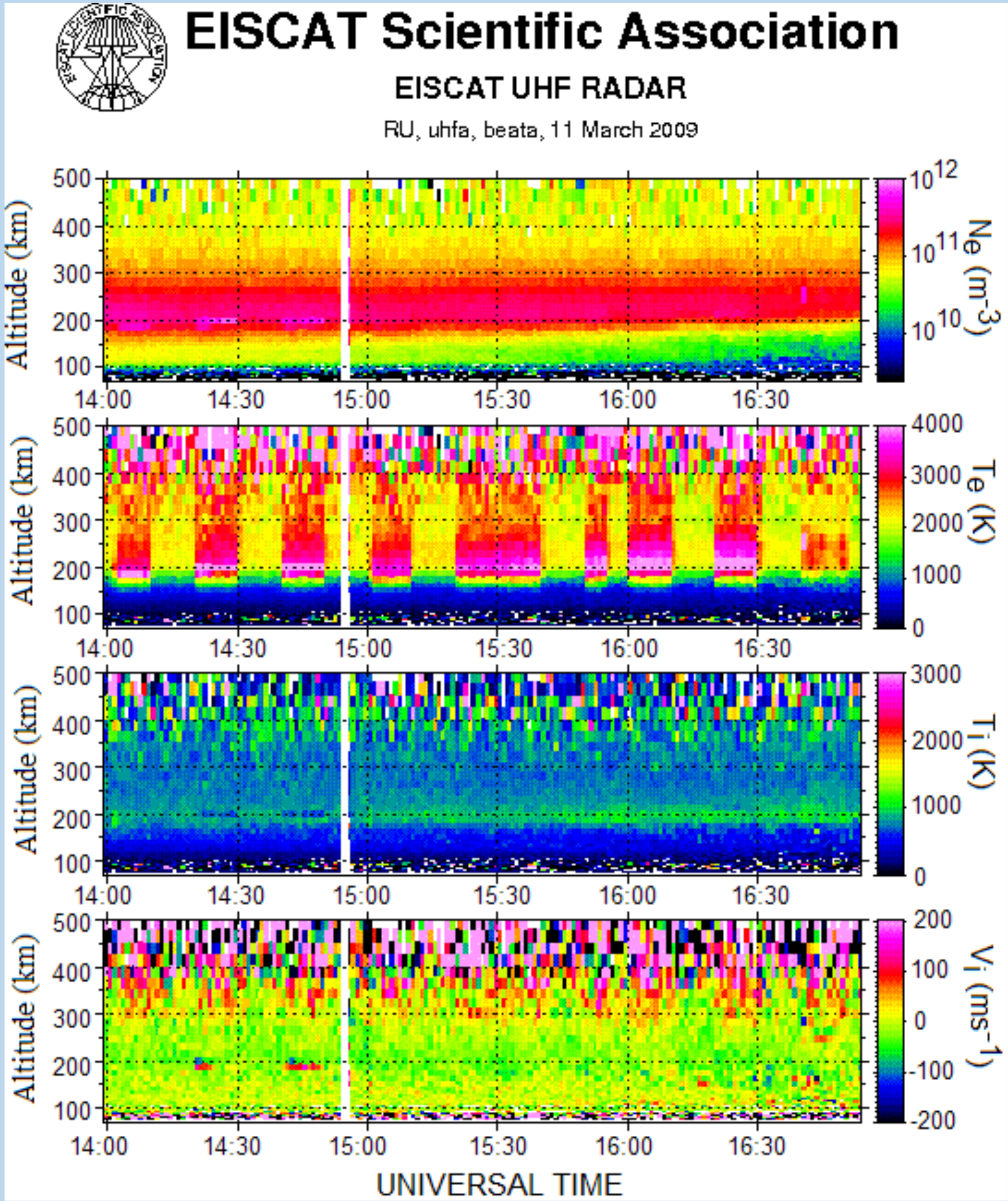
EISCAT Scientific Association
EISCAT UHF RADAR
RU, uhfa, beata, 11 March 2009
Altitude (km)
Ne (m-3)
Te (K)
Ti (K)
Vi (ms-1)
14:00 14:30 15:00 15:30 16:00 16:30
UNIVERSAL TIME

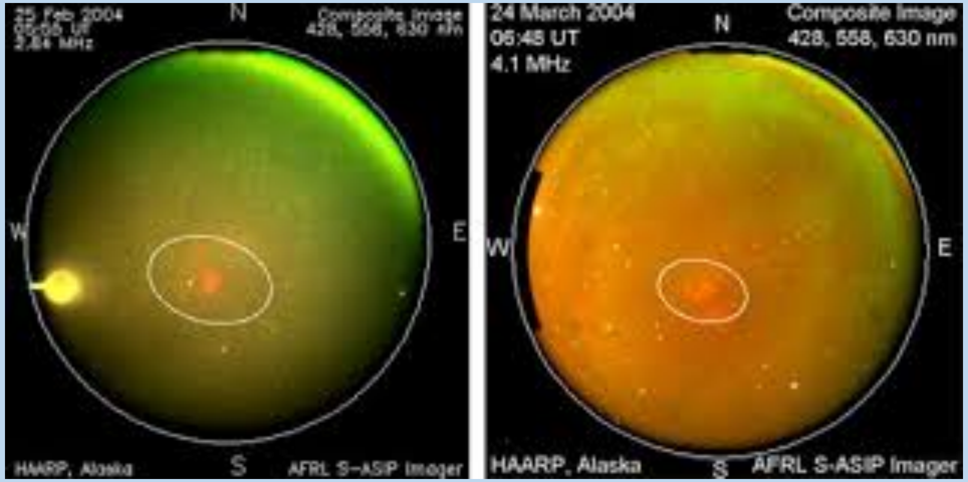
24 March 2004
06:48 UT
4.1 MHz
Composite Image
428, 558, 630 nm
N
S
E
W
HAARP, Alaska
AFRL S-ASIP Imager

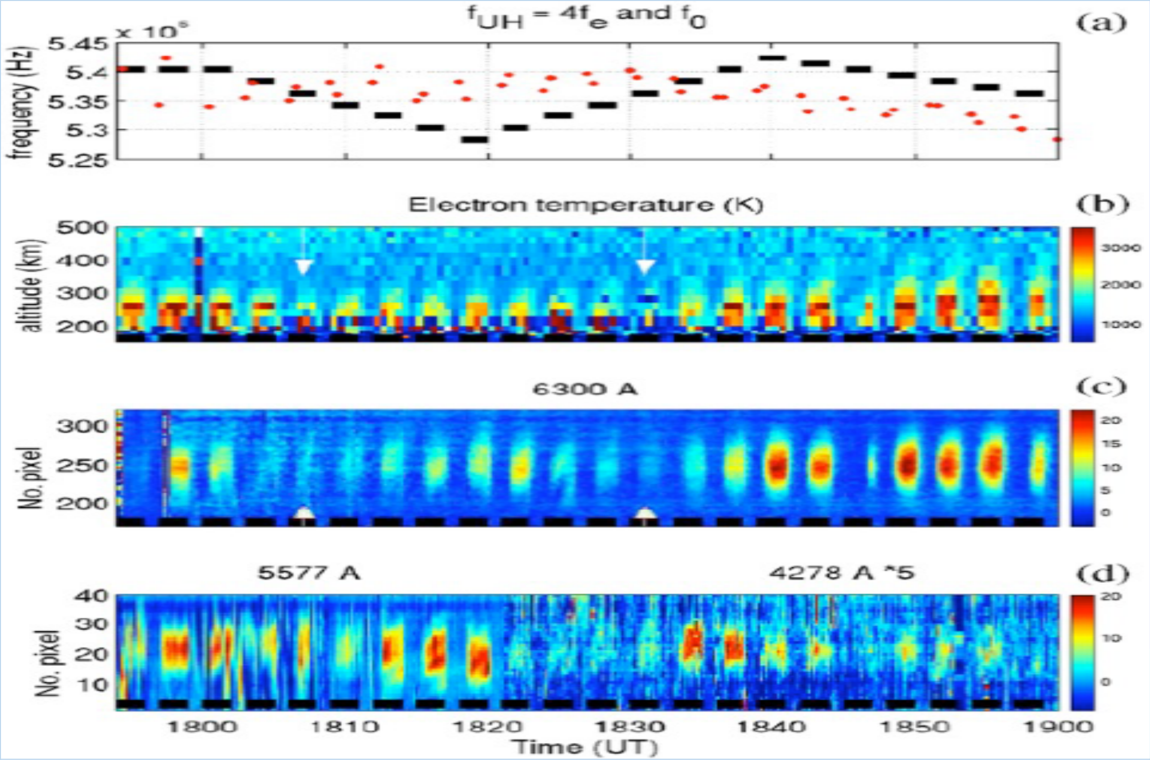
fUH = 4fe and f0
(a)
frequency (Hz)
Electron temperature (K)
(b)
altitude (km)
6300 A
(c)
No. pixel
5577 A
4278 A *5
(d)
1800 1810 1820 1830 1840 1850 1900
Time (UT)

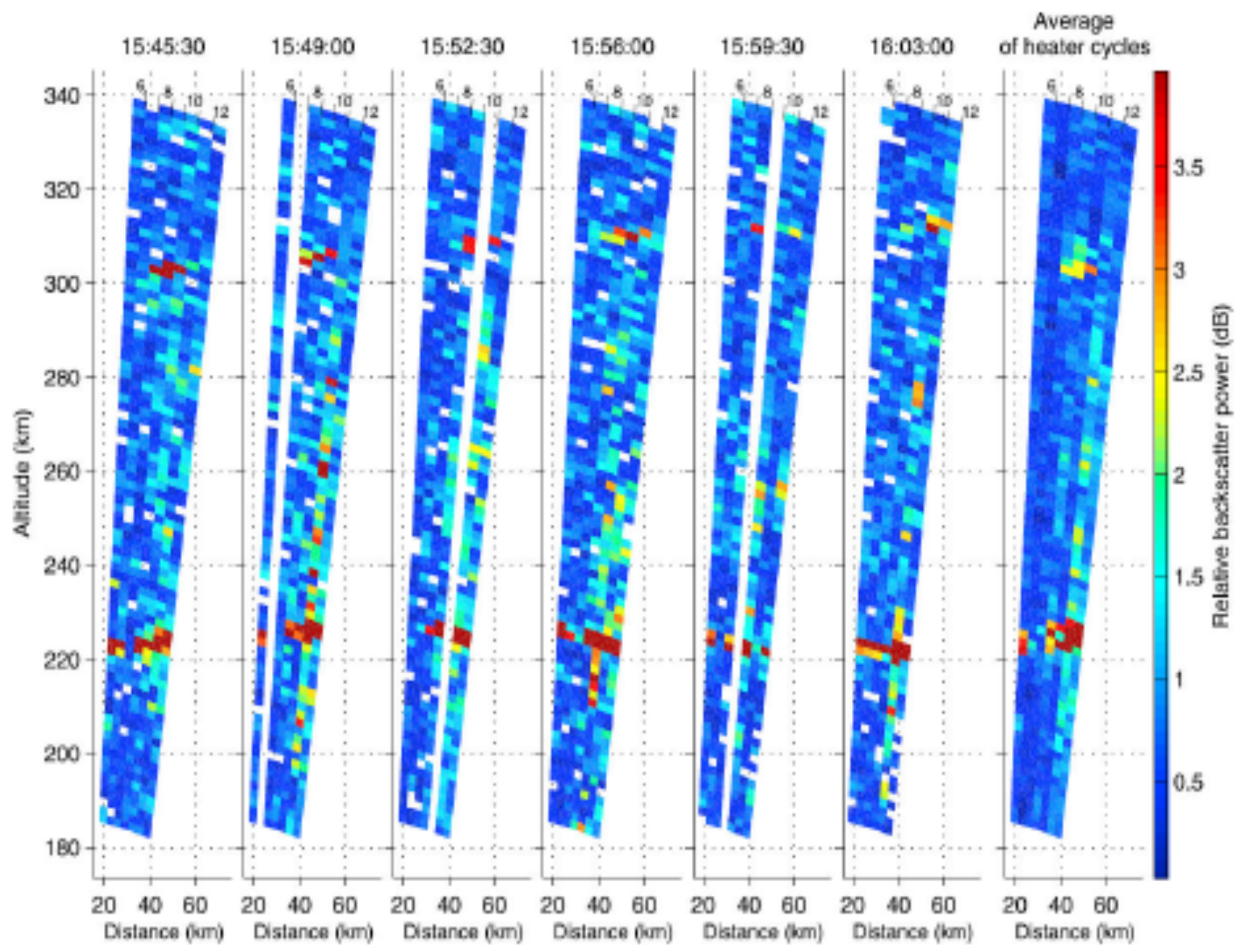

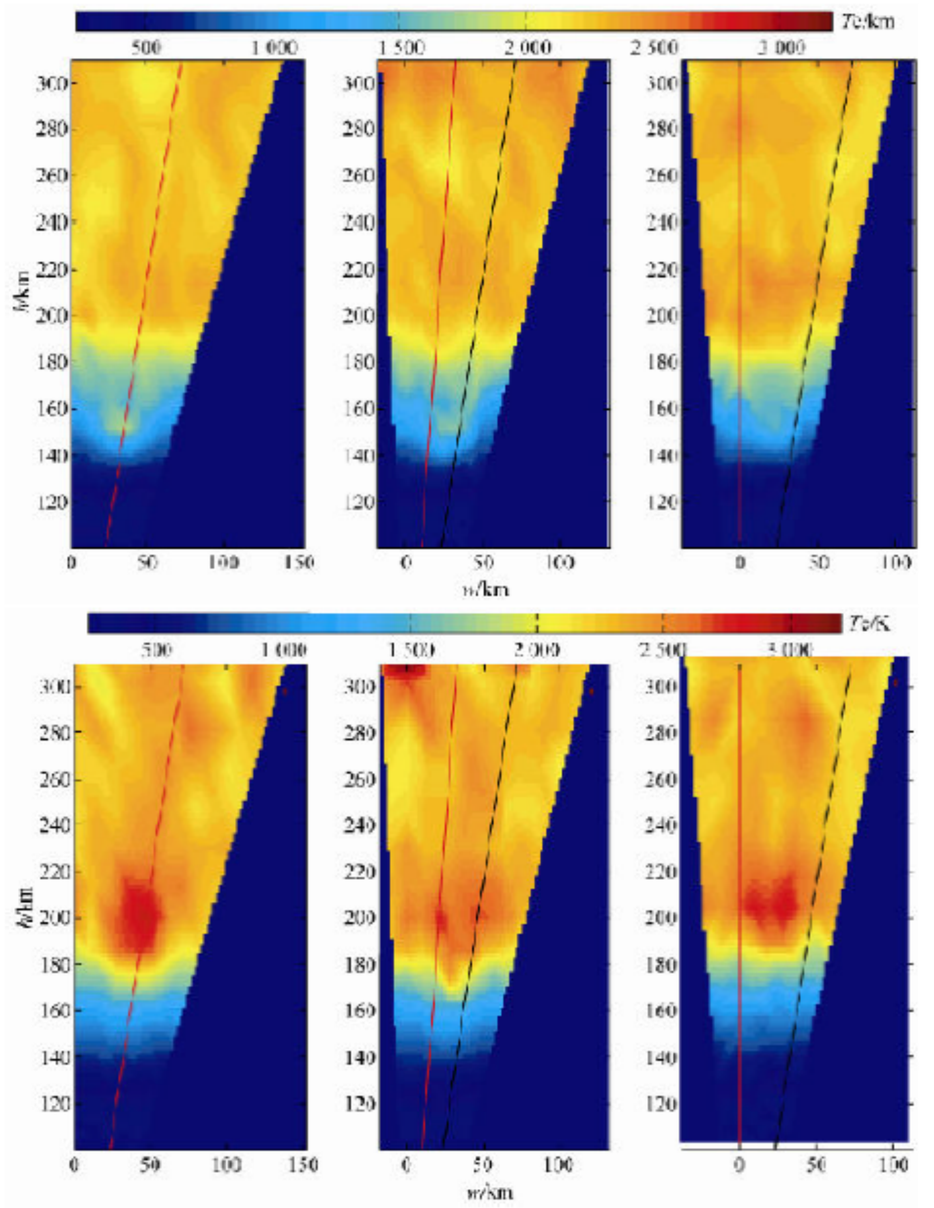

Spatial distributions of backscattered power and electron temperature in the heated volume

Small-scale Structure
IV: Natural plasma irregularities

- EISCAT occasionally sees powerful, strongly asymmetric spectra

- They occur infrequently, and are typically very short-lived, being typically seen for ~<10s.

- They have been seen to be linked to auroral phenomena such as rayed arcs

- Theories of generation include ion-acoustic instability, ion-ion two-stream instability or Langmuir wave decay from electron beams

- Likely they come from very small regions (sub-beamwidth)

- This has led to the construction of a small interferometer to

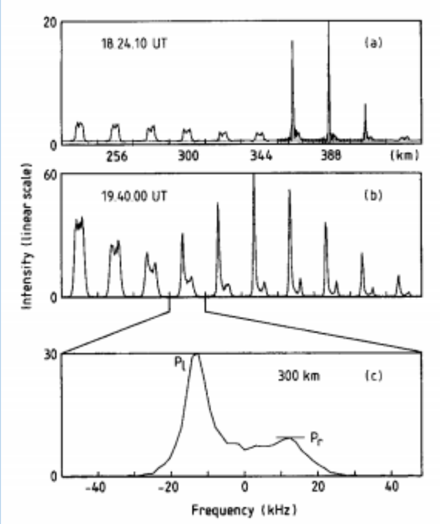

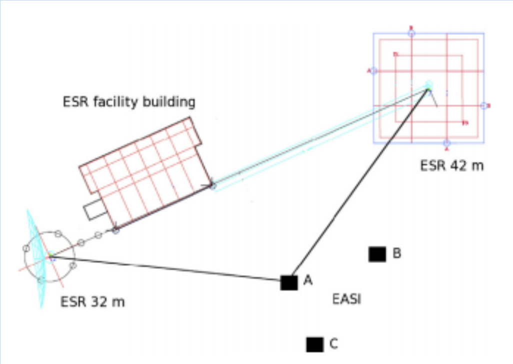

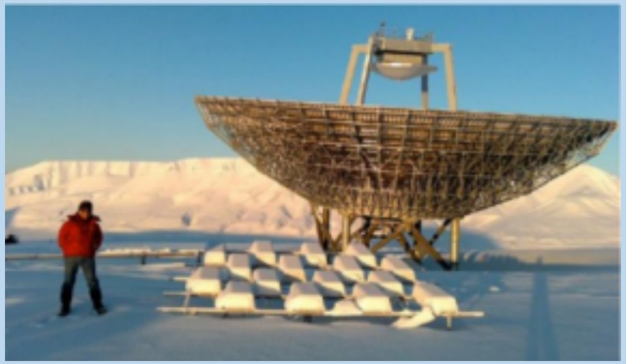

Microscale Structure:
V: Coherent ionospheric structure

The EISCAT mainland radars cannot look at very low elevation

Hence the EISCAT cannot satisfy orthogonality condition for backscatter from FAIs

However this can be done by putting a transmitter further south (bisector vector perp. to field)

In this case, Kiruna has been used as a receiver for coherent scatter @ 930 MHz.

Narrow spectra with phase speeds limited to around 420 m/s (ion-acoustic speed)

Likely to indicate scatter from a narrow region around 100km

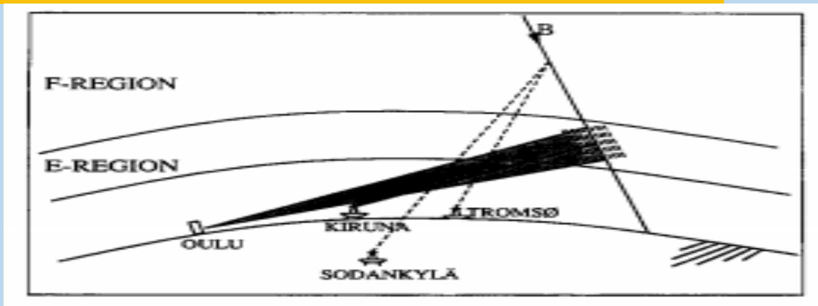

COSCAT passive spectra recorded at Kiruna
From 03:07:20 on 09/03 1991
To 03:47:20 on 09/03 1991
Filter Half Width 25 kHz

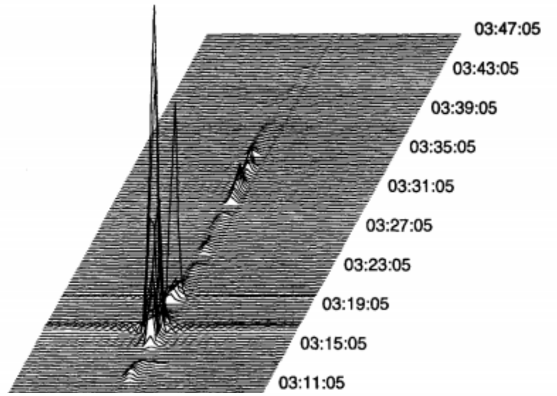

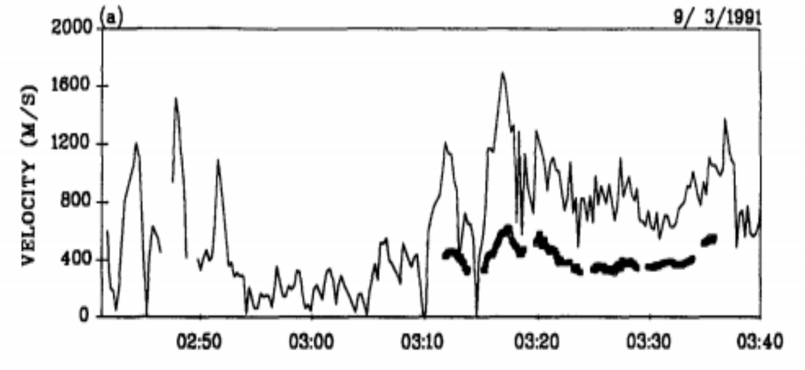

Small-scale Structure:
VI: Meteors

- ISRs normally record quite high rates of meteor contamination
- Meteors typically show up as short-lived undecoded signals at E-region ranges
- These are cluttering echoes which might normally be thrown away
- From meteors we can see “head echoes” as well as meteor train ionisation
- Different class of radars studies meteor trains for wind information etc
- Multi-beam/multi-radar capabilities can provide trajectory information
- Useful for mapping solar system origins of entering material

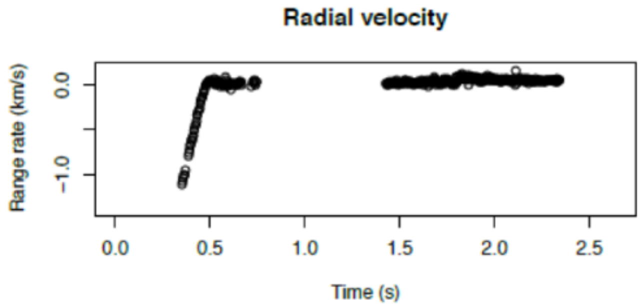

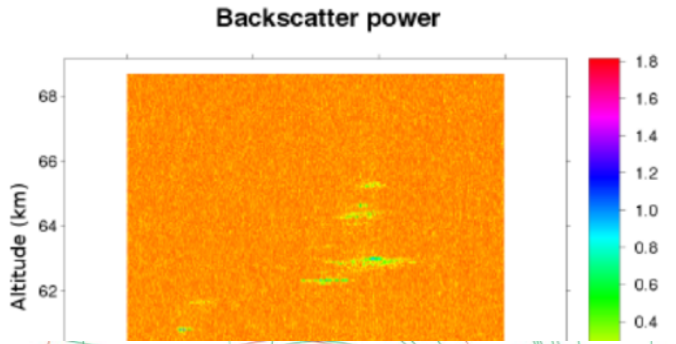

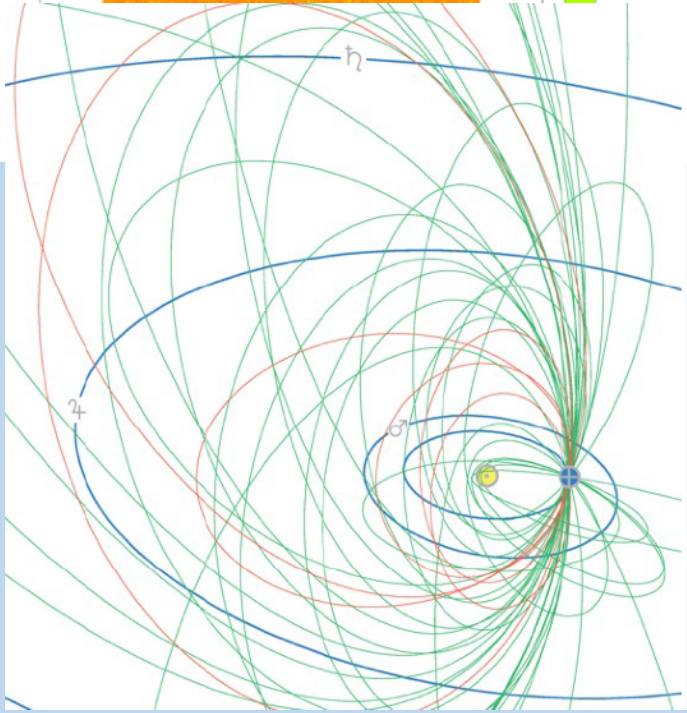

Small-scale structure: VII: Space debris

Because of their sensitivity, ISRs are excellent tools for observing satellites and space debris in LEO

These are the cluttering echoes which we would otherwise throw away

Long-term “beam park” observations can be very useful for monitoring development of debris clouds etc

Targetted acquisition and tracking can enable orbit determination, maintenance of catalogues etc.

In general this is not what we do, but there is use of ISRs and ISR like radars in space debris tracking applications (e.g. PFISR and LEOLabs)

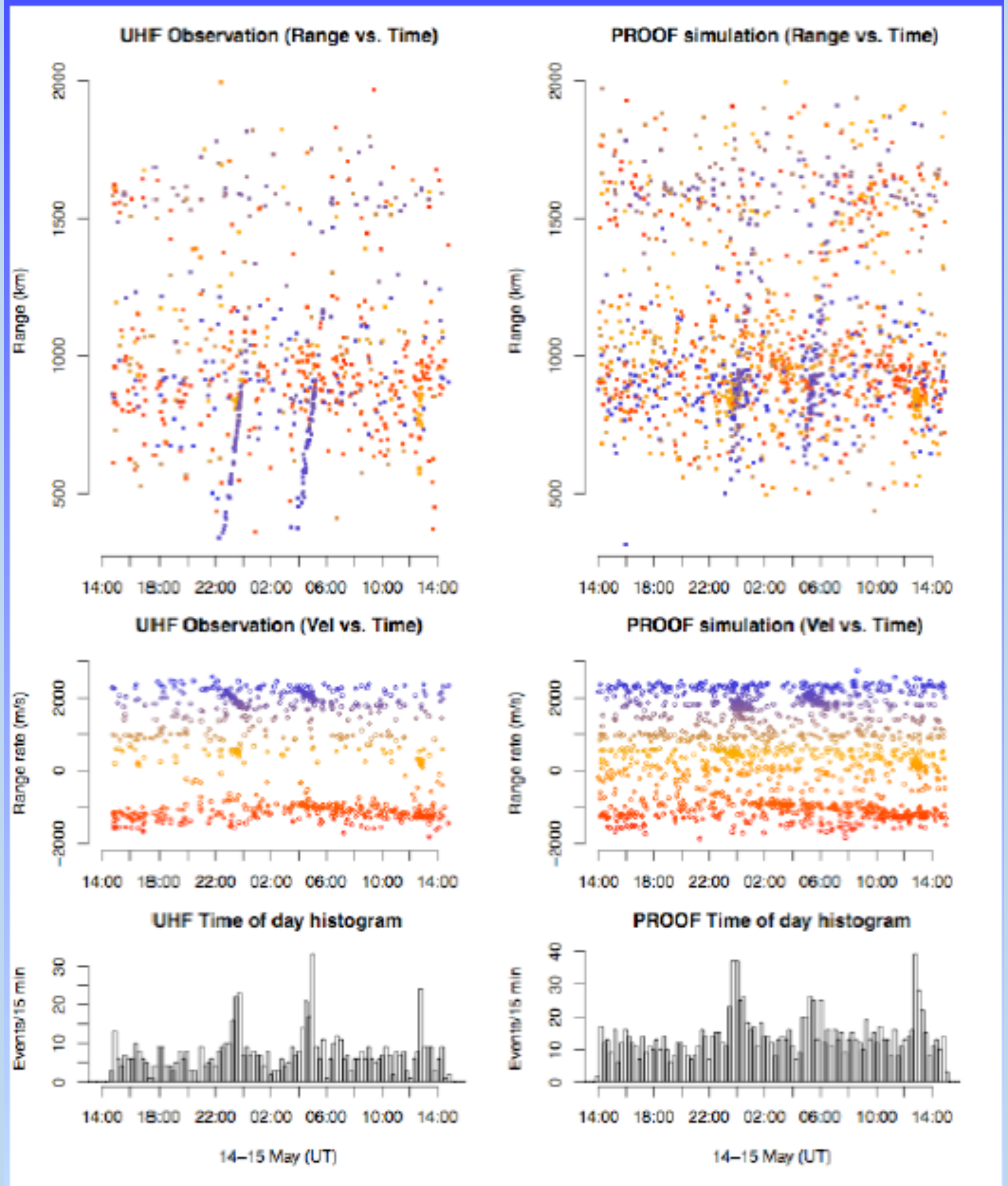

Temporal structure:
I: Day to day variability

- Multi-day runs often find a lot of variability, especially at high latitudes

- Driven by:
  - Solar wind/IMF variability
  - Magnetospheric responses
  - Transport phenomena
  - Changes in neutral wind
  - Composition changes

- Some radars (especially PFISR) have now made very long continuous runs, useful for climatological studies

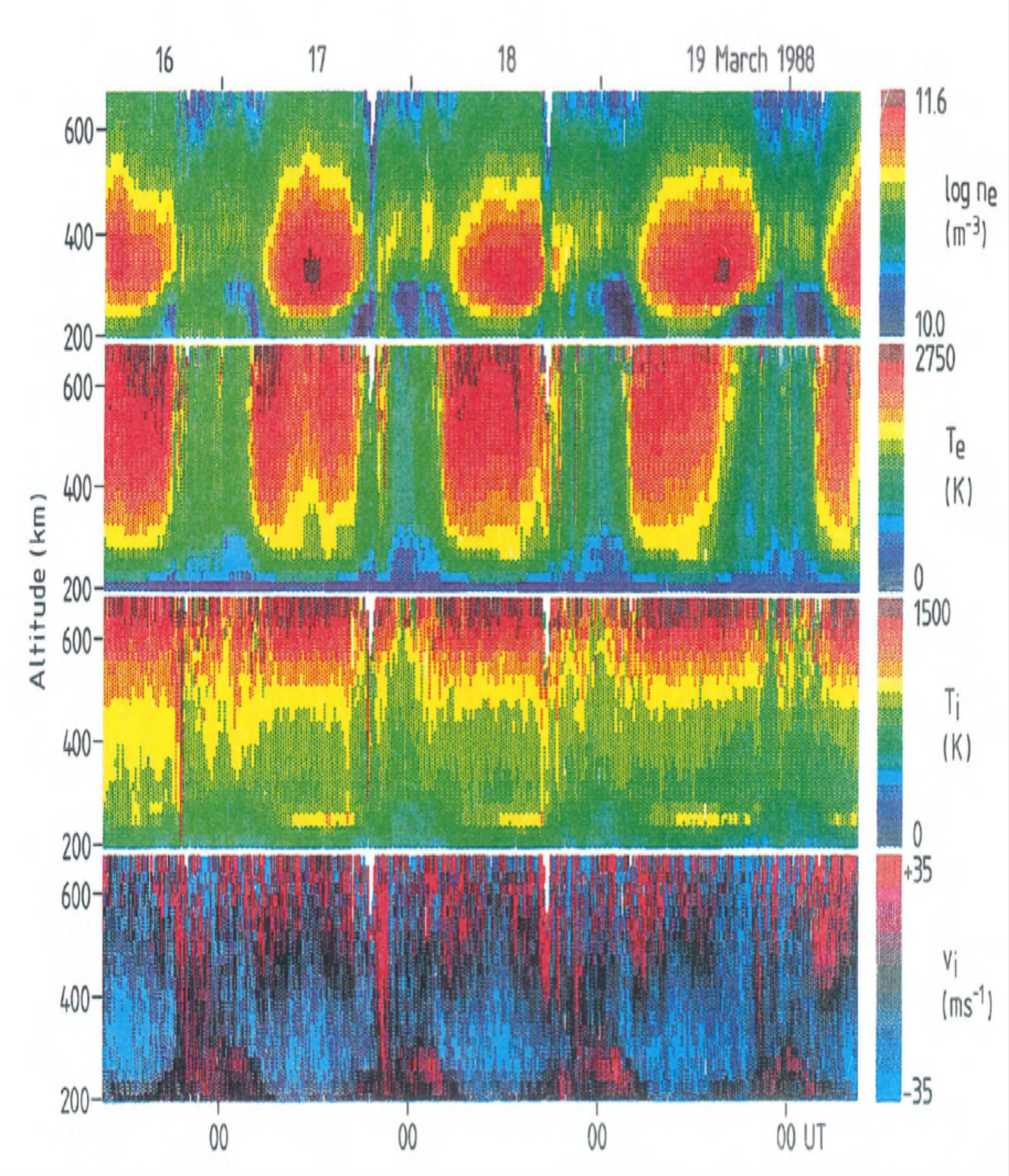

Millstone Hill Data – Explain April 1 and April 3, 2004

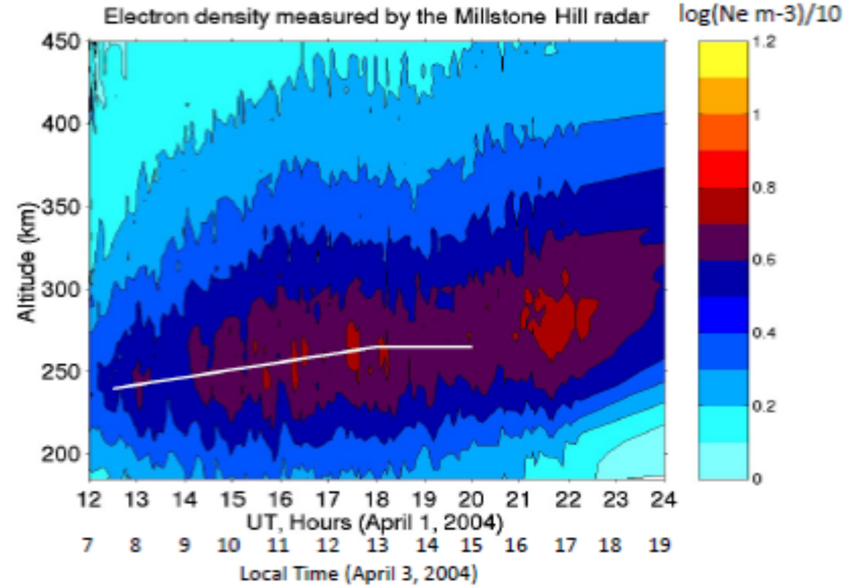

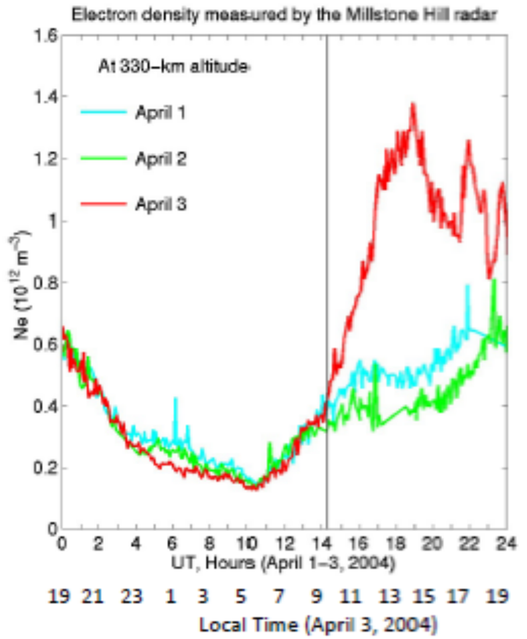

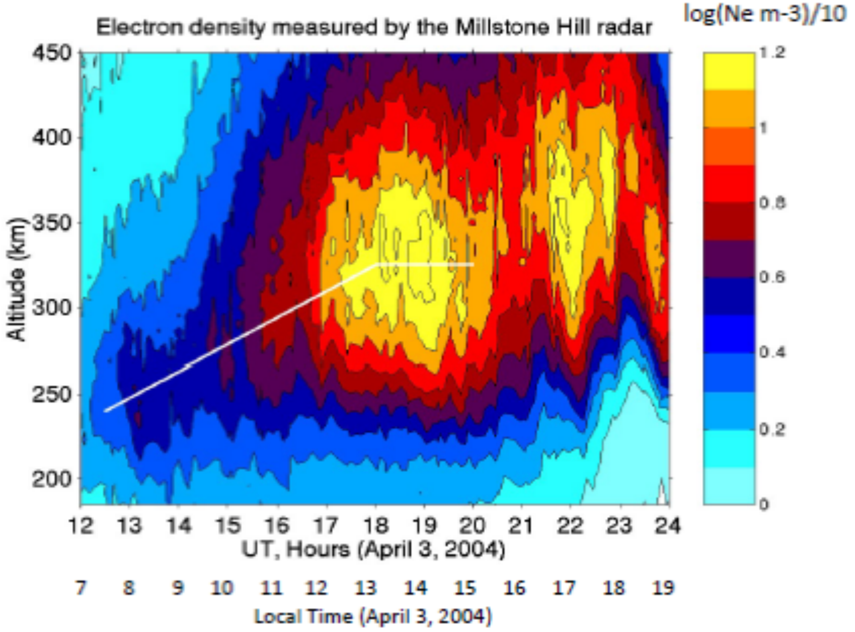

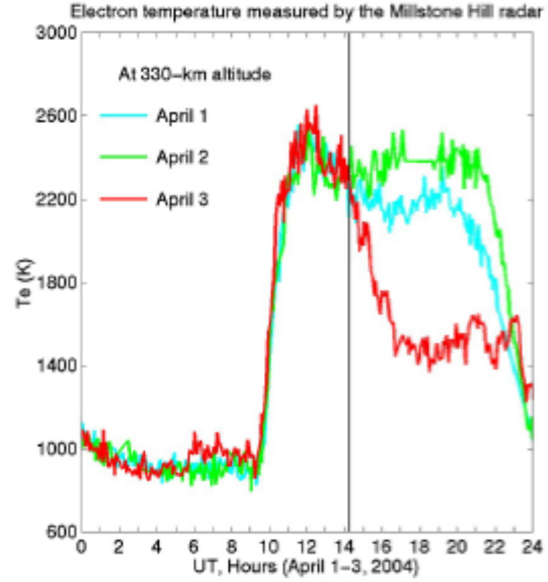

EISCAT Svalbard Radar data: Spring, Summer, Autumn, Winter

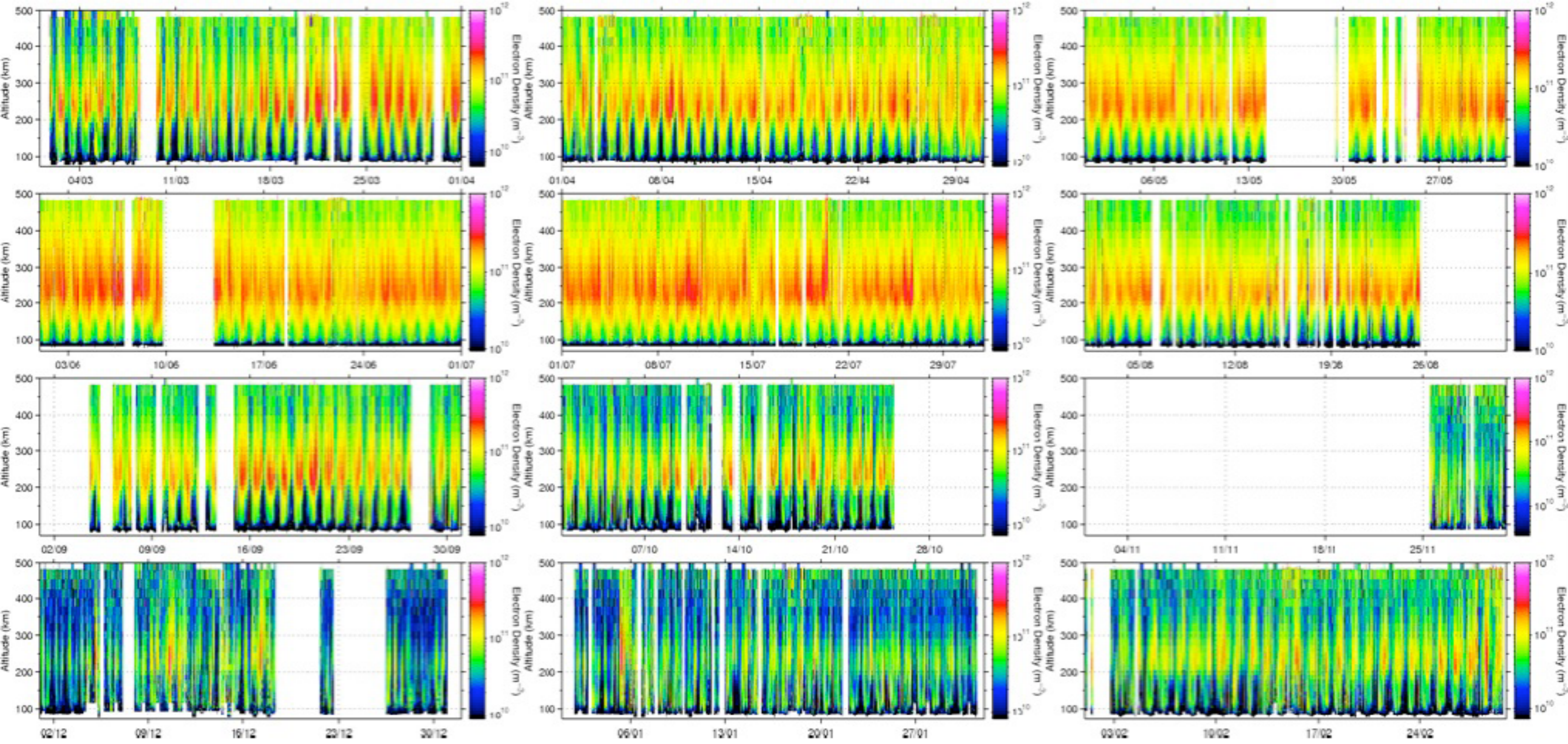

Temporal structure II: Statistical studies

Once ISRs had been running a few years, lots of people started doing statistical studies

A good way of learning about the physics, because any day of data exhibits so many different dependences

Using statistics, these factors become controllable: time, season, IMF, solar zenith angle, Kp, values of other parameters etc etc.

Statistical data sets can also be put together, e.g convection pattern statistics can be used to derive field-aligned currents and horizontal currents

These had previously been measured by other techniques e.g. satellites, but ISR data had some unique and important properties (e.g.

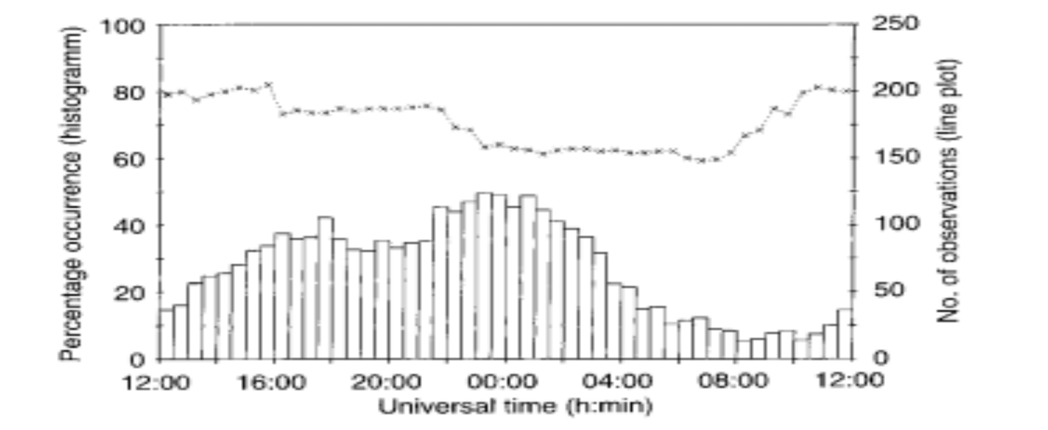

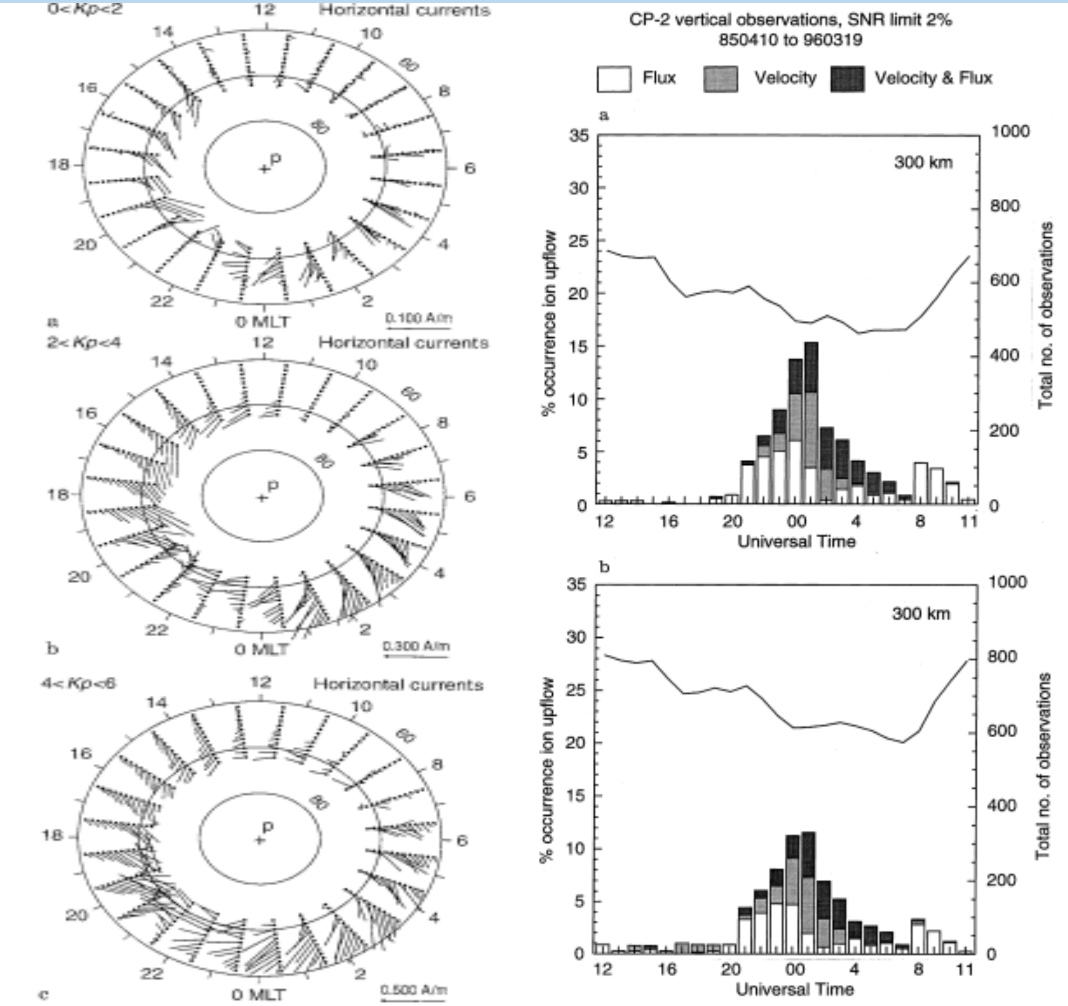

Temporal structure III: Long-term trends

- Now ISRs have been running for multiple solar cycles, people are doing longer-term trends.
- Vickers et al (2013) used ion momentum equation, simplified for field-aligned velocity, on a 13 year data set to derive variation of [O] at 350km with solar activity.
- Find factor 5-6 variation in [O] between solar min and solar max
- Also suggested a small overall decline in [O} at 350km from one solar maximum to the next
- Would suggest long-term thermospheric cooling, but effect was hardly significant

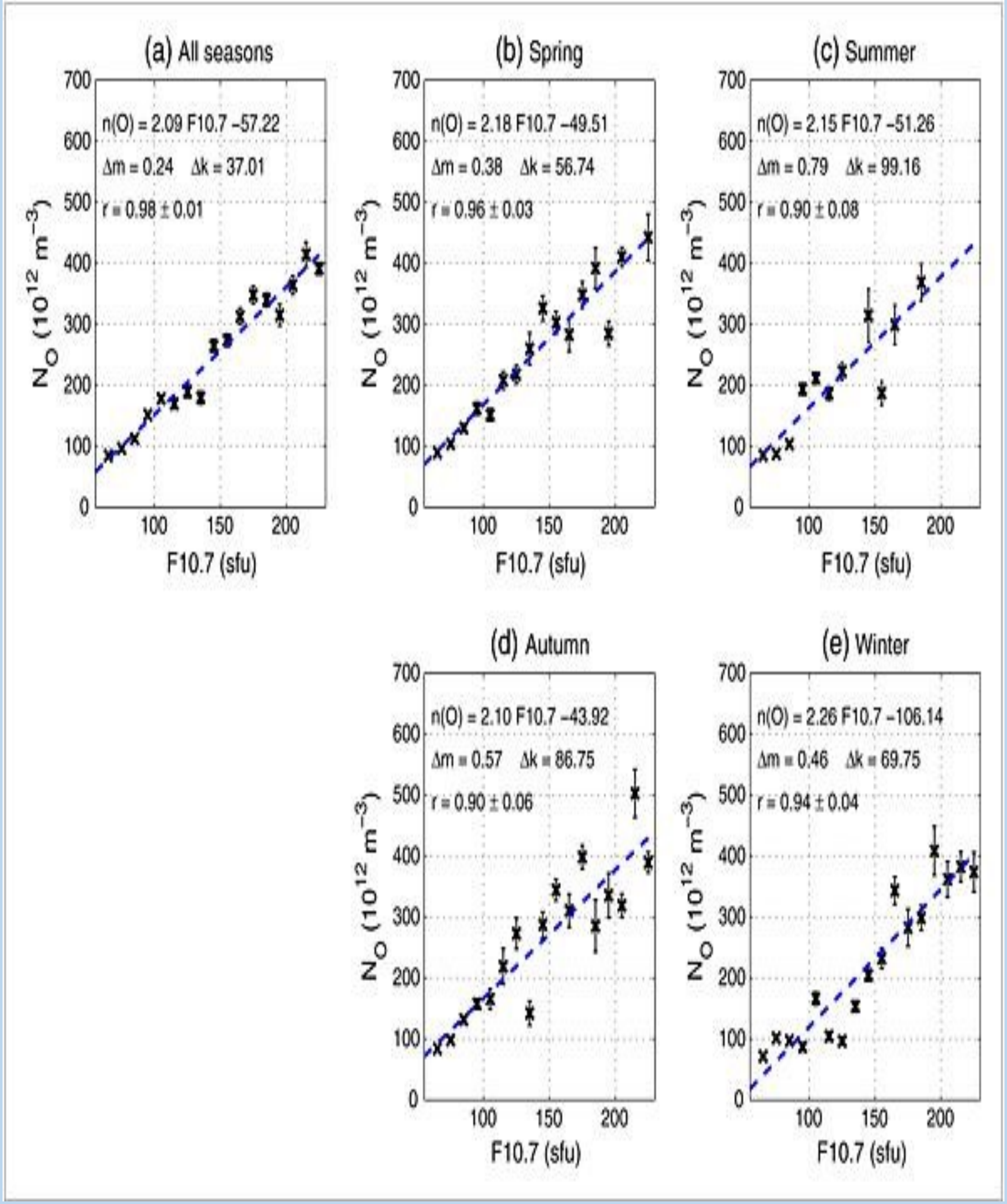

Ogawa et al (2014): 32 years of thermosphere cooling

Upper atmosphere has cooled steadily for three decades

Increasing amounts of greenhouse gases released by human activities do not just affect only the lower atmosphere: Scientists project that anthropogenic carbon emissions have caused a cooling trend in the upper atmosphere, between 200 and 400 kilometers, over the past few decades. Cooling in this atmospheric region can affect the operations of satellites and the orbits of space junk. However, data about cooling trends in the upper atmosphere are still incomplete, and better data are needed to confirm this projection.

Ogawa et al. present the first quantitative measurements that match projected upper atmospheric cooling. The authors analyzed data from the European Incoherent Scatter radar, which studies the interactions between the Sun and Earth on the basis of disturbances in Earth's ionosphere and magnetosphere.

From the radar's raw data spanning from 1981 to 2013, the authors teased out information about changes in upper atmospheric temperature. They calculated a cooling trend of 10–15 kelvins per decade near altitudes of 220–380 kilometers and little to no cooling at 400 kilometers.

The authors note that this height profile of their observed trend is in accord with those projected by previous models, but their estimated levels of cooling actually exceed the modeled ones. They speculate that this excess could be related to increases in anthropogenic carbon emissions. Further, their findings may have an impact on future modeling of the upper atmosphere, which will be important for planning future satellite missions. (*Geophysical Research Letters*, doi:10.1002/2014GL060591, 2014) —JW

Yasunobu Ogawa

The European Incoherent Scatter radar near Tromsø, Norway, was used to study climate change in the upper atmosphere.

EISCAT_3D Science Case

- EISCAT_3D Preparatory Phase project included a dedicated work package on building the science case
- Succession of working groups drawn from the EISCAT user community
- Different "focus area" in each of the first three years (atmospheric science, plasma physics, space weather - also solar system science and new techniques as background tasks)
- Annual updates of the science case and table of capabilities
- Appendices covering observing modes and supporting instruments. Feed into data requirements.
- McCrea, I., A. Aikio, L. Alfonsi, E. Belova, S. Buchert, M. Clilverd, N. Engler, B. Gustavsson, C. Heinselman, Johan Kero, M. Kosch, H. Lamy, T. Leyser, Y. Ogawa, K. Oksavik, A. Pellinen-Wannberg, F. Pitout, M. Rapp, I. Stanislawska and J. Vierinen, The science case for the EISCAT_3D radar, Progress in Earth and Planetary Science, 2:21, DOI 10.1186/s40645-015-0051-8, 2015.

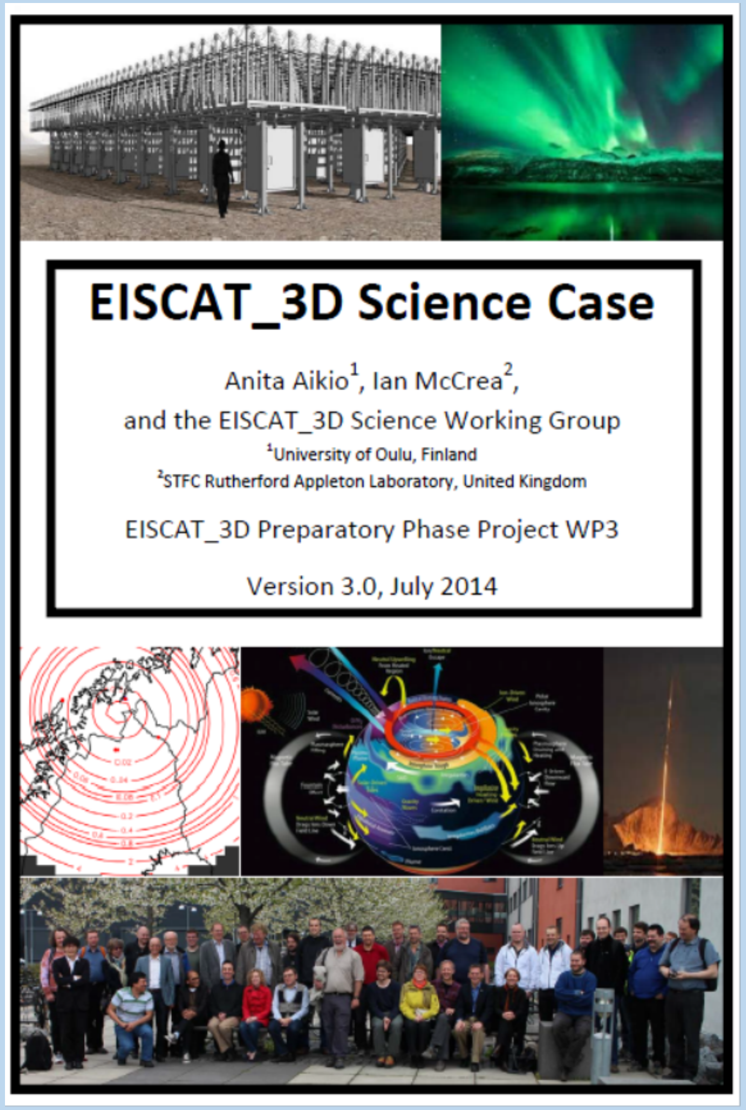

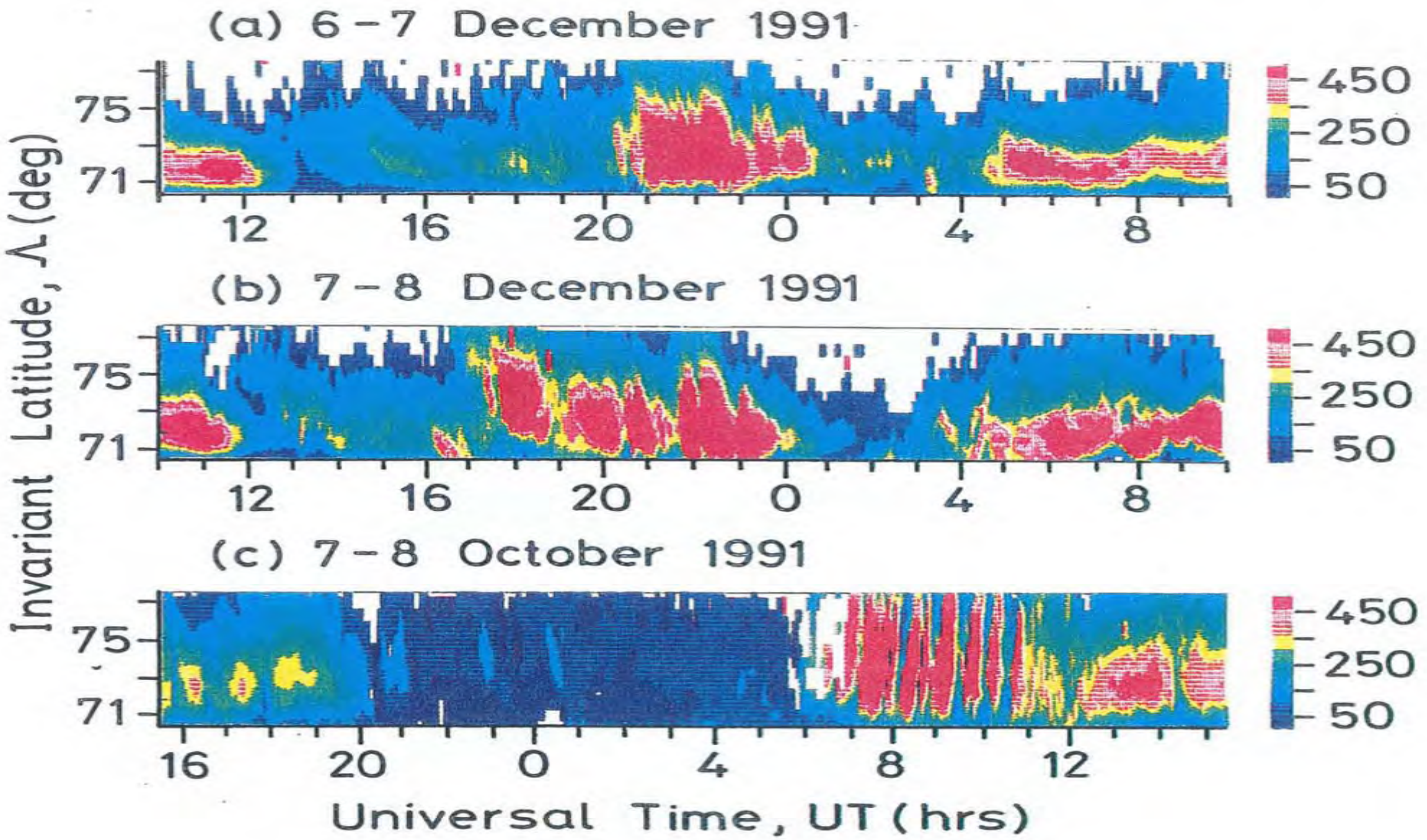
(a) 6 - 7 December 1991
(b) 7 - 8 December 1991
(c) 7 - 8 October 1991
Invariant Latitude, Λ (deg)
Universal Time, UT (hrs)
75
71
12
16
20
0
4
8
450
250
50

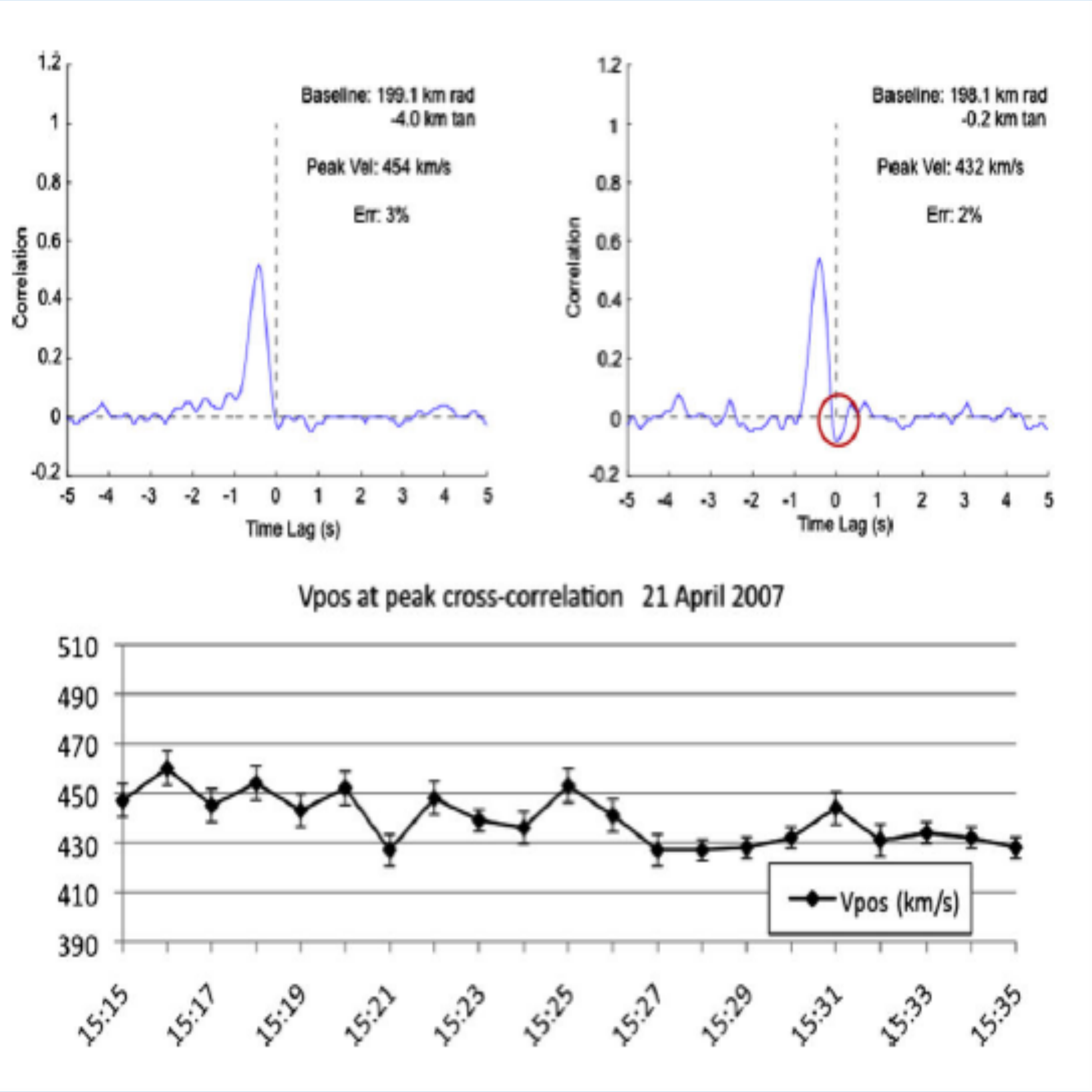
Baseline: 199.1 km rad
-4.0 km tan
Peak Vel: 454 km/s
Err: 3%
Correlation
Time Lag (s)
Baseline: 198.1 km rad
-0.2 km tan
Peak Vel: 432 km/s
Err: 2%
Correlation
Time Lag (s)
Vpos at peak cross-correlation 21 April 2007
Vpos (km/s)

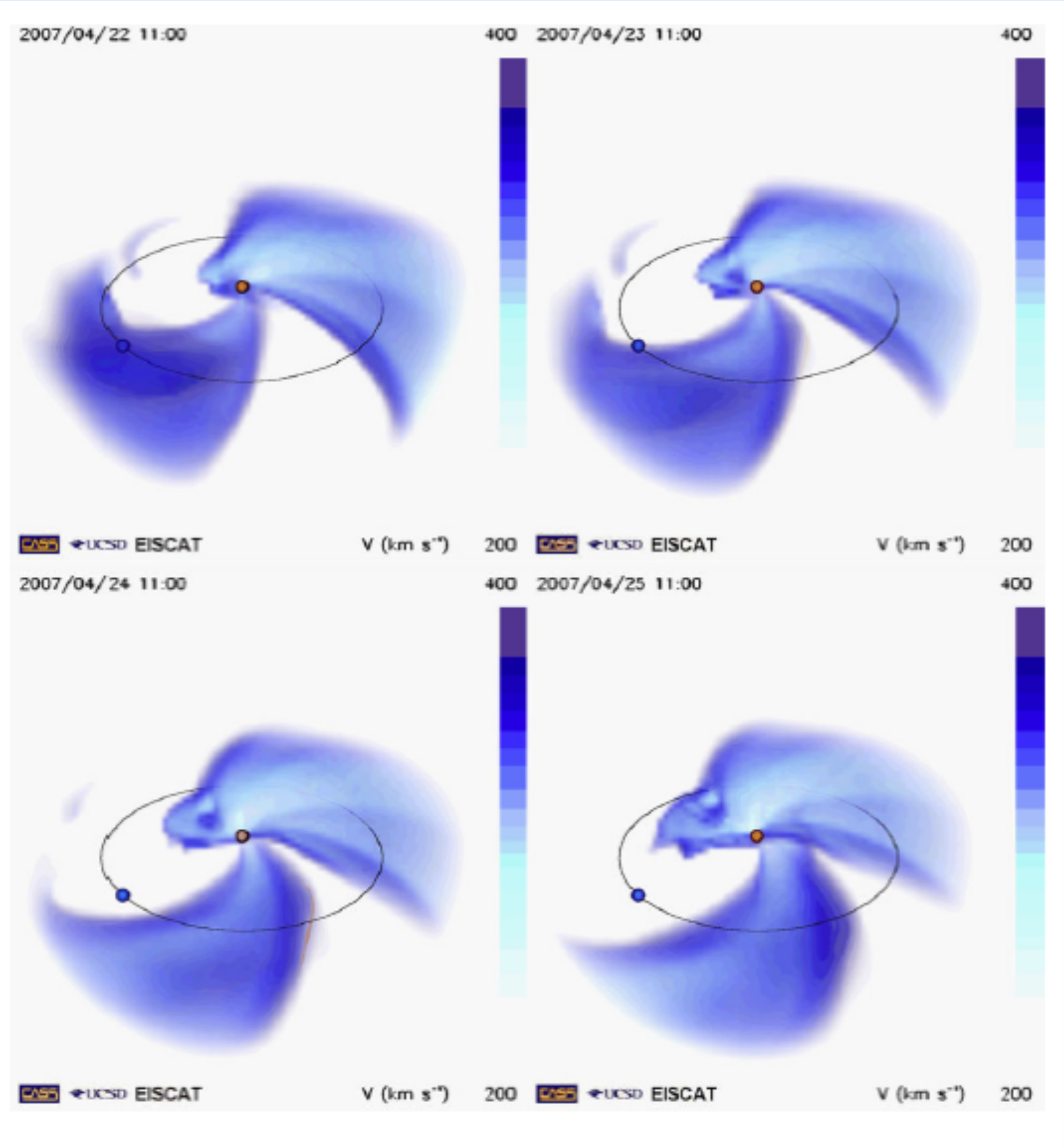
2007/04/22 11:00
2007/04/23 11:00
2007/04/24 11:00
2007/04/25 11:00
EISCAT
V (km s⁻¹)
400
200

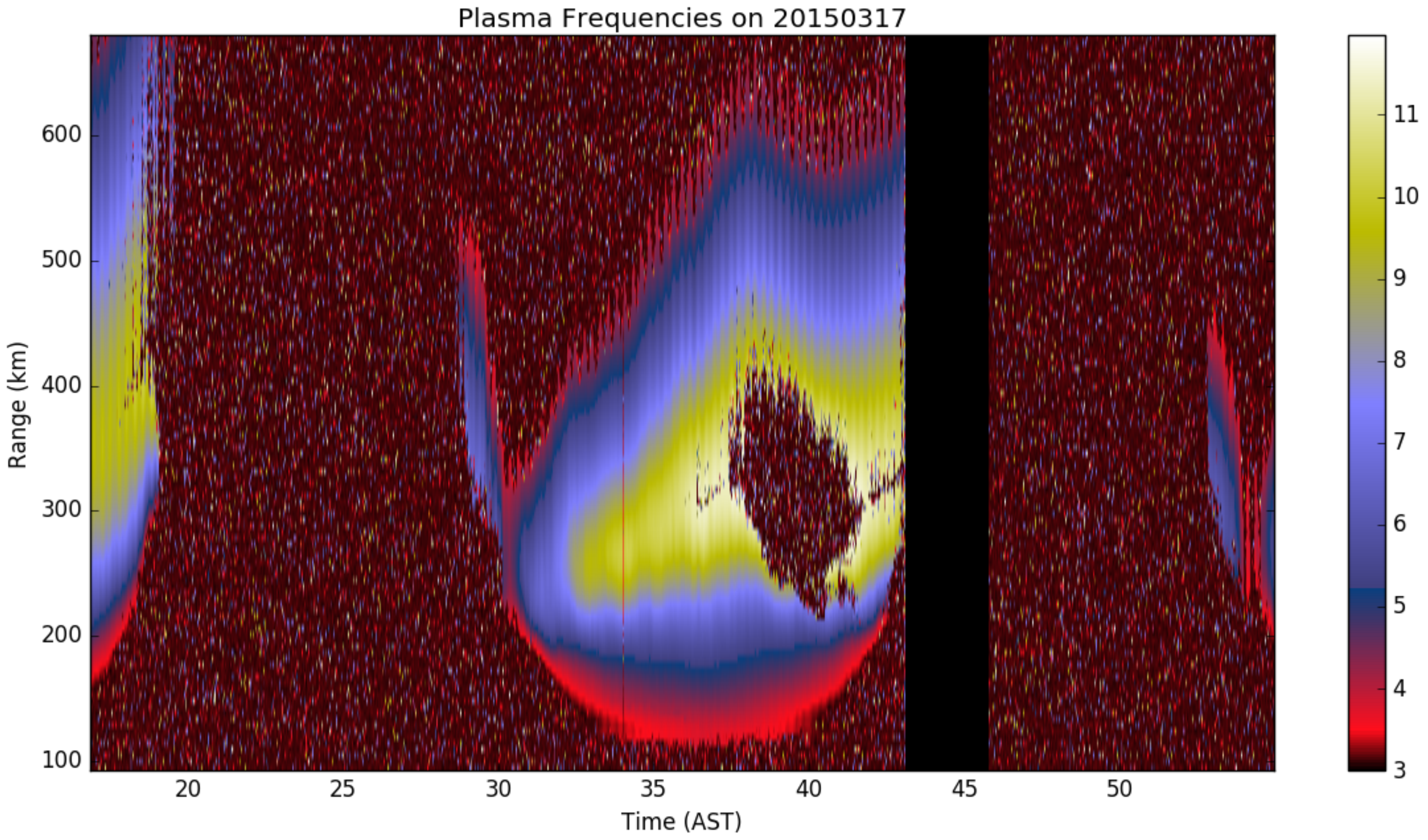

Plasma Frequencies on 20150317
Range (km)
600
500
400
300
200
100
20
25
30
35
40
45
50
Time (AST)
11
10
9
8
7
6
5
4
3

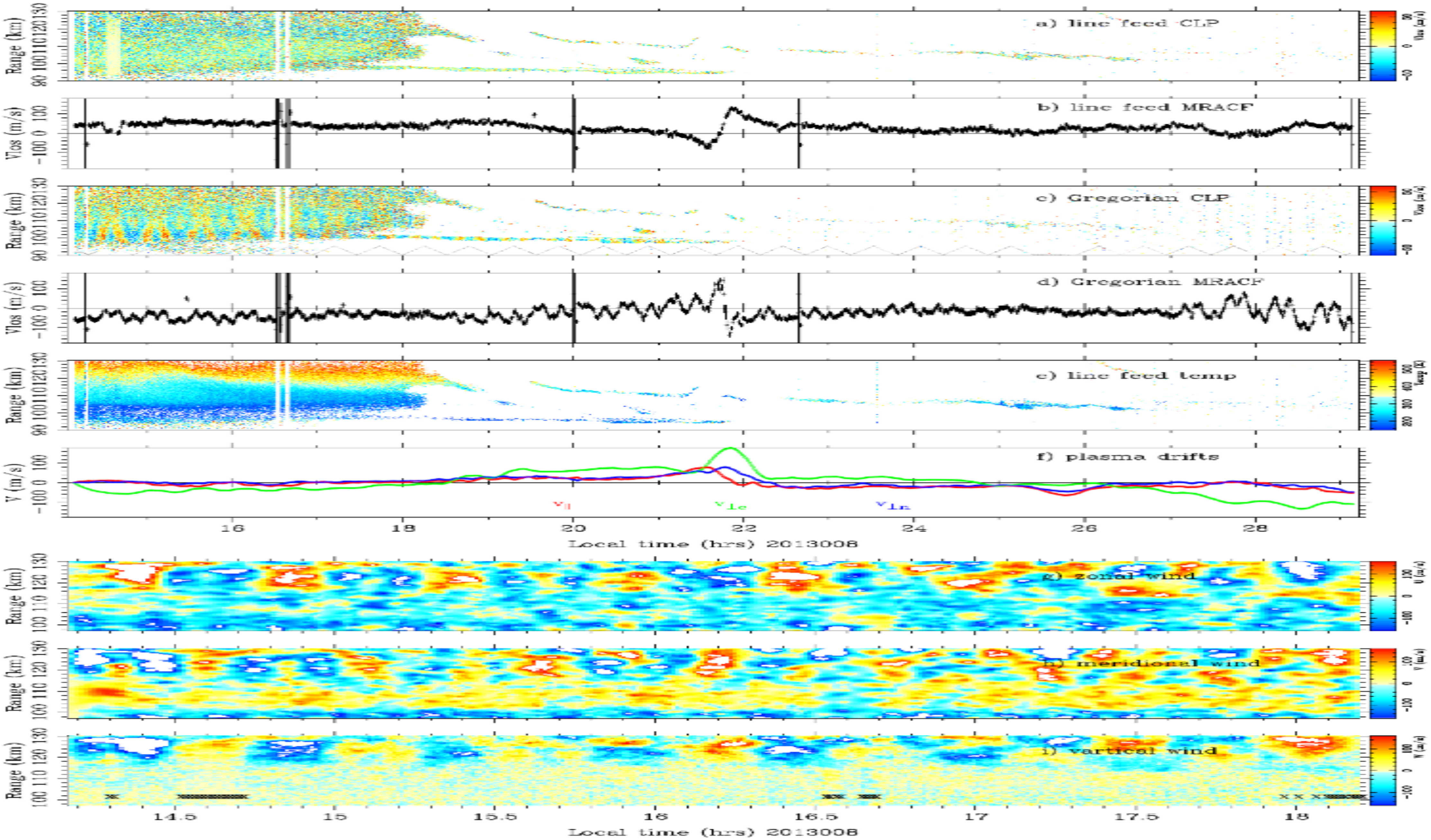

a) line feed CLP
b) line feed MRACF
c) Gregorian CLP
d) Gregorian MRACF
e) line feed temp
f) plasma drifts
g) zonal wind
h) meridional wind
i) vertical wind
Range (km)
Vlos (m/s)
V (m/s)
Local time (hrs) 2013008

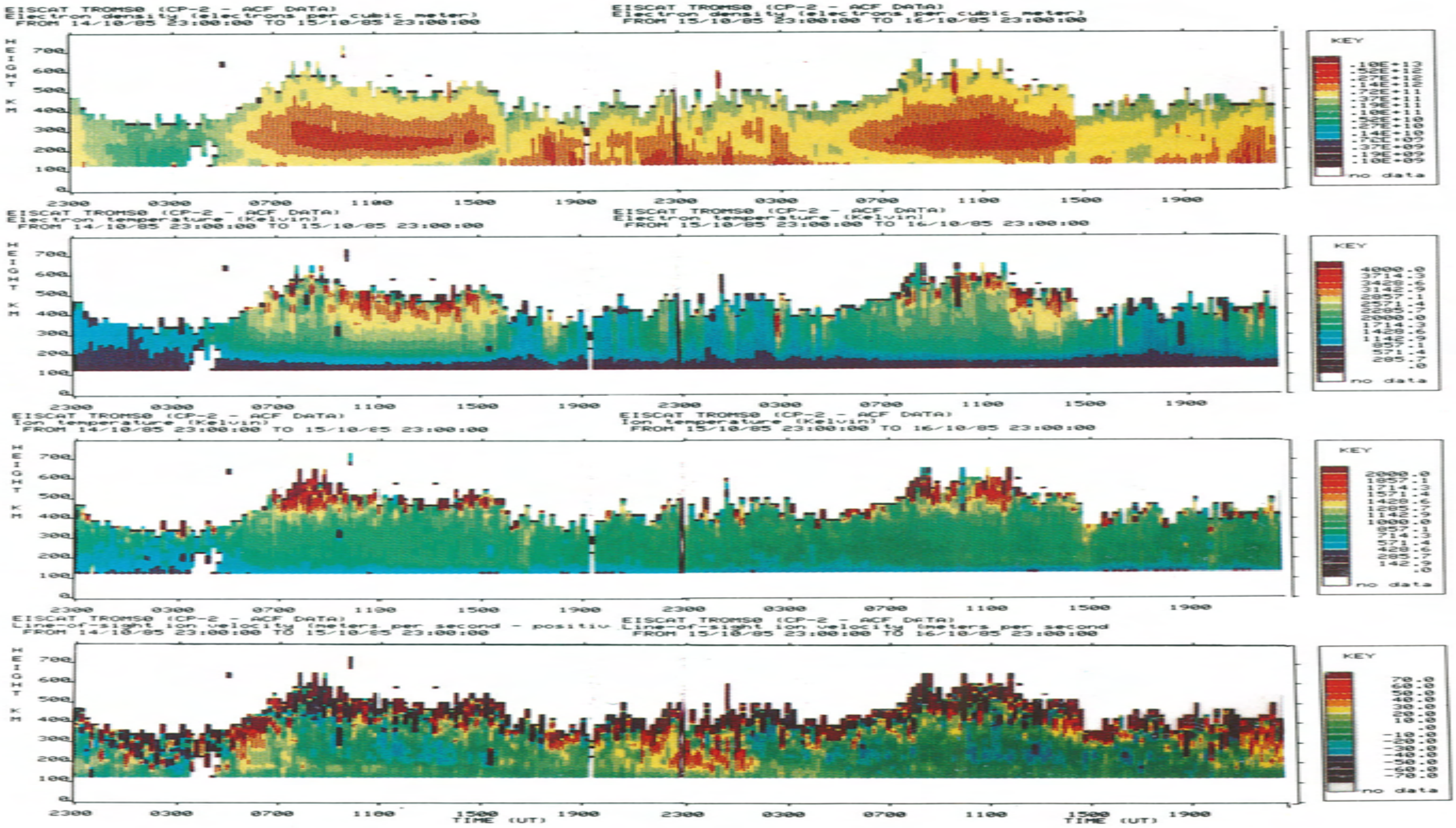

EISCAT TROMSØ (CP-2 - ACF DATA)
Electron density (electrons per cubic meter)
FROM 14/10/85 23:00:00 TO 15/10/85 23:00:00
EISCAT TROMSØ (CP-2 - ACF DATA)
Electron density (electrons per cubic meter)
FROM 15/10/85 23:00:00 TO 16/10/85 23:00:00
HEIGHT KM
KEY
.10E+13
.52E+12
.27E+12
.14E+12
.72E+11
.37E+11
.19E+11
.10E+11
.52E+10
.27E+10
.14E+10
.37E+09
.19E+09
.10E+09
no data
EISCAT TROMSØ (CP-2 - ACF DATA)
Electron temperature (Kelvin)
FROM 14/10/85 23:00:00 TO 15/10/85 23:00:00
EISCAT TROMSØ (CP-2 - ACF DATA)
Electron temperature (Kelvin)
FROM 15/10/85 23:00:00 TO 16/10/85 23:00:00
KEY
4000.0
3714.3
3428.6
3142.9
2857.1
2571.4
2285.7
2000.0
1714.3
1428.6
1142.9
857.1
571.4
285.7
.0
no data
EISCAT TROMSØ (CP-2 - ACF DATA)
Ion temperature (Kelvin)
FROM 14/10/85 23:00:00 TO 15/10/85 23:00:00
EISCAT TROMSØ (CP-2 - ACF DATA)
Ion temperature (Kelvin)
FROM 15/10/85 23:00:00 TO 16/10/85 23:00:00
KEY
2000.0
1857.1
1714.3
1571.4
1428.6
1285.7
1142.9
1000.0
857.1
714.3
571.4
428.6
285.7
142.9
.0
no data
EISCAT TROMSØ (CP-2 - ACF DATA)
Line-of-sight ion velocity (meters per second - positiv
FROM 14/10/85 23:00:00 TO 15/10/85 23:00:00
EISCAT TROMSØ (CP-2 - ACF DATA)
Line-of-sight ion velocity (meters per second
FROM 15/10/85 23:00:00 TO 16/10/85 23:00:00
KEY
70.0
60.0
50.0
40.0
30.0
20.0
10.0
.0
-10.0
-20.0
-30.0
-40.0
-50.0
-60.0
-70.0
no data
TIME (UT)